CHAPTER B8
FLOW OF FLUIDS

Tadeusz J. Swierzawski
Consultant, Energy Systems
Burlington, Massachusetts

INTRODUCTION

The primary objective of this chapter is to show the user the most important logical milestones and the general background of equations and formulas recommended for specific practical applications of fluid flow in pipes, nozzles, and orifices. For details, Refs. 1 through 4 or other equivalent textbooks should be consulted.

Nomenclature

A nomenclature section is provided to minimize repeating of variable definitions. Unless otherwise stated, all symbols used in this chapter are defined as described in the following lists. Units presented here are mostly those of practical range of applications. The SI units of each physical quantity under consideration appear in parentheses; however, in all equations presented in this chapter only the base U.S. customary units (English units) must be used. For details see ''Survey of Dimensions and Units.''

Variables

a	Acceleration, ft/s^2 (m/s^2) (m = meter, s = second)
A	Cross-sectional area of pipe, flow duct, or orifice, ft^2 (cm^2)
A_f	Flow area occupied by liquid phase, ft^2 (cm^2)
A_g	Flow area occupied by gaseous phase, ft^2 (cm^2)
c	Velocity of sound, ft/s (m/s)
C	Flow coefficient defined by Eq. (B8.45), dimensionless
C_A	Allen flow constant defined by Eq. (B8.88)
C_c	Coefficient of contraction, dimensionless
C_d	Discharge coefficient, dimensionless

c_p	Specific heat at constant pressure, Btu/($lb_m \cdot °F$) (kJ/(kg · K)) (kJ = kilojoule, kg = kilogram, K = kelvin)
c_v	Specific heat at constant volume, Btu/($lb_m \cdot °F$) (kJ/(kg · K))
C_v	Velocity coefficient, dimensionless
d	Nozzle or orifice diameter, in (mm) (mm = millimeter)
d_g	Flow height for gaseous phase, in (mm)
D	Pipe inside diameter, ft, in (mm)
E	Energy, Btu, kWh (kJ, kWh)
$\dot{E}$	Energy flow rate, Btu/s, kW (kJ/s, kW)
f	D'Arcy-Weisbach friction factor, dimensionless
f_T	Friction factor in zone of complete turbulence (dimensionless)
F	Force, lb_f, (N) (N = newton)
F_a	Area factor for thermal expansion of primary elements (see Fig. B8.22)
Fr	Froude number, dimensionless
F_{wa}	Approach velocity factor defined by Eq. (B8.42), dimensionless
g	Acceleration due to gravity (local), ft/s^2 (m/s^2)
g_c	32.174 ($lb_m \cdot ft$)/($lb_f \cdot s^2$), dimensional conversion factor (does not exist in SI units)
g_s	32.174 ft/s^2 (9.80665 m/s^2)—standard (normal) acceleration due to gravity (standard acceleration of free fall)
$\dot{G} = \dot{m}/A$	Mass flux, lb_m/($ft^2 \cdot s$) (kg/($m^2 \cdot s$))
$\dot{G}_c$	Maximum (critical) mass flux, lb_m/($ft^2 \cdot s$) (kg/($m^2 \cdot s$))
$\dot{G}_{fs}$	Superficial mass flux of liquid phase, lb_m/($ft^2 \cdot s$) (kg/($m^2 \cdot s$))
$\dot{G}_{gs}$	Superficial mass flux of gaseous phase, lb_m/($ft^2 \cdot s$) (kg/($m^2 \cdot s$))
h	Specific enthalpy (static), Btu/lb_m (kJ/kg)
h_f	Specific enthalpy of liquid phase, Btu/lb_m (kJ/kg)
h_g	Specific enthalpy of gaseous phase, Btu/lb_m (kJ/kg)
h_{fg}	Latent heat of vaporization ($h_g - h_f$), Btu/lb_m (kJ/kg)
h_0	Stagnation enthalpy, Btu/lb_m (kJ/kg)
H	Enthalpy, Btu (kJ)
H_f	Loss of static pressure head, ft (m)
$j_f = \dot{G}_{fs}\, v_f$	Superficial velocity (volumetric flux) of liquid phase, ft/s (m/s)
$j_g = \dot{G}_{gs}\, v_g$	Superficial velocity (volumetric flux) of gaseous phase, ft/s (m/s)
J	778.169 ft · lb_f/Btu; mechanical equivalent of heat, dimensional conversion factor (does not exist in SI units)
k	C_p/C_v—isentropic exponent, dimensionless
K	Flow resistance coefficient (K-factor), dimensionless
L	Length, ft (m)
m	Mass, lb_m (kg)
$\dot{m}$	Mass flow rate, lb_m/s (kg/s)

Ma	w/c—Mach number, dimensionless
p	Absolute pressure, lb_f/ft^2, lb_f/in^2 = psia (N/m^2 = Pa, kPa, bar; Pa − pascal, 1 bar = 10^5 Pa = 100 kPa)
p_g	$p - p_{amb}$, gauge pressure (p_{amb} is the ambient pressure expressed in the same units as p)
p_o	Stagnation pressure, lb_f/ft^2, lb_f/in^2 (N/m^2, kPa, bar)
P	Power, kW (kW)
q	Heat per unit mass, Btu/lb_m (kJ/kg)
Q	Heat, Btu (kJ)
$\dot{Q}$	Heat flow rate, Btu/s (kJ/s)
r_h	Hydraulic radius, ft (mm)
R	Gas constant, $(ft \cdot lb_f)/(lb_m \cdot °R)$ $((N \cdot m)/(kg \cdot K))$ where $1\ N \cdot m = 1\ J$)
Re	Reynolds number, dimensionless
s	Specific entropy, $Btu/(lb_m \cdot °R)$ $(kJ/(kg \cdot K))$
s_f	Specific entropy of liquid phase, $Btu/(lb_m \cdot °R)$ $(kJ/(kg \cdot K))$
s_g	Specific entropy of gaseous phase, $Btu/(lb_m \cdot °R)$ $(kJ/(kg \cdot K))$
s_{fg}	$s_g - s_f$, $Btu/(lb_m \cdot °R)$ $(kJ/(kg \cdot K))$
s_0	Stagnation entropy, $Btu/(lb_m \cdot °R)$ $(kJ/(kg \cdot K))$
S	Entropy, Btu/°R (kJ/K)
S^*	Slip ratio, dimensionless
t	Time, s, h (s, h)
t_F	°F (t_C = Celsius temperature, °C)
T	Thermodynamic temperature, °R (K)
T_o	Stagnation temperature, °R (K)
u	Specific internal energy, Btu/lb_m (kJ/kg)
U	Internal energy, Btu (kJ)
v	Specific volume, ft^3/lb_m; (m^3/kg)
v_f	Specific volume of saturated liquid, ft^3/lb_m (m^3/kg)
v_g	Specific volume of saturated steam, ft^3/lb_m (m^3/kg)
v_{fg}	$v_g - v_f$, ft^3/lb_m (m^3/kg)
V	Volume, ft^3 (m^3, 1 = liter)
$\dot{V}$	Volumetric flow rate, ft^3/h (m^3/h, l/s)
w	Velocity, ft/s (m/s)
W	Work, $ft \cdot lb_f$ (kJ)
$\dot{W}_t$	Technical work rate (power), $ft \cdot lb_f/s$, kW (kW)
x	Mass quality of steam, dimensionless
y	Distance to fixed surface, ft (m)
z	Elevation, ft (m)

Greek Symbols

α	Void fraction, dimensionless
α_s	Quantity defined by Eq. (B8.61)
β	d/D, dimensionless diameter ratio
β_s	Critical pressure ratio, dimensionless
γ	Specific weight, lb_f/ft^3; (N/m^3)
ε	Absolute roughness, ft (the same unit as the pipe diameter D); (mm)
μ	Dynamic (absolute) viscosity, $(lb_f \cdot s)/ft^2$ $((N \cdot s)/m^2)$
μ_f	Dynamic viscosity of liquid phase, $(lb_f \cdot s)/ft^2$ $((N \cdot s)/m^2)$
μ_g	Dynamic viscosity of gaseous phase, $(lb_f \cdot s)/ft^2$ $((N \cdot s)/m^2)$
ν	Kinematic viscosity, ft^2/s (m^2/s)
ν_f	Kinematic viscosity of liquid phase, ft^2/s (m^2/s)
ν_g	Kinematic viscosity of gaseous phase, ft^2/s (m^2/s)
π	Pi, approximately 3.14159, dimensionless
ρ	Density, lb_m/ft^3; (kg/m^3)
ρ_f	Density of gaseous phase, lb_m/ft^3 (kg/m^3)
ρ_g	Density of liquid phase, lb_m/ft^3 (kg/m^3)
τ	Shearing stress, lb_f/ft^2 (N/m^2)
T	Thrust, lb_f (N)
Ψ^2_{LO}	Two-phase pressure drop multiplier, dimensionless
Ψ_s	Quantity defined by Eq. (B8.52)

Subscripts

f, l	Liquid or water phase, saturated liquid
g	Steam phase, saturated steam

Basic Fluid Properties

A *fluid* is a substance which can flow and which deforms continuously under the action of shearing forces. Fluids offer no resistance to distortion of form; they yield continuously to tangential forces, no matter how small. Ordinarily, fluids are classified as being liquids or gases. Some classifications also include the vapor form within the group of fluids.

Liquids change volume and density very slightly with considerable variation in pressure, and when the pressure is removed, they do not dilate significantly. They are practically incompressible.

A *gas* is a fluid which tends to expand to fill completely any vessel in which it is contained. It is easily compressed, and a change in pressure is accompanied by a considerable change in its volume and density.

A *perfect (or ideal) gas* satisfies two conditions: (1) it obeys the Clapeyron equation $pV = mRT$ at all pressures, and (2) its specific heats are constant regardless of pressures and temperatures. In (1) above, p, V, and T are pressure, volume, and absolute temperature, respectively, and m and R represent the mass of gas and the gas constant, all in proper units. From (2) it follows also that the specific-heat ratio, $k = c_p/c_v$, is also constant.

The behavior of real gases is more complex. Real gases at low pressure tend to obey perfect gas law. As the pressure increases, however, the discrepancy increases and becomes serious near the critical point. If higher degrees of accuracy are required, textbooks in thermodynamics list corrections (as, for example, van der Waals' equation) which take into account deviations from ideal conformance. For practical purposes, gas and steam properties are published in the form of tables, charts, and appropriate computer programs. For example, the ASME (American Society of Mechanical Engineers) steam tables[5] are accompanied by computer diskettes that contain a steam properties calculation program. This FORTRAN source code may be copied, compiled, and utilized in compiled code of other programs.

Survey of Dimensions and Units

Dimensions, although discussed in other sections of this handbook, are briefly reviewed here to recall some fundamentals. The proper use of units and dimensions will save time and avoid errors. It is a good practice to include the units of all physical quantities, as well as their magnitudes, in performed calculations.

A *dimension* is a general expression for a particular kind of physical quantity (e.g., length, mass, time). A *unit* is a reference standard used to measure a physical quantity (e.g., one meter, one inch, and one foot are alternative units of the dimension length).

Four fundamental dimensions are required for analyses of thermodynamic or/and fluid flow systems. Length, mass, time, and temperature are usually chosen.

U.S. Customary Units. The U.S. Customary Units (English system of dimensions and units) belong to the group of engineering systems where force instead of mass is a base dimension and the mass unit is derived from Newton's relationship that force equals mass times acceleration:

$$F = ma \tag{B8.1}$$

Then, the derived unit of mass in this system is $(lb_f \cdot s^2)/ft = 1$ slug. A *slug* is the mass that can be accelerated at the rate of 1 ft/s^2 by a force of 1 standard pound-force. By definition, 1 standard pound-force will also accelerate 1 pound-mass at the rate of 32.174 ft/s^2. It follows that the slug is the mass of size 32.174 times that of the pound-mass (Fig. B8.1), and $g_c = 32.174\ lb_m/slug = 32.174\ (lb_m \cdot ft)/(lb_f \cdot s^2)$ is the dimensional conversion factor between the two systems of dimensions (based on mass versus that based on force). The density ρ is the mass per unit volume of the fluid and is not to be confused with specific weight γ, the weight per unit volume. The interrelation of density and specific weight is $\gamma = \rho g/g_c$. In thermodynamic calculations, this system is still using the unit of mass lb_m (for example, $Q = mc\,\Delta T$).

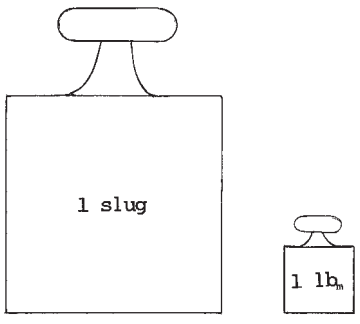

FIGURE B8.1 Slug versus pound mass.

Click for view of double page spread

TABLE B8.1 Conversion Factors for Pressure

To obtain → / Multiply, by ↓	atm	bar	$\frac{\text{lbf}}{\text{in.}^2}$	in. Hg (0°C)
atm	1	1.013 25	$\frac{1\,013\,250 \times 2.54^2}{980.665 \times 453.592\,37}$ = 14.695 948 8	$\frac{1\,013\,250/980.665}{13.595\,088\,9 \times 2.54}$ = 29.921 280 0
bar	$\frac{1.0}{1.013\,25}$ = 0.986 923 267	1	$\frac{2.54^2 \times 10^6}{980.665 \times 453.592\,37}$ = 14.503 773 8	$\frac{10^6/980.665}{13.595\,088\,9 \times 2.54}$ = 29.530 007 4
$\frac{\text{lbf}}{\text{in.}^2}$	$\frac{980.665 \times 453.592\,37}{1\,013\,250 \times 2.54^2}$ = 0.068 045 963 9	$\frac{980.665 \times 453.592\,37}{2.54^2 \times 10^6}$ = 0.068 947 572 9	1	$\frac{453.592\,37/2.54^3}{13.595\,088\,9}$ = 2.036 022 34
in. Hg (0 C)	$\frac{13.595\,088\,9 \times 2.54}{1\,013\,250/980.665}$ = 0.033 421 030 1	$\frac{13.595\,088\,9 \times 2.54}{10^6/980.665}$ = 0.033 863 858 8	$\frac{13.595\,088\,9 \times 2.54^3}{453.592\,37}$ = 0.491 153 746	1
ft H_2O (20 C)	$\frac{0.998\,278\,282 \times 30.48}{1\,013\,250/980.665}$ = 0.029 449 006 6	$\frac{0.998\,278\,282 \times 30.48}{10^6/980.665}$ = 0.029 839 205 9	$\frac{0.998\,278\,282 \times 12}{453.592\,37/2.54^3}$ = 0.432 781 092	$\frac{0.998\,278\,282 \times 12}{13.595\,088\,9}$ = 0.881 151 971
mm Hg (0 C)	$\frac{13.595\,088\,9}{10\,132\,500/980.665}$ = 0.001 315 788 59	$\frac{13.595\,088\,9}{10^7/980.665}$ = 0.001 333 222 79	$\frac{13.595\,088\,9 \times 2.54^2}{453.592\,37 \times 10}$ = 0.019 336 761 7	$\frac{1.0}{25.4}$ = 0.039 370 078 7
$\frac{\text{kp}}{\text{cm}^2}$	$\frac{980.665}{1\,013.25}$ = 0.967 841 105	0.980 665	$\frac{2.54^2 \times 10^3}{453.592\,37}$ = 14.223 343 3	$\frac{10^3}{13.595\,088\,9 \times 2.54}$ = 28.959 044 7
kPa	$\frac{1.0}{101.325}$ = 0.009 869 232 67	0.01	$\frac{2.54^2 \times 10^4}{980.665 \times 453.592\,37}$ = 0.145 037 738	$\frac{10^4/980.665}{13.595\,0889 \times 2.54}$ = 0.295 300 074

Source: Ref. 5.

	ft H_2O (20°C)	mm Hg (0°C)	$\frac{kp}{cm^2}$	kPa
	$\frac{1\,013\,250/980.665}{0.998\,278\,282 \times 30.48}$ $= 33.957\,002\,9$	$\frac{10\,132\,500/980.665}{13.595\,088\,9}$ $= 760.000\,512$	$\frac{1.013\,25}{0.980\,665}$ $= 1.033\,227\,45$	101.325
	$\frac{10^6/980.665}{0.998\,278\,282 \times 30.48}$ $= 33.512\,956\,2$	$\frac{10^7/980.665}{13.595\,088\,9}$ $= 750.062\,188$	$\frac{10^3}{980.665}$ $= 1.019\,716\,21$	100
	$\frac{453.592\,37/2.54^3}{0.998\,278\,282 \times 12}$ $= 2.310\,636\,99$	$\frac{453.592\,37 \times 10}{13.595\,088\,9 \times 2.54^2}$ $= 51.714\,967\,4$	$\frac{453.592\,37}{2.54^2 \times 10^3}$ $= 0.070\,306\,958\,0$	$\frac{980.665 \times 453.592\,37}{2.54^2 \times 10^4}$ $= 6.894\,757\,29$
	$\frac{13.595\,088\,9}{0.998\,278\,282 \times 12}$ $= 1.134\,878\,01$	25.4	$\frac{13.595\,088\,9 \times 2.54}{10^3}$ $= 0.034\,531\,525\,8$	$\frac{13.595\,088\,9 \times 2.54}{10^4/980.665}$ $= 3.386\,385\,88$
	1	$\frac{9.982\,782\,82 \times 30.48}{13.595\,088\,9}$ $= 22.381\,260\,1$	$\frac{0.998\,278\,282 \times 30.48}{10^3}$ $= 0.030\,427\,522\,0$	$\frac{0.998\,278\,282 \times 30.48}{10^4/980.665}$ $= 2.983\,920\,59$
	$\frac{13.595\,088\,9}{9.982\,782\,82 \times 30.48}$ $= 0.044\,680\,236\,8$	1	$13.595\,088\,9 \times 10^{-4}$ $= 0.001\,359\,508\,89$	$\frac{13.595\,088\,9}{10^5/980.665}$ $= 0.133\,322\,279$
	$\frac{10^3}{0.998\,278\,282 \times 30.48}$ $= 32.864\,983\,2$	$\frac{10^4}{13.595\,088\,9}$ $= 735.559\,736$	1	$\frac{9.806\,65}{10^{-1}}$ $= 98.066\,5$
	$\frac{10^4/980.665}{0.998\,278\,282 \times 30.48}$ $= 0.335\,129\,562$	$\frac{10^5/980.665}{13.595\,088\,9}$ $= 7.500\,621\,88$	$\frac{10^{-1}}{9.806\,65}$ $= 0.010\,197\,162$	1

TABLE B8.2 Conversion Factors for Specific Volume

To obtain → / Multiply, by ↓	$\frac{ft^3}{lbm}$	$\frac{in^3}{lbm}$	$\frac{US\ gal}{lbm}$	$\frac{liter}{kg}$	$\frac{m^3}{kg}$
$\frac{ft^3}{lbm}$	1	1 728	$\frac{1\,728}{231}$ = 7.480 519 48	$\frac{30.48^3}{453.592\,37}$ = 62.427 960 6	$\frac{30.48^3 \times 10^{-6}}{0.453\,592\,37}$ = 0.062 427 960 6
$\frac{in^3}{lbm}$	$\frac{1.0}{1\,728}$ = 0.000 578 703 704	1	$\frac{1.0}{231}$ = 0.004 329 004 33	$\frac{2.54^3}{453.592\,37}$ = 0.036 127 292 0	$\frac{2.54^3 \times 10^{-6}}{0.453\,592\,37}$ = 0.000 036 127 292
$\frac{US\ gal}{lbm}$	$\frac{231}{1\,728}$ = 0.133 680 556	231	1	$\frac{231 \times 2.54^3}{453.592\,37}$ = 8.345 404 45	$\frac{231 \times 2.54^3 \times 10^{-6}}{0.453\,592\,37}$ = 0.008 345 404 45
$\frac{liter}{kg}$	$\frac{453.592\,37}{30.48^3}$ = 0.016 018 463 4	$\frac{453.592\,37}{2.54^3}$ = 27.679 904 7	$\frac{453.592\,37}{231 \times 2.54^3}$ = 0.119 826 427	1	0.001
$\frac{m^3}{kg}$	$\frac{0.453\,592\,37}{30.48^3 \times 10^{-6}}$ = 16.018 463 4	$\frac{0.453\,592\,37}{2.54^3 \times 10^{-6}}$ = 27 679.904 7	$\frac{0.453\,592\,37}{231 \times 2.54^3 \times 10^{-6}}$ = 119.826 427	1000	1

Source: Ref. 5.

Also, the interconversion between heat expressed by British thermal units, and work, expressed by $ft \cdot lb_f$, is required in this dimensional system (J = 778.169 $ft \cdot lb_f/Btu$).

International System. The International System "SI" (Systeme international d'unites) of units is founded on four base units: meter (m) of length, kilogram (kg) of mass, second of time, and kelvin (K) of thermodynamic temperature.[6] It must be explained that the Celsius temperature scale is the commonly used scale for temperature measurements in metric systems. The Celsius scale is not in itself part of the SI, but a difference of one degree on that scale equals one kelvin. Zero on the thermodynamic scale is fixed by convention to be 273.15 kelvin (K) below zero degrees Celsius.

When two or more units expressed in *base* SI units are multiplied or divided as required to obtain derived quantities, the result is a *unit value.* No numerical constant (dimensional conversion factor) is introduced. Such units are called *coherent.* SI is a coherent system of units. For some derived SI units, special names and symbols exist; for example, force expressed by 1 $kg \cdot m/s^2$ has a derived name *newton* (N), pressure expressed by 1 N/m^2 has a derived name *pascal* (Pa), energy expressed by 1 $N \cdot m$ has a derived name *joule* (J), power expressed by 1 J/s has a derived name *watt* (W), and so forth. There are certain units outside the SI which are recognized as having to be retained because of their practical importance. As is general practice in the power industry worldwide, 1 bar = 10^5 Pa = 100 kPa (pressure expressed in bars is close to that expressed in *atmospheres*) has been used as the unit for absolute pressure. The symbol p_g is recommended for gauge pressure, defined as $p_g = p - p_{amb}$, where p_{amb} is the ambient pressure. Other recognized units outside the SI are: 1 minute (min) = 60 s, 1 hour (h) = 60 min, 1 day (d) = 24 h, 1 litre (l) = 1 dm^3, 1 tonne (t) = 10^3 kg.

In order to avoid large or small numerical values, decimal multiples of the SI units are added to the coherent system within the framework of the SI. They are formed by means of the following SI prefixes. Some of them are: G (giga) = 10^9, M (mega) = 10^6, k (kilo) = 10^3, h (hecto) = 10^2, d (deci) = 10^{-1}, c (centi) = 10^{-2}, m (milli) = 10^{-3}, μ (micro) = 10^{-6}. Therefore, for example, the compound prefix for 1 mm^2/s = $(10^{-3}\ m)^2/s$ is equal to 10^{-6} m^2/s. The choice of the appropriate multiple of an SI unit is governed by convenience. The multiple chosen for a particular application is the one which will lead to numerical values within a practical range. For certain quantities in particular applications, the same multiple is customarily used; for example, the millimeter is used for dimensions in most mechanical engineering drawings.

Because of the increasing international commitment of U.S. engineering, industry, and commerce, the need for an accelerated growth in acceptance of the capability of SI units by the engineering profession is recognized. However, for this edition of the *Piping Handbook,* the English units of the engineering system of dimensions and units have been recommended. As a result of this recommendation, all equations in this chapter are written in such a way that the dimensional conversion factors (g_c, J) must be used. In parentheses, after all, the corresponding SI units and calculated values are presented. For those who must deliver calculation results in other units, useful conversion factors are given in Tables B8.1 through B8.6.

Click for view of double page spread

TABLE B8.3 Conversion Factors for Specific Enthalpy and Specific Entropy

To obtain → / Multiply, by ↓	$\frac{\text{Btu}}{\text{lbm}}$	$\frac{\text{ft} \times \text{lbf}}{\text{lbm}}$	$\frac{\text{hp} \times \text{hr}}{\text{lbm}}$
$\frac{\text{Btu}}{\text{lbm}}$	1	$\frac{2.326 \times 10^7}{980.665 \times 30.48}$ $= 778.169\,262$	$\frac{2.326}{980.665 \times 30.48 \times 0.198}$ $= 3.930\,147\,79 \times 10^{-4}$
$\frac{\text{ft} \times \text{lbf}}{\text{lbm}}$	$\frac{980.665 \times 30.48}{2.326 \times 10^7}$ $= 0.001\,285\,067\,46$	1	$\frac{1.0}{1\,980\,000}$ $= 5.050\,505\,05 \times 10^{-7}$
$\frac{\text{hp} \times \text{hr}}{\text{lbm}}$	$\frac{980.665 \times 30.48 \times 0.198}{2.326}$ $= 2\,544.433\,58$	1 980 000	1
$\frac{\text{lbf/in.}^2}{\text{lbm/ft}^3}$	$\frac{980.665 \times 30.48 \times 144}{2.326 \times 10^7}$ $= 0.185\,049\,715$	144	$\frac{144}{1\,980\,000}$ $= 7.272\,727\,27 \times 10^{-5}$
$\frac{\text{kp} \times \text{m}}{\text{g}}$	$\frac{9.806\,65}{2.326}$ $= 4.216\,100\,60$	$\frac{10^5}{30.48}$ $= 3\,280.839\,90$	$\frac{1.0}{30.48 \times 19.8}$ $= 0.001\,656\,989\,85$
$\frac{\text{kcal}}{\text{g}}$	$\frac{4\,186.8}{2.326}$ $= 1800$	$\frac{4\,186.8 \times 10^7}{980.665 \times 30.48}$ $= 1\,400\,704.67$	$\frac{4\,186.8 \times 10^3}{980.665 \times 30.48 \times 198}$ $= 0.707\,426\,602$
$\frac{\text{kJ}}{\text{kg}}$	$\frac{1.0}{2.326}$ $= 0.429\,922\,614$	$\frac{10^7}{980.665 \times 30.48}$ $= 334.552\,563$	$\frac{10^3}{980.665 \times 30.48 \times 198}$ $= 1.689\,659\,41 \times 10^{-4}$

Source: Ref. 5.

$\frac{\text{lbf/in.}^2}{\text{lbm/ft}^3}$	$\frac{\text{kp} \times \text{m}}{\text{g}}$	$\frac{\text{kcal}}{\text{g}}$	$\frac{\text{kJ}}{\text{kg}}$
$\frac{2.326 \times 10^7}{980.665 \times 30.48 \times 144}$ $= 5.403\ 953\ 21$	$\frac{2.326}{9.806\ 65}$ $= 0.237\ 185\ 991$	$\frac{2.326}{4\ 186.8}$ $= 5.555\ 555\ 6 \times 10^{-4}$	2.326
$\frac{1.0}{144}$ $= 0.069\ 444\ 444\ 4$	30.48×10^{-5} $= 0.000\ 304\ 8$	$\frac{980.665 \times 30.48}{4\ 186.8 \times 10^7}$ $= 7.139\ 263\ 69 \times 10^{-7}$	$980.665 \times 30.48 \times 10^{-7}$ $= 0.002\ 989\ 066\ 920$
$\frac{1\ 980\ 000}{144}$ $= 13\ 750$	30.48×19.8 $= 603.504$	$\frac{980.665 \times 30.48}{4\ 186.8/0.198}$ $= 1.413\ 574\ 21$	$\frac{980.665 \times 30.48 \times 198}{1000}$ $= 5\ 918.352\ 50$
1	$30.48 \times 144 \times 10^{-5}$ $= 0.043\ 891\ 2$	$\frac{980.665 \times 30.48 \times 144}{4\ 186.8 \times 10^7}$ $= 1.028\ 053\ 97 \times 10^{-4}$	$\frac{980.665 \times 30.48 \times 144}{10^7}$ $= 0.430\ 425\ 636$
$\frac{10^5}{30.48 \times 144}$ $= 22.783\ 610\ 4$	1	$\frac{9.806\ 65}{4\ 186.8}$ $= 0.002\ 342\ 278\ 11$	9.806 65
$\frac{4\ 186.8 \times 10^7}{980.665 \times 30.48 \times 144}$ $= 9\ 727.115\ 78$	$\frac{4\ 186.8}{9.806\ 65}$ $= 426.934\ 784$	1	4 186.8
$\frac{10^7}{980.665 \times 30.48 \times 144}$ $= 2.323\ 281\ 69$	$\frac{1.0}{9.806\ 65}$ $= 0.101\ 971\ 621$	$\frac{1.0}{4\ 186.8}$ $= 2.388\ 458\ 97 \times 10^{-4}$	1

Click for view of double page spread

TABLE B8.4 Conversion Factors for Specific Entropy, Specific Heat, and Gas Constant

To obtain → / Multiply, by ↓	$\frac{Btu}{lbm \times R}$	$\frac{ft \times lbf}{lbm \times R}$	$\frac{kw \times hr}{lbm \times R}$
$\frac{Btu}{lbm \times R}$	1	$\frac{2.326 \times 10^7}{980.665 \times 30.48}$ = 778.169 262	$\frac{2.326 \times 453.592\,37}{3\,600\,000}$ = 0.000 293 071 070
$\frac{ft \times lbf}{lbm \times R}$	$\frac{980.665 \times 30.48}{2.326 \times 10^7}$ = 0.001 285 067 46	1	$\frac{453.592\,37 \times 30.48}{3.6 \times 10^{13}/980.665}$ = $3.766\,160\,97 \times 10^{-7}$
$\frac{kw \times hr}{lbm \times R}$	$\frac{3\,600\,000}{2.326 \times 453.592\,37}$ = 3 412.141 63	$\frac{3.6 \times 10^{13}/980.665}{453.592\,37 \times 30.48}$ = 2 655 223.73	1
$\frac{bar \times cm^3}{g \times K}$	$\frac{1.0}{41.868}$ = 0.023 884 589 7	$\frac{10^6}{30.48 \times 980.665 \times 9/5}$ = 18.586 253 5	$\frac{453.592\,37}{3.6 \times 10^7 \times 9/5}$ = $6.999\,882\,25 \times 10^{-6}$
$\frac{kcal}{g \times K}$	1000	$\frac{2\,326 \times 10^7}{980.665 \times 30.48}$ = 778 169.262	$\frac{2\,326 \times 453.592\,37}{3\,600\,000}$ = 0.293 071 070
$\frac{kp \times m}{g \times K}$	$\frac{9.806\,65}{4.186\,8}$ = 2.342 278 11	$\frac{10^5}{30.48 \times 9/5}$ = 1 822.688 83	$\frac{980.665 \times 453.592\,37}{3.6 \times 10^8 \times 9/5}$ = 0.000 686 453 953
$\frac{kJ}{kg \times K}$	$\frac{1.0}{4.186\,8}$ = 0.238 845 897	$\frac{10^7 \times 5/9}{980.665 \times 30.48}$ = 185.862 535	$\frac{453.592\,37}{3.6 \times 10^6 \times 9/5}$ = $6.999\,882\,25 \times 10^{-5}$

Source: Ref. 5.

$\frac{\text{bar} \times \text{cm}^3}{\text{g} \times \text{K}}$	$\frac{\text{kcal}}{\text{g} \times \text{K}}$	$\frac{\text{kp} \times \text{m}}{\text{g} \times \text{K}}$	$\frac{\text{kJ}}{\text{kg} \times \text{K}}$
41.868	0.001	$\frac{4.186\,8}{9.806\,65}$ $= 0.426\,934\,784$	4.186 8
$\frac{30.48 \times 980.665 \times 9/5}{10^6}$ $= 0.053\,803\,204\,6$	$\frac{980.665 \times 30.48}{2\,326 \times 10^7}$ $= 1.285\,067\,46 \times 10^{-6}$	$30.48 \times 10^{-5} \times 9/5$ $= 0.000\,548\,64$	$\frac{980.665 \times 30.48 \times 10^{-7}}{5/9}$ $= 0.005\,380\,320\,46$
$\frac{3.6 \times 10^7 \times 9/5}{453.592\,37}$ $= 142\,859.546$	$\frac{3\,600\,000}{2\,326 \times 453.592\,37}$ $= 3.412\,141\,63$	$\frac{3.6 \times 10^8 \times 9/5}{980.665 \times 453.592\,37}$ $= 1.456\,761\,95$	$\frac{3.6 \times 10^6 \times 9/5}{453.592\,37}$ $= 14\,285.954\,6$
1	$\frac{1.0}{41\,868}$ $= 2.388\,458\,97 \times 10^{-5}$	$\frac{1.0}{98.066\,5}$ $= 0.010\,197\,1621$	0.1
41 868	1	$\frac{4\,186.8}{9.806\,65}$ $= 426.934\,784$	4 186.8
98.066 5	$\frac{9.806\,65}{4\,186.8}$ $= 0.002\,342\,278\,11$	1	9.806 65
10	$\frac{1.0}{4\,186.8}$ $= 0.000\,238\,845\,897$	$\frac{1.0}{9.806\,65}$ $= 0.101\,971\,621$	1

TABLE B8.5 Conversion Factors for (Dynamic) Viscosity

To obtain → / Multiply, by ↓	Pa × s *	$\frac{\text{lbf} \times \text{sec}}{\text{ft}^2}$	$\frac{\text{lbm}}{\text{ft} \times \text{sec}}$	$\frac{\text{lbm}}{\text{hr} \times \text{ft}}$	$\frac{\text{g}}{\text{cm} \times \text{sec}}$ (poise)	$\frac{\text{kg}}{\text{m} \times \text{sec}}$
Pa × s *	1	$\frac{(0.3048)^2}{9.80665 \times 0.453\,59237}$ = 0.020 885 4342	$\frac{0.3048}{0.453\,592\,37}$ = 0.671 968 975	$\frac{0.3048 \times 3600}{0.453\,592\,37}$ = 2419.088 31	10	1
$\frac{\text{lbf sec}}{\text{ft}^2}$	$\frac{9.806\,65 \times 0.453\,592\,37}{(0.3048)^2}$ = 47.880 259 0	1	$\frac{980.665}{30.48}$ = 32.174 048 6	$\frac{980.665 \times 3\,600}{30.48}$ = 115 826.575	$\frac{980.665 \times 453.592\,37}{30.48^2}$ = 478.802 590	$\frac{980.665 \times 453.592\,37}{10 \times 30.48^2}$ = 47.880 259 0
$\frac{\text{lbm}}{\text{ft} \times \text{sec}}$	$\frac{0.453\,592\,37}{0.3048}$ = 1.488 163 94	$\frac{30.48}{980.665}$ = 0.031 080 950 2	1	3 600	$\frac{453.592\,37}{30.48}$ = 14.881 639 4	$\frac{453.592\,37}{304.8}$ = 1.488 163 94
$\frac{\text{lbm}}{\text{hr} \times \text{ft}}$	$\frac{0.453\,592\,37}{0.3048 \times 3600}$ = 0.413 378 873 × 10^{-3}	$\frac{30.48}{980.665 \times 3\,600}$ = 8.633 597 27 × 10^{-6}	$\frac{1.0}{3\,600}$ = 0.000 277 777 778	1	$\frac{453.592\,37}{30.48 \times 3\,600}$ = 0.004 133 788 73	$\frac{453.592\,37}{304.8 \times 3\,600}$ = 0.000 413 378 873
$\frac{\text{g}}{\text{cm} \times \text{sec}}$ (poise)	0.1	$\frac{30.48^2}{980.665 \times 453.592\,37}$ = 0.002 088 543 42	$\frac{30.48}{453.592\,37}$ = 0.067 196 897 5	$\frac{3\,600 \times 30.48}{453.592\,37}$ = 241.908 831	1	0.1
$\frac{\text{kg}}{\text{m} \times \text{sec}}$	1	$\frac{10 \times 30.48^2}{980.665 \times 453.592\,37}$ = 0.020 885 434 2	$\frac{304.8}{453.592\,37}$ = 0.671 968 975	$\frac{10 \times 3\,600 \times 30.48}{453.592\,37}$ = 2 419.088 31	10	1

* SI Units for ASME use.
Source: Ref. 5.

TABLE B8.6 Conversion Factors for Kinematic Viscosity

To obtain → / Multiply, by ↓	$\frac{m^2}{s}$ *	$\frac{ft^2}{sec}$	$\frac{\frac{cm^2}{sec}}{(stoke)}$	$\frac{cm^2}{hr}$	$\frac{m^2}{hr}$
$\frac{m^2}{s}$ *	1	$\frac{1.0}{(0.3048)^2} = 10.763\ 9104$	$(100)^2 = 10\ 000$	$(100)^2 \times 3600 = 36 \times 10^6$	3600
$\frac{ft^2}{sec}$	$(0.3048)^2 = 0.092\ 903\ 04$	1	$(30.48)^2 = 929.030\ 4$	$(30.48)^2 \times 3\ 600 = 3\ 344\ 509.440\ 000$	$(0.304\ 8)^2 \times 3\ 600 = 334.450\ 944\ 000$
$\frac{cm^2}{sec}$ (Stoke)	$\frac{1.0}{(100)^2} = 10^{-4}$	$\frac{1.0}{(30.48)^2} = 0.001\ 076\ 391\ 04$	1	3 600	$\frac{3\ 600}{(100)^2} = 0.36$
$\frac{cm^2}{hr}$	$\frac{1.0}{(100)^2 \times 3600} = 27.777\ 777\ 8 \times 10^{-9}$	$\frac{1.0}{(30.48)^2 \times 3600} = 0.2\ 989\ 975\ 12 \times 10^{-6}$	$\frac{1.0}{3\ 600} = 0.000\ 277\ 777\ 778$	1	$\frac{1.0}{(100)^2} = 0.000\ 1$
$\frac{m^2}{hr}$	$\frac{1.0}{3600} = 277.777\ 778 \times 10^{-6}$	$\frac{1.0}{(0.3048)^2 \times 3\ 600} = 2.989\ 975\ 12 \times 10^{-3}$	$\frac{(100)^2}{3\ 600} = 2.777\ 777\ 78$	$(100)^2 = 10\ 000$	1

* SI Units for ASME use.
Source: Ref. 5.

THEORETICAL BACKGROUND

Some basic fluid properties used in this chapter are discussed in the following paragraphs; for more detailed information see Refs. 1 and 2 listed at the end of this chapter.

Viscosity

It is an experimental fact that a fluid in immediate contact with a solid boundary has the same velocity as the boundary itself. For the case of Fig. B8.2, in which a fluid separates closely spaced parallel plates, the force F applied to the upper, moving plate, is directly proportional to the surface area A of the upper plate and its velocity w, and is inversely proportional to the distance y between the plates. The last statement is expressed in the form of Newton's law of viscosity:

$$F = \mu \frac{Aw}{y} \tag{B8.2}$$

in which μ is the proportionality factor and is called the *dynamic* (*or absolute*) *viscosity* of the fluid. *Poise* (P) and *stokes* (St) are special names for CGS units. They and their multiples should not be used together with SI units. Conversion factors for dynamic viscosity, from other units, are presented in Table B8.5.

Water at 68°F (20°C) has a dynamic viscosity of 1.002 centipoise (0.001 $N \cdot s/m^2$ or $Pa \cdot s$). The viscosity of liquids decreases with increasing temperature, but the viscosity of a gas increases with increasing temperature.

Because the shear stress is $\tau = F/A$, Equation (B8.2) could be written as $\tau = \mu\, w/y$ or in differential form as $\tau = \mu\, dw/dy$. The ratio dw/dy is called the *rate of angular deformation* of the fluid for one-dimensional flow. *Viscosity* is that property

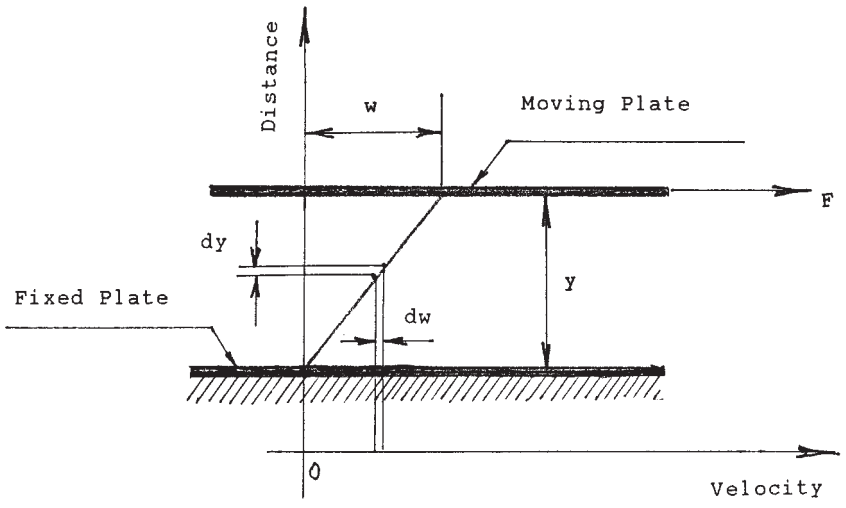

FIGURE B8.2 Established steady state velocity profile in the fluid.

of a fluid by virtue of which it offers resistance to shear. In Newtonian fluids, there is a linear relation between the applied shear stress and the resulting rate of deformation [μ = constant in Eq. (B8.2)]. In non-Newtonian fluids, this relationship is not linear. Gases and thin liquids tend to be Newtonian fluids, while thick hydrocarbons may be non-Newtonian.

The kinematic viscosity ν, which is the ratio of dynamic viscosity to mass density ρ, is:

$$\nu = \frac{\mu}{\rho} g_c \tag{B8.3}$$

Conversion factors for kinematic viscosity are presented in Table B8.6.

Pressure Variation in a Static Fluid

The static pressure existing at a point within a fluid body is known also as the *hydrostatic pressure.* In the case of gaseous fluids, the density of the fluid column is relatively small unless great vertical heights are involved. In such cases the average density of fluid should be used for the static pressure calculation. With denser fluids such as liquids, the increase in pressure due to depth within the liquid can be of great significance. When applied to the two-fluid mixture in a container filled with a gas at the pressure p_1, as shown in Fig. B8.3, the expression for static pressure at a horizontal plane located at distance z below the free surface is:

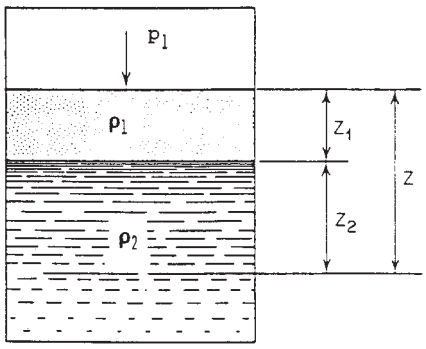

FIGURE B8.3 Hydrostatic pressure in two-fluid system.

$$p = p_1 + \frac{g}{g_c}(\rho_1 z_1 + \rho_2 z_2) \tag{B8.4}$$

Standard atmospheric pressure is defined as that pressure produced by a column of mercury of 760 mm length at a mercury density of 13.5950889 g/cm^3 at 32°F (0°C) and at an acceleration due to gravity of g_n = 32.174 ft/s^2 (9.80665 m/s^2). On this basis, then:

1 standard atmosphere = 14.6959488 psia (1.01325 bar)

For many engineering calculations, it is sufficiently accurate to use 14.7 psia as being equivalent to 1 standard atmosphere.

Continuity

Applying the law of conservation of mass to a flow process yields a mass balance, or continuity equation. The mass balance in physical processes is that the mass of

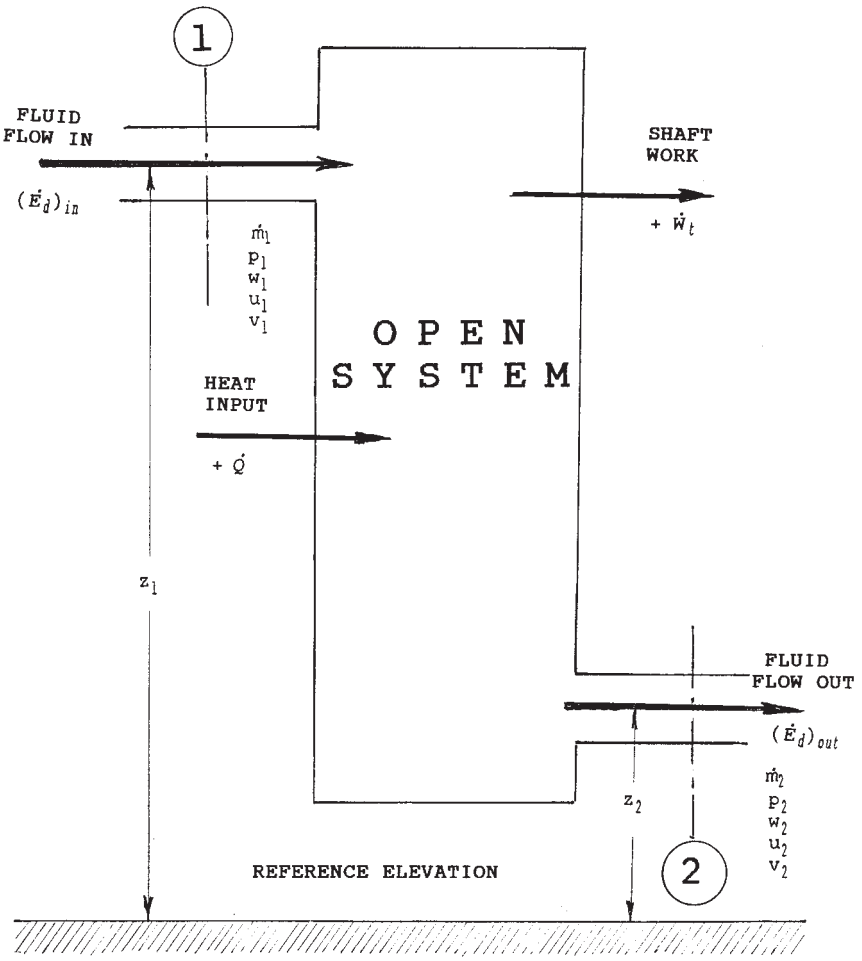

FIGURE B8.4 Energy balance in an open system.

substance added to the system is equal to the mass subtracted from the system, plus accumulation of any mass in the system.

Conservation of Energy

The first law of thermodynamics can be formulated as the principle of conservation of energy[2]:

$$E_{\text{in}} = \Delta E_s + E_{\text{out}} \tag{B8.5}$$

where E_{in} represents all types of energy added to the system within a defined control boundary during a specified time interval, ΔE_s is the change in the total energy of the system, and E_{out} represents all kinds of energy substracted from the system in the same time interval. In the steady-flow system $\Delta E_s = 0$, and

$$\dot{E}_{in} = \dot{E}_{out} \tag{B8.6}$$

With fluid flow through the system, as shown in Fig. B8.4, the energy entering (or leaving) this system by a duct (or a pipeline) will consist of potential (external), kinetic, and internal energy of the fluid, and also the external pumping work, the energy transmitted by a pump to force the fluid to flow continuously across the boundary of the system. Then the total rate of steady-flow energy transported in a duct (or a pipe) is:

$$\dot{E}_d = \dot{m}\left[\frac{1}{J}\left(pv + \frac{w^2}{2g_c} + \frac{g}{g_c}z\right) + u\right] \tag{B8.7}$$

where $J = 778.169$ (ft · lb$_f$)/Btu (dimensional conversion factor).

The sum of the specific internal energy u and the external pumping work $(p\ v)/J$

$$h = u + \frac{pv}{J} \tag{B8.8}$$

is called the *specific enthalpy*. Since, *u, p,* and *v* are all properties, then also *h* must be a state function or a property. The sum defined by h_o:

$$h_0 = h + \frac{w^2}{2g_c J} \tag{B8.9}$$

is called the *stagnation enthalpy*.

Then, for a steady state flow system presented in Fig. B8.4, with a mass flow rate of $\dot{m} = \dot{m}_1 = \dot{m}_2$, by using Eqs. (B8.6), (B8.7), and (B8.8) the following is found:

$$\dot{Q} - \frac{\dot{W}_t}{J} = \dot{m}\left[(h_2 - h_1) + \frac{(w_2^2 - w_1^2)}{2Jg_c} + \frac{g}{Jg_c}(z_2 - z_1)\right] \tag{B8.10}$$

In a differential form, per unit mass, this equation may be modified by introducing an internal friction term (viscous friction and other irreversible phenomena distinguishing a real fluid from an ideal one) to yield the following equation, which is known from literature as the *mechanical energy balance:*

$$d\left(\frac{w^2}{2g_c}\right) + \frac{g}{g_c}dz + vdp = -d'w_t - d'w_f \tag{B8.11}$$

where $d'w_t$ = specific "technical work" transmitted across the boundary of the system,

$d'w_f$ = specific work done against fluid friction.

STEADY SINGLE-PHASE INCOMPRESSIBLE FLOW IN PIPING

Characteristics of Incompressible Flow

Although there is no such thing in reality as an incompressible fluid, this term is applied to liquids. Yet sound waves, which are really pressure waves, travel through liquids. This is an evidence of the elasticity of liquids. In problems involving water hammer, it is necessary to consider the compressibility of the liquid. The compressibility of a liquid is expressed by its bulk modulus of elasticity which influences the wave speed in the liquid.

It should be explained here that when density changes of compressible fluids (gases or steam) are gradual and do not change by more than about 10 percent, the flow may be treated as incompressible with the use of an average density.

Bernoulli's equation is a special case of Eq. (B8.11) applied to nonviscous, incompressible fluids (ideal fluid) which do not exchange shaft work with surroundings:

$$v = \frac{1}{\rho} = \text{const}, \qquad d'w_f = 0, \qquad \text{and} \qquad d'w_t = 0$$

In real flow systems, however, the Bernoulli equation must be suplemented by a frictional head loss H_f (expressed in feet of a column of the fluid) and by a pump-head term H_p (total dynamic head, TDH, expressed in feet of a column of fluid). Then, for real systems the following is found:

$$\frac{w_1^2}{2g} + \frac{p_1}{\gamma} + z_1 + H_p = \frac{w_2^2}{2g} + \frac{p_2}{\gamma} + z_2 + H_f \tag{B8.12}$$

The frictional head loss is given by the following D'Arcy-Weisbach equation:

$$H_f = \frac{\Delta p}{\gamma} = f\frac{w^2}{2g}\frac{L}{D} \tag{B8.13}$$

and the corresponding pressure drop (expressed in lb_f/ft^2) is:

$$\Delta p = f\rho\frac{w^2}{2g_c}\frac{L}{D} \tag{B8.14}$$

where f is the D'Arcy-Weisbach friction factor, which is four times the Fanning friction factor used in some publications.

For laminar flow:

$$f = \frac{64}{\text{Re}} \tag{B8.15}$$

which plots as a straight line with a slope (-1) on the Moody diagram (Fig. B8.5). It applies to all roughnesses, as the head loss in laminar flow is independent of wall roughness. The Reynolds number is:

$$\text{Re} = \frac{Dw}{\nu} \tag{B8.16}$$

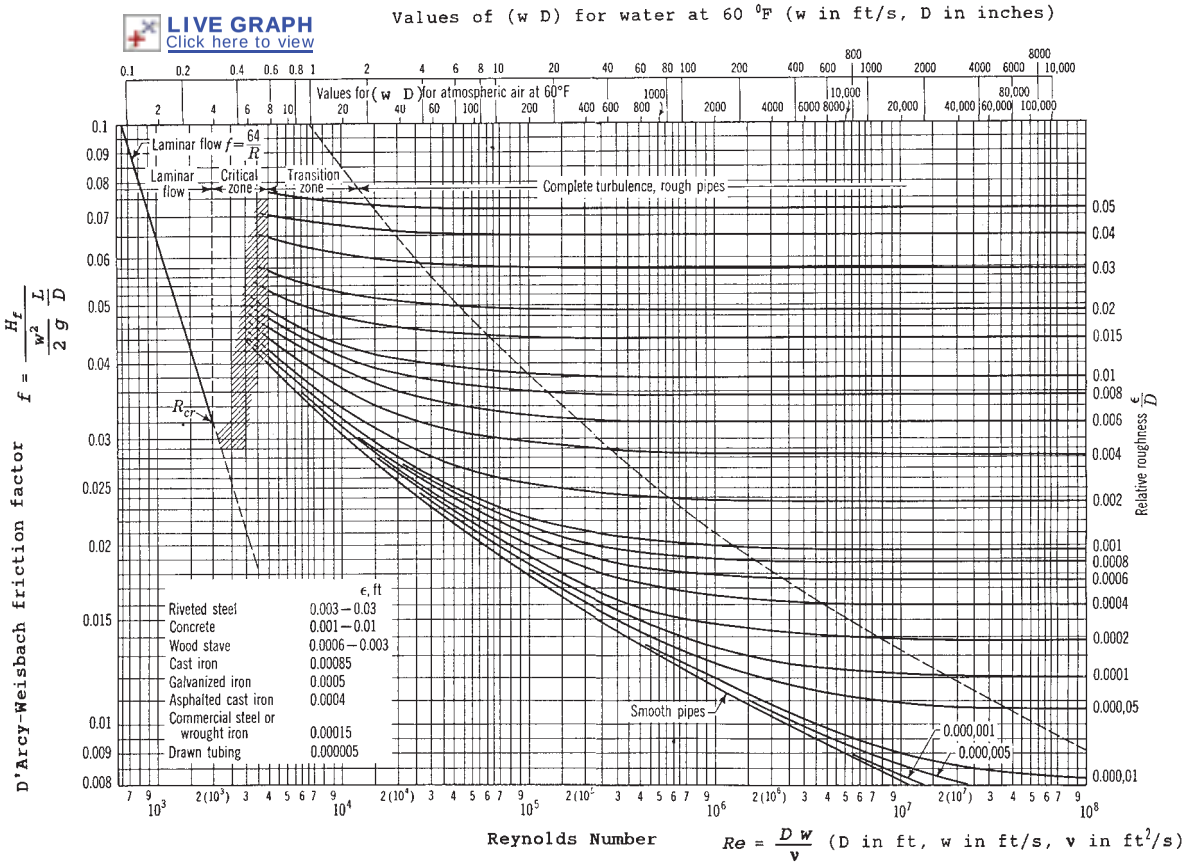

FIGURE B8.5 Moody diagram. (*From Ref. 1.*)

Expressions for calculating the loss of pressure in turbulent flow are based upon experimental data. An empirical transition function for commercial pipes for the region between smooth pipes and the complete turbulence zone (see the Moody diagram) has been developed by Colebrook:

$$\frac{1}{\sqrt{f}} = -0.86 \ln \left(\frac{\varepsilon/D}{3.7} + \frac{2.51}{\mathrm{Re}\sqrt{f}} \right) \tag{B8.17}$$

where the absolute roughness ε, expressed in feet (millimeters), is used as a measure of pipe wall irregularities of commercial pipes. Formula (B8.17) is the basis for the Moody diagram in the ''transition zone'' flow. The Moody diagram is widely accepted for hand calculations. For computerized calculations of the pressure drop, however, the Colebrook equation is built into the software.

Pressure losses which occur in piping systems due to bends, elbows, joints, valves, and so forth are called *form losses.* Recommended values of local flow resistance coefficients (K-factors) may be found in Refs. 7 and 8. Form losses may also be expressed in terms of the equivalent length L_e of pipe that has the same pressure-head loss for the same flow rate; thus

$$f \frac{L_e}{D} \frac{w^2}{2g} = K \frac{w^2}{2g} \tag{B8.18}$$

After solving for L_e:

$$L_e = \frac{K D}{f} \tag{B8.19}$$

Applications: Water Systems

General Design Considerations. Water system design requirements and design parameters are developed in the system descriptions which include piping and instrumentation diagrams (P&IDs), descriptions of the system individual components (pumps, valves, heat exchangers, etc.), design flow rates, valve alignments, control valve operation, and pipe sizes. Pipe sizes are determined by evaluation of water velocities in the system. Selection of velocities must consider many factors including:

- Pipe material
- Water quality
- System flow balance requirements
- Economic evaluation of pipe cost versus pumping costs
- Available pump head
- Water hammer prevention

Typical water flow velocities in ft/s (m/s) for various applications based on general industry practices are shown in Table B8.7.

A steady-state analysis of a water system is generally performed twice. The first calculation is needed to obtain data required for the purchase of the system components. This initial analysis is performed after the system description and

TABLE B8.7 Typical Water Flow Velocities

Condenser pump suction	3 ft/s (1 m/s)
Condenser pump discharge	10 ft/s (3 m/s)
Booster pump discharge	10 ft/s (3 m/s)
Feed pump suction (no deaerator)	10 ft/s (3 m/s)
(For systems with deaerators, the downcomer sizes should be optimized with a pump NPSH decay in mind—see section ''Transient Flow Analysis'')	
Feed pump discharge	20–25 ft/s (6–7.5 m/s)
Circulating water system	≤9 ft/s (3 m/s)
General service	5–10 ft/s (1.5–3 m/s)

Source: Stone & Webster

general arrangement drawings have been issued. The initial analysis proceeds as follows:

1. Issue the system description and general arrangement drawings.
2. Develop a preliminary piping layout based on P&IDs and general arrangement drawings.
3. Determine the system operating mode or modes (valve lineup, number of pumps, etc.) which are critical for equipment purchase.
4. Calculate the pressure drop in the piping for design flow rates.
5. Develop a system resistance curve.
6. Calculate the flow balance in branching systems.
7. Revise the system description (if required) to achieve desired system flow balance.
8. Develop a revised system resistance curve (if required).
9. Calculate values of parameters required for the purchase of system components (pump head, system pressures, control valve pressure drop, etc.).

The final steady-state hydraulic analysis of a system is usually performed after major equipment has been purchased and piping drawings have been prepared. This analysis is to confirm acceptable operation for all operating modes by reconciling the as-built piping and installed equipment with the initial analysis.

The final analysis proceeds as follows:

1. Determine the pressure drop in the system based on piping drawings and equipment suppliers data for design flow rates (if required).
2. Develop system resistance curves (if required).
3. Plot pump curves on the system resistance curve to determine the system flow rates.
4. Compare design flow rates with calculated flow rates for all operating modes.

Due to problems which occur during construction, the as-built drawings often differ from the piping drawings. In most instances, these changes are minor and do not affect the results of the analysis. Should any major changes occur during construction, the effect on the analysis results would need to be evaluated.

Piping Configurations. Piping systems may be arranged in series, in parallel, or as branching pipes. For pipes in series, the total pressure head loss is the sum of head losses in the pipe sections, and the flow rate is the same at all sections. For pipes in parallel, the pressure head loss is the same for each flow path, and the total flow rate is the sum of flows in parallel sections. For branching pipes, the analyst must combine the above two principles. The total energy at a junction must be the same for all branches of the pipe.

Analysis of a piping system begins with a determination of the pressure drop (pressure head loss) due to friction losses, form losses (in various types of piping components) and pressure losses in equipment for the design flow rate. For ease in evaluating the total system performance, the head loss should be calculated for each pipe branch separately. The manual head loss calculations often are done on pressure drop sheets. Calculations of head loss should include a schematic sketch of the piping layout. The calculation should be a clear record of the design basis for head loss calculations in order that as the design evolves, the significance of pipe changes is apparent. A second head loss calculation may be required if the pipeline is expected to operate at flow rates considerably different from the design flow rate.

Having calculated the head loss in each branch of the system for the design flow rate, the performance of the entire system can be calculated. System resistance curves, flow balances, pump design points, and system pressures are some of the products of the system analysis.

The complexity of the system analysis depends on the number of pipes in series, pipes in parallel, and pipe branches. Obviously the greater the number of pipes, the more complex the analysis becomes. The analysis is done either by manual calculation or by computer analysis. Computerized calculations are preferable.

Manual calculations are suited for relatively simple piping systems. Manual analysis with the use of graphs provides an easy method for analyzing systems with a number of pipes in parallel, pipes in series, and branching pipes. This technique is based on the assumption that head loss varies with the square of velocity. Table B8.8 presents flow data for water through various sizes of Schedule 40 steel pipe.

The hydraulic grade line (HGL) and energy grade line (EGL) are two useful engineering tools in the hydraulic design of any system in which a liquid is in a dynamic state.[1] The graphical representation with respect to any selected datum, of the static head for each point along the pipe under consideration as ordinate, plotted against distance along the pipe as the abscissa is called the *hydraulic grade line.* Similar graphical representation of the total pressure (or Bernoulli head: static + dynamic), as described by Eq. (B8.12), is called the *energy grade line.* Figure B8.6 illustrates the HGL and EGL for a sample system.

Economic Optimization of Line Sizes. The objective of this subject is balancing the savings in cost obtained by reduction in the size of the piping diameter against the increased cost of pumping equipment and power necessary to provide for increased pressure drop.

For given flows, as the pipe diameter decreases, the flow velocity increases, which decreases the cost of erected piping, including fittings, hangers, supports, and labor as represented by cost *a* in Fig. B8.7. However, the piping pressure drop ratio increases to the 5th power with reduction in the pipe internal diameter ratio, as shown in the accompanying table. The same is true with the pumping power, which is proportional to the pressure drop in the line, as represented by cost *b*

$d2/d1$	$(d1/d2)^5$
0.99	1.050
0.98	1.106
0.97	1.165
0.96	1.230
0.95	1.292
0.90	1.694
0.80	3.052
0.70	5.950

in Fig. B8.7. In addition, there is the cost of the pump and the pump drive, which increases as greater pumping power is required, as represented by cost *c*.

The total cost, which is the sum of these three costs ($T_{COST} = a + b + c$) in \$/year, is shown on Fig. B8.7 as reaching a minimum value at the optimum flow velocity. The analysis for each piping system should consider the optimization of flow velocity (optimum internal diameter) of the pipe under consideration. It is important to note that cost *b* depends strongly on the plant operating mode or the load factor, and on other economic indicators for a particular project. Industry data containing updated prices of equipment, piping, and labor are needed to implement this optimization procedure.

Sample Problem B8.1. What is the pressure drop $p_A - p_B$ (see Fig. B8.8), when water at 200°F (93.3°C) flows in a piping system at the rate of $\dot{m} = 450{,}200$ lb_m/h (204,207 kg/h), $p_A = 500$ psia (34.47 bar)?

Pipe Data. For 6-in nominal size, schedule 40 pipe, the internal diameter $d = 6.065$ in, $D = 0.5054$ ft, $A = 0.200$ ft^2.

Properties of Fluid. From the ASME Steam Tables software (Ref. 5) for $T = 200$°F and $p = 500$ psia, the dynamic viscosity of water (see attached computer printout, Table B8.9) is

$$\mu = 63.43 * 10^{-7}\ (lb_f \cdot s)/ft^2$$

From the same computer printout, the specific volume of water at $T = 200$°F and $p = 500$ psia is

$$v = 0.01661\ ft^3/lb_m$$

Then, the kinematic viscosity of water is [see Eq. (B8.3)]:

$$\nu = \frac{\mu}{\rho} g_c = (63.43 * 10^{-7})\,(0.01661)\,(32.174)$$

$$= 3.39 * 10^{-6}\ ft^2/s$$

The flow velocity is calculated from the continuity equation

$$w = \frac{\dot{m}}{\rho A}$$

$$\text{where } \dot{m} = \frac{450{,}200}{3600} = 125.06\ lb_m/s$$

TABLE B8.8 Flow of Water Through Schedule 40 Steel Pipe

Discharge		Pressure drop per 100 ft and velocity in Schedule 40 pipe for water at 60°F															
gal/min	ft^3/s	Velocity, ft/s	Press. drop, lb/in^2	Velocity, ft/s	Press. drop, lb/in^2	Velocity, ft/s	Press. drop, lb/in^2	Velocity, ft/s	Press. drop, lb/in^2	Velocity, ft/s	Press. drop, lb/in^2	Velocity, ft/s	Press. drop, lb/in^2	Velocity, ft/s	Press. drop, lb/in^2	Velocity, ft/s	Press. drop, lb/in^2
		⅛ in		¼ in		⅜ in		½ in									
0.2	0.000446	1.13	1.86	0.616	0.359												
0.3	0.000668	1.69	4.22	0.924	0.903	0.504	0.159	0.317	0.061	¾ in							
0.4	0.000891	2.26	6.98	1.23	1.61	0.672	0.345	0.422	0.086								
0.5	0.00111	2.82	10.5	1.54	2.39	0.840	0.539	0.528	0.167	0.301	0.033						
0.6	0.00134	3.39	14.7	1.85	3.29	1.01	0.751	0.633	0.240	0.361	0.041						
0.8	0.00178	4.52	25.0	2.46	5.44	1.34	1.25	0.844	0.408	0.481	0.102	1 in		1¼ in			
1	0.00223	5.65	37.2	3.08	8.28	1.68	1.85	1.06	0.600	0.602	0.155	0.371	0.048			1½ in	
2	0.00446	11.29	134.4	6.16	30.1	3.36	6.58	2.11	2.10	1.20	0.526	0.743	0.164	0.429	0.044		
3	0.00668			9.25	64.1	5.04	13.9	3.17	4.33	1.81	1.09	1.114	0.336	0.644	0.090	0.473	0.043
4	0.00891			12.33	111.2	6.72	23.9	4.22	7.42	2.41	1.83	1.49	0.565	0.858	0.150	0.630	0.071
5	0.01114	2 in				8.40	36.7	5.28	11.2	3.01	2.75	1.86	0.835	1.073	0.223	0.788	0.104
6	0.01337	0.574	0.044	2½ in		10.08	51.9	6.33	15.8	3.61	3.84	2.23	1.17	1.29	0.309	0.946	0.145
8	0.01782	0.765	0.073			13.44	91.1	8.45	27.7	4.81	6.60	2.97	1.99	1.72	0.518	1.26	0.241
10	0.02228	0.956	0.108	0.670	0.046			10.56	42.4	6.02	9.99	3.71	2.99	2.15	0.774	1.58	0.361
15	0.03342	1.43	0.224	1.01	0.094	3 in				9.03	21.6	5.57	6.36	3.22	1.63	2.37	0.755
20	0.04456	1.91	0.375	1.34	0.158	0.868	0.056	3½ in		12.03	37.8	7.43	10.9	4.29	2.78	3.16	1.28
25	0.05570	2.39	0.561	1.68	0.234	1.09	0.083	0.812	0.041	4 in		9.28	16.7	5.37	4.22	3.94	1.93
30	0.06684	2.87	0.786	2.01	0.327	1.30	0.114	0.974	0.056			11.14	23.8	6.44	5.92	4.73	2.72
35	0.07798	3.35	1.05	2.35	0.436	1.52	0.151	1.14	0.704	0.882	0.041	12.99	32.2	7.51	7.90	5.52	3.64
40	0.08912	3.83	1.35	2.68	0.556	1.74	0.192	1.30	0.095	1.01	0.052	14.85	41.5	8.59	10.24	6.30	4.65
45	0.1003	4.30	1.67	3.02	0.668	1.95	0.239	1.46	0.117	1.13	0.064			9.67	12.80	7.09	5.85
50	0.1114	4.78	2.03	3.35	0.839	2.17	0.288	1.62	0.142	1.26	0.076	5 in		10.74	15.66	7.88	7.15
60	0.1337	5.74	2.87	4.02	1.18	2.60	0.406	1.95	0.204	1.51	0.107			12.89	22.2	9.47	10.21
70	0.1560	6.70	3.84	4.69	1.59	3.04	0.540	2.27	0.261	1.76	0.143	1.12	0.047			11.05	13.71
80	0.1782	7.65	4.97	5.36	2.03	3.47	0.687	2.60	0.334	2.02	0.180	1.28	0.060			12.62	17.59
90	0.2005	8.60	6.20	6.03	2.53	3.91	0.861	2.92	0.416	2.27	0.224	1.44	0.074	6 in		14.20	22.0
100	0.2228	9.56	7.59	6.70	3.09	4.34	1.05	3.25	0.509	2.52	0.272	1.60	0.090	1.11	0.036	15.78	26.9
125	0.2785	11.97	11.76	8.38	4.71	5.43	1.61	4.06	0.769	3.15	0.415	2.01	0.135	1.39	0.055	19.72	41.4
150	0.3342	14.36	16.70	10.05	6.69	6.51	2.24	4.87	1.08	3.78	0.580	2.41	0.190	1.67	0.077		
175	0.3899	16.75	22.3	11.73	8.97	7.60	3.00	5.68	1.44	4.41	0.774	2.81	0.253	1.94	0.102		
200	0.4456	19.14	28.8	13.42	11.68	8.68	3.87	6.49	1.85	5.04	0.985	3.21	0.323	2.22	0.130	8 in	
225	0.5013	...	...	15.09	14.63	9.77	4.83	7.30	2.32	5.67	1.23	3.61	0.401	2.50	0.162	1.44	0.043
250	0.557	...	...	...	...	10.85	5.93	8.12	2.84	6.30	1.46	4.01	0.495	2.78	0.195	1.60	0.051
275	0.6127	...	...	...	...	11.94	7.14	8.93	3.40	6.93	1.79	4.41	0.583	3.05	0.234	1.76	0.061
300	0.6684	...	...	...	...	13.00	8.36	9.74	4.02	7.56	2.11	4.81	0.683	3.33	0.275	1.92	0.072
325	0.7241	...	...	...	...	14.12	9.89	10.53	4.09	8.19	2.47	5.21	0.797	3.61	0.320	2.08	0.083
350	0.7798			...	...	...	...	11.36	5.41	8.82	2.84	5.62	0.919	3.89	0.367	2.24	0.095
375	0.8355			...	...	...	...	12.17	6.18	9.45	3.25	6.02	1.05	4.16	0.416	2.40	0.108
400	0.8912			...	...	...	...	12.98	7.03	10.08	3.68	6.42	1.19	4.44	0.471	2.56	0.121

TABLE B8.8 Flow of Water Through Schedule 40 Steel Pipe (*Continued*)

Discharge		Pressure drop per 100 ft and velocity in Schedule 40 pipe for water at 60°F															
gal/min	ft^3/s	Velocity, ft/s	Press. drop, lb/in^2	Velocity, ft/s	Press. drop, lb/in^2	Velocity, ft/s	Press. drop, lb/in^2	Velocity, ft/s	Press. drop, lb/in^2	Velocity, ft/s	Press. drop, lb/in^2	Velocity, ft/s	Press. drop, lb/in^2	Velocity, ft/s	Press. drop, lb/in^2	Velocity, ft/s	Press. drop, lb/in^2
425	0.9469			...	...	...	...	13.80	7.89	10.71	4.12	6.82	1.33	4.72	0.529	2.73	0.136
450	1.003	10 in		...	...	...	...	14.61	8.80	11.34	4.60	7.22	1.48	5.00	0.590	2.89	0.151
475	1.059	1.93	0.054			...	...	...	...	11.97	5.12	7.62	1.64	5.27	0.653	3.04	0.166
500	1.114	2.03	0.059			...	...	...	...	12.60	5.65	8.02	1.81	5.55	0.720	3.21	0.182
550	1.225	2.24	0.071			...	...	...	...	13.85	6.79	8.82	2.17	6.11	0.861	3.53	0.219
600	1.337	2.44	0.083			...	...	...	...	15.12	8.04	9.63	2.55	6.66	1.02	3.85	0.258
650	1.448	2.64	0.097	12 in		...	...	...	...	...	...	10.43	2.98	7.22	1.18	4.17	0.301
700	1.560	2.85	0.112	2.01	0.047			...	...	...	...	11.23	3.43	7.78	1.35	4.49	0.343
750	1.671	3.05	0.127	2.15	0.054	14 in		...	...	...	...	12.03	3.92	8.33	1.55	4.81	0.392
800	1.782	3.25	0.143	2.29	0.061			...	...	...	...	12.83	4.43	8.88	1.75	5.13	0.443
850	1.894	3.46	0.160	2.44	0.068	2.02	0.042	...	...	...	...	13.64	5.00	9.44	1.96	5.45	0.497
900	2.005	3.66	0.179	2.58	0.075	2.13	0.047	...	...	...	...	14.44	5.58	9.99	2.18	5.77	0.554
950	2.117	3.86	0.198	2.72	0.083	2.25	0.052			...	...	15.24	6.21	10.55	2.42	6.09	0.613
1000	2.228	4.07	0.218	2.87	0.091	2.37	0.057	16 in		...	...	16.04	6.84	11.10	2.68	6.41	0.675
1100	2.451	4.48	0.260	3.15	0.110	2.61	0.068			...	...	17.65	8.23	12.22	3.22	7.05	0.807
1200	2.674	4.88	0.306	3.44	0.128	2.85	0.080	2.18	0.042	...	...	...	...	13.33	3.81	7.70	0.948
1300	2.896	5.29	0.355	3.73	0.150	3.08	0.093	2.36	0.048	...	...	...	...	14.43	4.45	8.33	1.11
1400	3.119	5.70	0.409	4.01	0.171	3.32	0.107	2.54	0.055					15.55	5.13	8.98	1.28
1500	3.342	6.10	0.466	4.30	0.195	3.56	0.122	2.72	0.063	18 in				16.66	5.85	9.62	1.46
1600	3.565	6.51	0.527	4.59	0.219	3.79	0.138	2.90	0.071					17.77	6.61	10.26	1.65
1800	4.010	7.32	0.663	5.16	0.276	4.27	0.172	3.27	0.088	2.58	0.050			19.99	8.37	11.54	2.08
2000	4.456	8.14	0.808	5.73	0.339	4.74	0.209	3.63	0.107	2.87	0.060	20 in		22.21	10.3	12.82	2.55
2500	5.570	10.17	1.24	7.17	0.515	5.93	0.321	4.54	0.163	3.59	0.091					16.03	3.94
3000	6.684	12.20	1.76	8.60	0.731	7.11	0.451	5.45	0.232	4.30	0.129	3.46	0.075	24 in		19.24	5.59
3500	7.798	14.24	2.38	10.03	0.982	8.30	0.607	6.35	0.312	5.02	0.173	4.04	0.101			22.44	7.56
4000	8.912	16.27	3.08	11.47	1.27	9.48	0.787	7.26	0.401	5.74	0.222	4.62	0.129	3.19	0.052	25.65	9.80
4500	10.03	18.31	3.87	12.90	1.60	10.67	0.990	8.17	0.503	6.46	0.280	5.20	0.162	3.59	0.065	28.87	12.2
5000	11.14	20.35	4.71	14.33	1.95	11.85	1.21	9.08	0.617	7.17	0.340	5.77	0.199	3.99	0.079	...	
6000	13.37	24.41	6.74	17.20	2.77	14.23	1.71	10.89	0.877	8.61	0.483	6.93	0.280	4.79	0.111	...	
7000	15.60	28.49	9.11	20.07	3.74	16.60	2.31	12.71	1.18	10.04	0.652	8.08	0.376	5.59	0.150	...	
8000	17.82	...	...	22.93	4.84	18.96	2.99	14.52	1.51	11.47	0.839	9.23	0.488	6.38	0.192	...	
9000	20.05	...	...	25.79	6.09	21.34	3.76	16.34	1.90	12.91	1.05	10.39	0.608	7.18	0.242	...	
10000	22.28	...	...	28.66	7.46	23.71	4.61	18.15	2.34	14.34	1.28	11.54	0.739	7.98	0.294	...	
12000	26.74	...	...	34.40	10.7	28.45	6.59	21.79	3.33	17.21	1.83	13.85	1.06	9.58	0.416	...	
14000	31.19	...	...	...	...	33.19	8.89	25.42	4.49	20.08	2.45	16.16	1.43	11.17	0.562	...	
16000	35.65	...	...	...	...	...	...	29.05	5.83	22.95	3.18	18.47	1.85	12.77	0.723	...	
18000	40.10	...	...	...	...	...	...	32.68	7.31	25.82	4.03	20.77	2.32	14.16	0.907	...	
20000	44.56	...	...	...	...	...	...	36.31	9.03	28.69	4.93	23.08	2.86	15.96	1.12	...	

Useful conversion of units:

1 inch = 25.4 mm; 1 ft = 0.3048 m; 1 ft^3 = 0.02832 m^3; $t_C = \frac{5}{9}(t_F - 32)$; for pressure conversions to other units see Table B8.1.

Note: For calculations for pipes other than Schedule 40, see explanation in Table B8.14.

Note: For pipe lengths other than 100 ft, the pressure drop is proportional to the length. Thus, for 50 ft of pipe, the pressure drop is approximately one-half the value given in the table ... for 300 ft, three times the given value, etc. Velocity is a function of the cross-sectional flow area; thus, it is constant for a given flow rate and is independent of pipe length.

Source: Ref. 7.

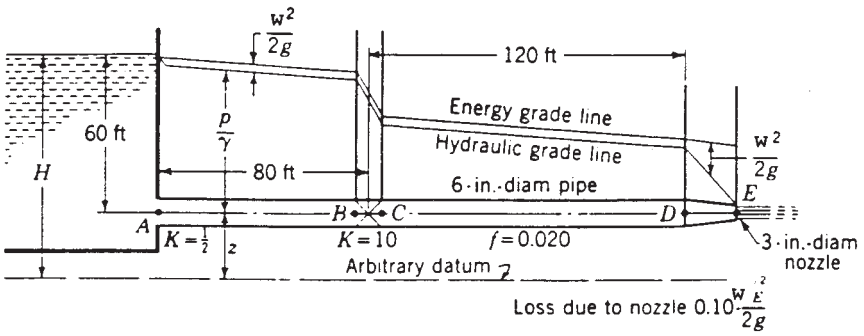

FIGURE B8.6 Hydraulic and energy grade lines. (*From Ref. 1.*)

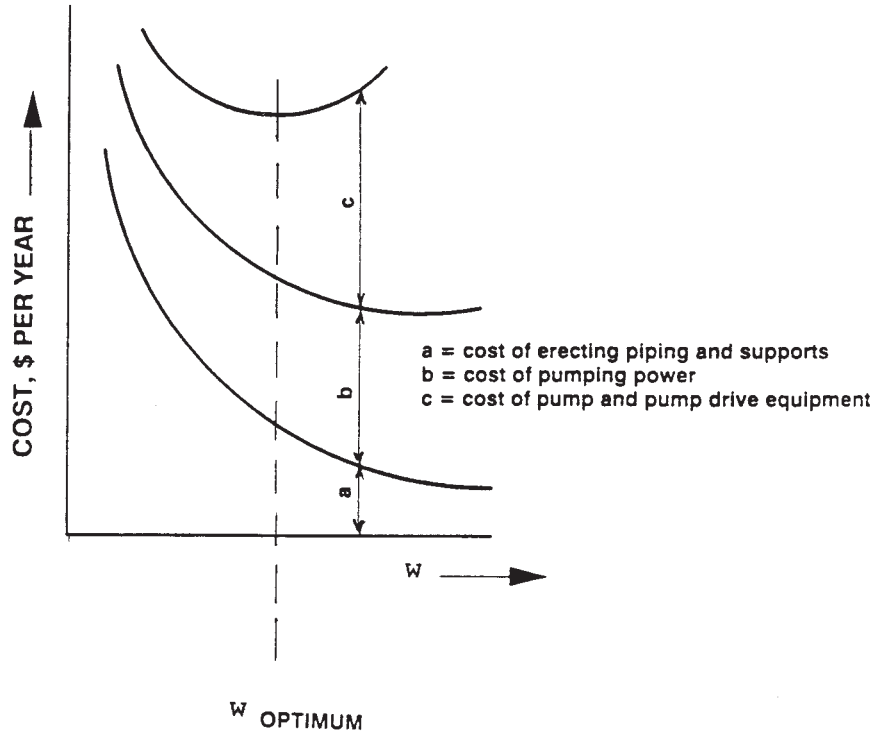

FIGURE B8.7 Flow velocity optimization plot.

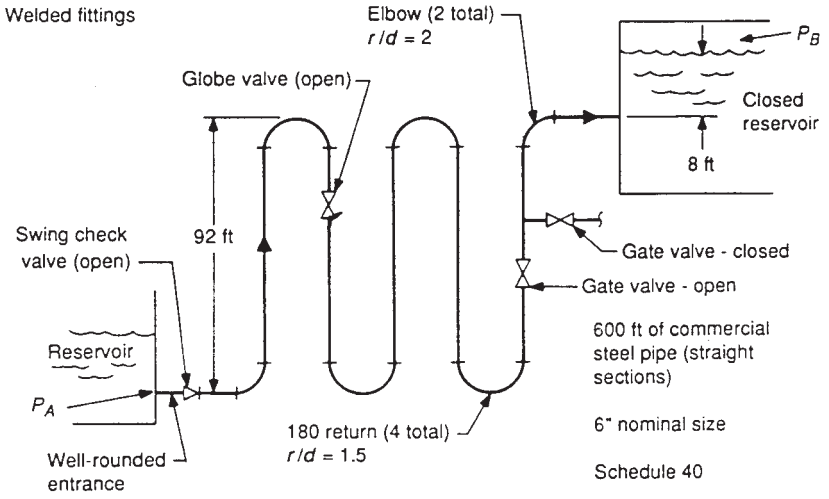

FIGURE B8.8 Reference for sample problem B8.1.

TABLE B8.9 Computer Printout of Steam/Water Properties

STEAM PROPERTIES		INPUT	*	RESULTS
ABS. PRESSURE,	bar	.0000		34.4738
	psia	500.0000		500.0000
TEMPERATURE,	C	.0000		93.3333
	F	200.0000		200.0000
ENTHALPY,	kJ/kg	.0000		393.5460
	Btu/lbm	.0000		169.1943
ENTROPY,	kJ/(kg.K)	.000000		1.228453
	Btu/(lbm.R)	.000000		.293411
SPEC.VOLUME	m3/kg	.000000		.001037
	ft3/lbm	.000000		.016609
QUALITY,	decimal	.000000		-1.000000
DYNAM. VISC	N.s/m2	.000000000		.000303681
	lbf.s/ft2	.000000000		.000006343

UNITS FOR INPUT: UNT = 1-SI, 2-BRITISH * 1995/TJS

UNT	PRESSURE	TEMPERAT	ENTHALPY	ENTROPY	QUALITY

Then:

$$w = \frac{125.06}{0.200} 0.01661 = 10.39 \text{ ft/s}$$

Using Eq. (B8.16), the Reynolds number is

$$\text{Re} = \frac{Dw}{\nu} = \frac{(0.5054)\,(10.39)}{3.39 * 10^{-6}} = 1.549 * 10^{6}$$

D'Arcy-Weisbach Friction Factor. For commercial steel pipe from Ref. 7, the relative roughness is

$$\frac{\varepsilon}{D} = 0.00015/0.5054 = 0.0003$$

and the friction factor in zone of complete turbulence is

$$f_T = 0.015$$

From Eq. (B8.17), using, for example, the Newton-Raphson method for solving equations [or using the Moody diagram, Fig. (B8.5)], for calculated values of Re and ε/D, the D'Arcy-Weisbach friction factor, f, is found:

$$f = 0.0154$$

Flow Resistance Coefficients[7]:

Local disturbance	$K(f_T = 0.015)$
Entrance	$K = 0.04$
4 180° turns	$(4)(22.18\ f_T) = 1.33$
1 globe valve (open)	$340\ f_T = 5.10$
1 tee flow through run	$20\ f_T = 0.33$
1 swing check valve (open)	$100\ f_T = 1.50$
2 long radius elbows	$(2)(14 f_T) = 0.42$
1 gate valve (open)	$8\ f_T = 0.12$
Exit	$K = 1.00$
	$\sum K = 9.77$

Total Resistance

$$\begin{aligned} K_{\text{tot}} &= \sum K + f\,\frac{L}{D} \\ &= 9.77 + 0.0154\,\frac{600}{0.5054} \\ &= 28.05 \end{aligned}$$

''Friction'' Pressure Drop in Pipe. From Eqs. (B8.14) and (B8.18):

$$\Delta p = K_{\text{tot}}\,\rho\,\frac{w^2}{2g_c}$$

$$= 28.05\,\frac{(10.39)^2}{(0.01661)(2)(32.174)}$$

$$= 2833.08\,\frac{\text{lb}_\text{f}}{\text{ft}^2}$$

$$= \frac{2833.08}{144} = 19.67 \text{ psi}$$

Pressure Difference $p_A - p_B$. From Bernoulli's equation (Eq. B8.12 with $H_f = 0$ and $H_p = 0$):

$$\frac{\rho_A\,w_A^2}{2g_c} + p_A + \frac{g}{g_c}\,z_A\,\rho_A$$

$$= \frac{\rho_B\,w_B^2}{2g_c} + p_B + \frac{g}{g_c}\,z_B\,\rho_B + \Delta\rho$$

$$\text{Assuming } \rho_A = \rho_B = \rho \quad \text{and} \quad g = 32.174\,\frac{\text{ft}}{\text{s}^2}$$

$$p_A - p_B = \frac{g}{g_c}\,(z_B - z_A)\,\frac{\rho}{144} + \Delta p$$

$$= \frac{100}{(144)(0.01661)} + 19.67 = 61.48 \text{ psi } (4.24 \text{ bar})$$

Applications: Oil and Other Liquid Systems

The calculation of oil flow through pipes is a much more complicated process than a similar calculation for water flow. Water properties are well-defined and many, including viscosity, are nearly constant within liquid temperature ranges, whereas oil is quite different. No two oils have the same physical properties, and any given oil is subject to important physical changes at expected variable temperatures. When considering oil flow in pipes, the most important variable physical property is viscosity.

Ordinary crude oil is not a homogeneous liquid; it is a very complex fluid composed of compounds of carbon and hydrogen which exist in petroleum in a wide variety of combinations. Physical properties change accordingly, and they also change as a result of temperature variations. Therefore, this handbook assumes that the user will research the fluid of interest in other sourcebooks (such as the *Petroleum Processing Handbook*[9]) to determine important properties including density and viscosity.

The ''Viscosity'' subsection in this handbook refers to Tables B8.5 and B8.6 for conversion among several common units of viscosity. The special names and symbols for derived CGS units (such as dyne, erg, poise, and stokes) should not be used

TABLE B8.10 Kinematic Viscosity Conversion Table (Centistokes to Engler, Saybolt, and Redwood units)

Centistokes	Engler degrees	Saybolt seconds at 130°F	Redwood seconds at 140°F	Centistokes	Engler degrees	Saybolt seconds at 130°F	Redwood seconds at 140°F	Centistokes	Engler degrees	Saybolt seconds at 130°F	Redwood seconds at 140°F
2.0	1.140	32.66	30.95	18.0	2.644	89.37	78.45	41.0	5.465	190.6	168.3
2.5	1.182	34.46	32.20	19.0	2.755	93.48	82.10	42.0	5.590	195.1	172.3
3.0	1.224	36.07	33.45	20.0	2.870	97.69	85.75	43.0	5.720	199.6	176.4
3.5	1.266	37.67	34.70	21.0	2.984	101.9	89.50	44.0	5.845	204.2	180.4
4.0	1.308	39.17	35.95	22.0	3.100	106.2	93.25	45.0	5.975	208.8	184.5
4.5	1.350	40.78	37.20	23.0	3.215	110.5	97.05	46.0	6.105	213.4	188.5
5.0	1.400	42.38	38.45	24.0	3.335	114.8	100.9	47.0	6.235	218.0	192.6
5.5	1.441	43.98	39.80	25.0	3.455	119.1	104.7	48.0	6.365	222.6	196.6
6.0	1.481	45.59	41.05	26.0	3.575	123.5	108.6	49.0	6.495	227.2	200.7
6.5	1.521	47.19	42.40	27.0	3.695	127.9	112.5	50.0	6.630	231.8	204.7
7.0	1.563	48.79	43.70	28.0	3.820	132.4	116.5	52.0	6.890	241.1	212.8
7.5	1.605	50.44	45.00	29.0	3.945	136.8	120.4	54.0	7.106	250.3	221.0
8.0	1.653	52.10	46.35	30.0	4.070	141.2	124.4	56.0	7.370	259.5	229.1
8.5	1.700	53.80	47.75	31.0	4.195	145.6	128.3	58.0	7.633	268.7	237.2
9.0	1.746	55.51	49.10	32.0	4.320	150.0	132.3	60.0	7.896	277.9	245.3
9.5	1.791	57.21	50.55	33.0	4.445	154.5	136.3	62.0	8.159	287.2	253.5
10.0	1.837	58.91	52.00	34.0	4.570	159.0	140.2	64.0	8.422	296.4	261.6
11.0	1.928	62.42	55.00	35.0	4.695	163.5	144.2	66.0	8.686	305.6	269.8
12.0	2.020	66.03	58.10	36.0	4.825	168.0	148.2	68.0	8.949	314.8	277.9
13.0	2.120	69.73	61.30	37.0	4.955	172.5	152.2	70.0	9.212	324.0	286.0
14.0	2.219	73.54	64.55	38.0	5.080	177.0	156.2	72.0	9.475	333.3	294.1
15.0	2.323	77.35	67.95	39.0	5.205	181.5	160.3	74.0	9.738	342.5	302.2
16.0	2.434	81.25	71.40	40.0	5.335	186.0	164.3	75.0	9.870	347.2	306.3
17.0	2.540	85.26	74.85								

Supplementary Kinematic Viscosity Conversion Table

Centistokes.....	2	6	10	20	30	40	50	60	70
Saybolt at 100°F.....	32.60	45.50	58.80	97.50	40.9	185.7	231.4	277.4	323.4
Saybolt at 210°F.....	32.83	45.82	59.21	98.18	141.9	187.0	233.0	279.3	325.7
Redwood at 70°F.....	30.20	40.50	51.70	85.40	123.7	163.2	203.3	243.5	283.9
Redwood at 200°F.....	31.20	41.50	52.55	86.90	126.0	166.7	208.3	250.0	291.7

Temperature conversion: $t_C = \frac{5}{9}(t_F - 32)$

70°F = 21.1°C; 140°F = 60.0°C
100°F = 37.8°C; 200°F = 93.3°C
130°F = 54.5°C; 210°F = 98.9°C

TABLE B8.11 Flow of Oils Through Commercial Pipes

Size of pipe and average inside diameter, inches	Capacity, gallons per minute*	Pressure drop in pounds per square inch per 100 ft of pipe based on oils of 20° Bé gravity					
		Viscosity in Saybolt Universal seconds					
		100	200	300	400	500	600
½ 0.622	2	6.59	14.3	21.7	29.1	36.9	43.6
	5	21.1	34.8	53.4	71.5	89.5	107.0
	7	37.7	49.2	74.6	101.0	129.0	152.0
	10	69.8	85.8	107.0	144.0	177.0	217.0
	15	143.0	174.0	194.0	217.0	267.0	325.0
¾ 0.824	2	2.16	4.74	7.04	9.48	11.6	14.2
	5	5.6	11.5	17.1	23.1	28.9	35.2
	7	9.96	16.1	24.5	32.8	40.5	48.9
	10	18.4	22.3	34.9	46.0	58.5	70.9
	15	37.9	45.7	51.5	70.4	88.3	106.0
1 1.05	5	2.06	4.32	6.68	8.85	11.0	13.4
	10	5.9	8.74	13.4	17.9	22.0	26.6
	15	11.9	14.5	19.7	26.6	33.2	40.3
	20	19.7	23.8	26.8	35.4	44.1	53.5
	25	29.0	35.1	39.3	44.2	54.5	66.8
1½ 1.61	10	0.783	1.57	2.40	3.22	3.98	4.86
	20	2.61	3.17	4.85	6.52	8.02	9.70
	30	5.30	6.43	7.15	9.68	12.1	14.7
	40	8.72	10.6	11.9	12.8	16.0	19.4
	50	12.7	15.7	17.4	18.8	19.8	24.2
2 2.067	10	0.266	0.578	0.875	1.17	1.47	1.79
	20	0.79	1.15	1.75	2.34	2.92	3.52
	30	1.60	1.93	2.62	3.50	4.40	5.30
	40	2.63	3.18	3.56	4.66	5.85	7.10
	50	3.86	4.68	5.28	5.88	7.26	8.85
4 4.026	50	0.174	0.198	0.307	0.412	0.494	0.612
	100	0.550	0.668	0.744	0.810	1.01	1.22
	150	1.09	1.36	1.50	1.62	1.74	1.84
	200	1.81	2.22	2.49	2.68	2.85	2.98
	250	2.67	3.26	3.67	3.97	4.20	4.41
6 6.065	100	0.0788	0.0956	0.115	0.158	0.194	0.236
	200	0.259	0.315	0.359	0.388	0.408	0.480
	500	1.27	1.55	1.74	1.88	2.01	2.20
	700	2.29	2.80	3.15	3.36	3.60	3.78
	1000	4.24	5.21	5.82	6.32	6.68	7.05
8 8.03	200	0.0696	0.0834	0.0947	0.102	0.128	0.155
	500	0.340	0.418	0.459	0.500	0.530	0.556
	1000	1.13	1.37	1.55	1.67	1.78	1.87
	1500	2.27	2.74	3.07	3.30	3.59	3.75
	2000	3.88	4.55	5.15	5.56	5.92	6.22
12 12.05	1000	0.165	0.203	0.228	0.242	0.258	0.272
	2000	0.552	0.670	0.750	0.810	0.866	0.905
	3000	1.15	1.34	1.50	1.63	1.73	1.83
	4000	1.91	2.22	2.50	2.69	2.84	3.00
	5000	2.90	3.34	3.63	3.97	4.22	4.41

* To change capacities from gallons per minute to barrels (42 gal) per hour, multiply pressure drops by 1.43. To change from pressure drops per square inch per 100 ft to pressure drops per square inch per mile, multiply by 52.8.

Other important conversion relations:

1 US gallon = 0.00378541 m^3, 1 ft = 0.3048 m,
1 inch = 25.4 mm, 1 mile = 1609.344 m.
For pressure conversions refer to TABLE B8.1.

with the SI. Apart from these, other units which do not belong to any coherent system should be defined in the oil-related problems. For readers who must use information from various existing sources, Table B8.10 is included. Together with Tables B8.5 and B8.6, this may lead to organized, easy-to-follow SI solutions to the encountered problems, especially in determining the pressure drop or flow rate of oil through pipes.

Typical pressure drops for oil flowing through pipes ranging from ½ to 12 inches in diameter appear in Table B8.11 for fluids with a density of approximately 7.78 lb_m/U.S. gal (0.932 kg/dm^3).

Figures B8.9 through B8.15 provide pressure drops versus flow rates for fluids ranging from gasoline to those with 10,000 Seconds Saybolt Universal (SSU) viscosity through 2- to 12-in Schedule 40 pipe. To use these figures with SI units, the following conversion factors should be applied: 1 U.S. gallon = 3.78541 dm^3, 1 U.S. mile = 1.609344 km (exactly), 1000 ft = 304.8 m (exactly). For pressure conversions see Table B8.1. The *specific gravity* of a substance is the ratio of its weight to the weight of an equal volume of water at chosen standard conditions.

Usually the engineer of an oil-burning plant will know only two things regarding the fuel oil supplied to him; namely, the specific gravity and the viscosity. The specific density or specific gravity can be used to convert volume measurements of fuel oil into mass, or vice versa. Using the API gravity system devised jointly by the American Petroleum Institute and the National Bureau of Standards (NBS), the API gravity of a mixture can be readily calculated proportionately (in degrees

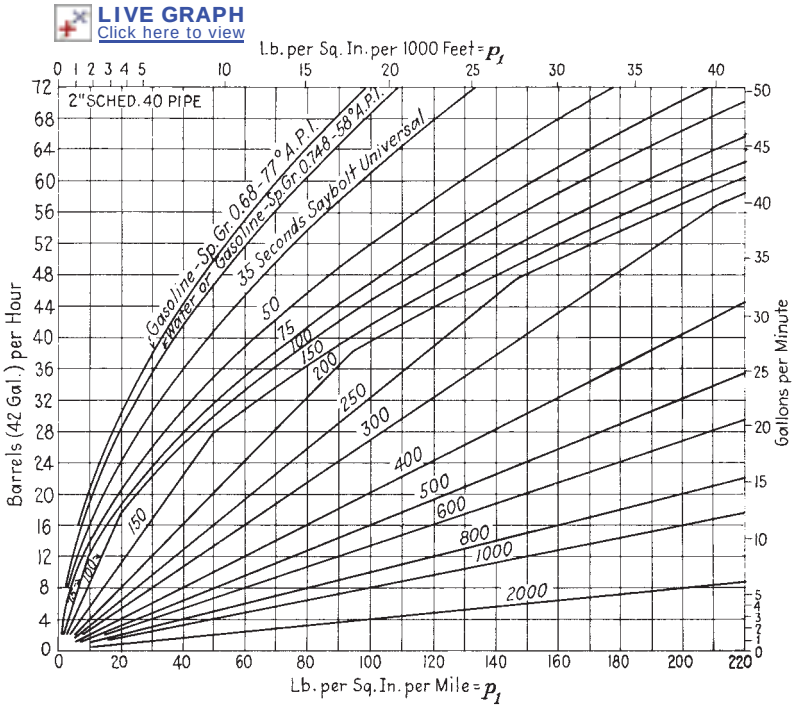

FIGURE B8.9 Pipe friction based on average Saybolt Universal viscosity and specific gravity of fluid in pipeline. Pressure drop $\Delta p = p_1 \times$ sp. gr.

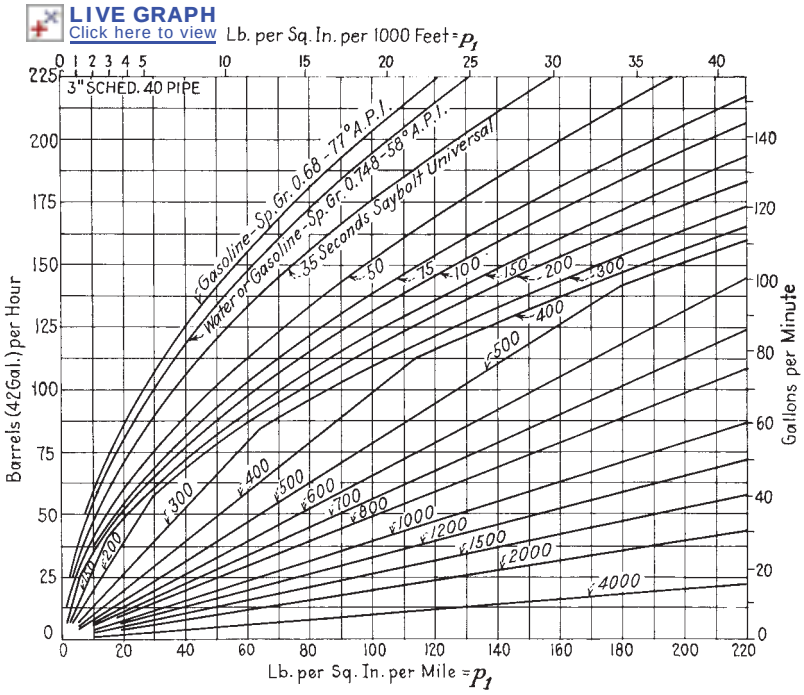

FIGURE B8.10 Pipe friction based on average Saybolt Universal viscosity and specific gravity of fluid in pipeline. Pressure drop $\Delta p = p_1 \times$ sp. gr.

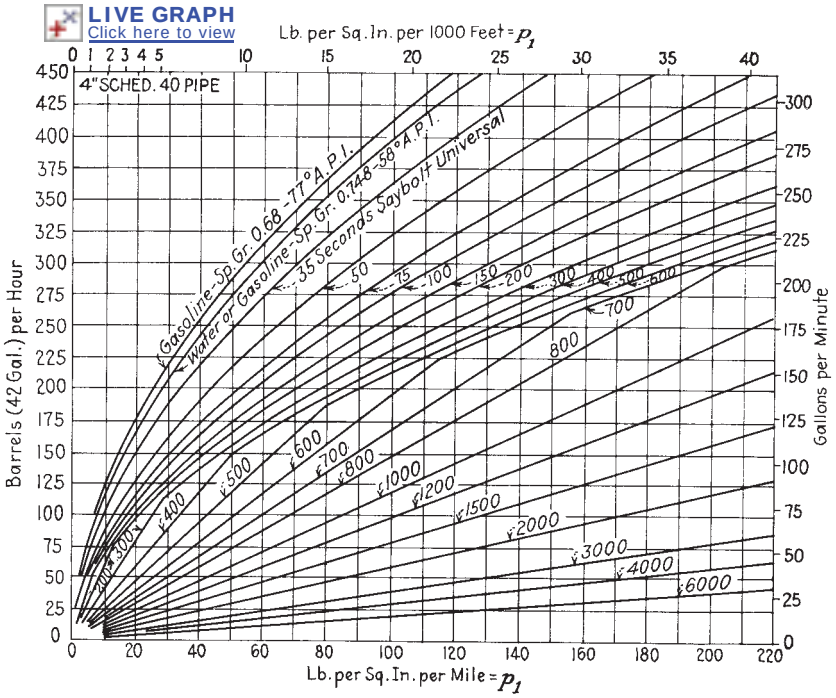

FIGURE B8.11 Pipe friction based on average Saybolt Universal viscosity and specific gravity of fluid in pipeline. Pressure drop $\Delta p = p_1 \times$ sp. gr.

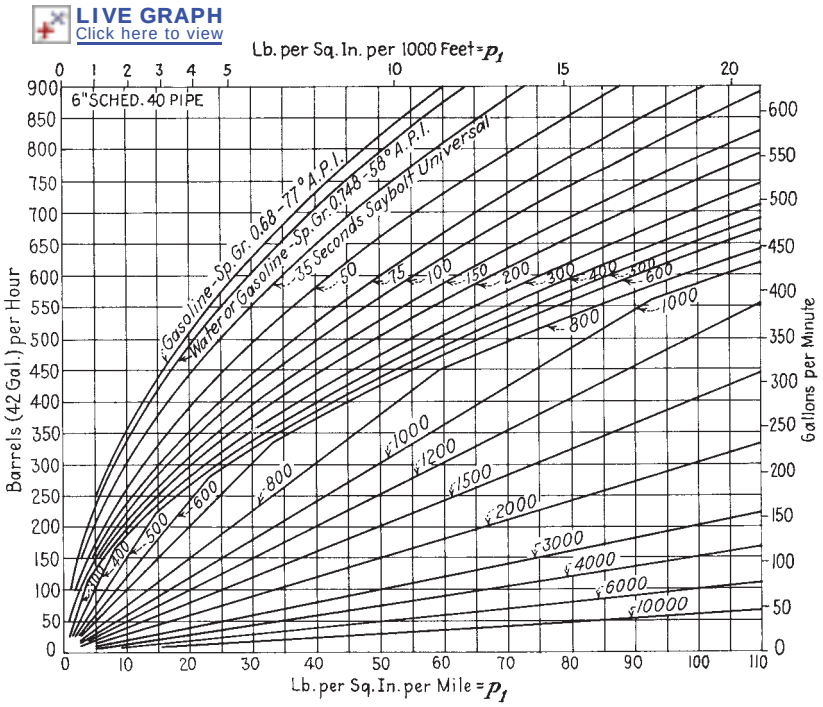

FIGURE B8.12 Pipe friction based on average Saybolt Universal viscosity and specific gravity of fluid in pipeline. Pressure drop $\Delta p = p_1 \times$ sp. gr.

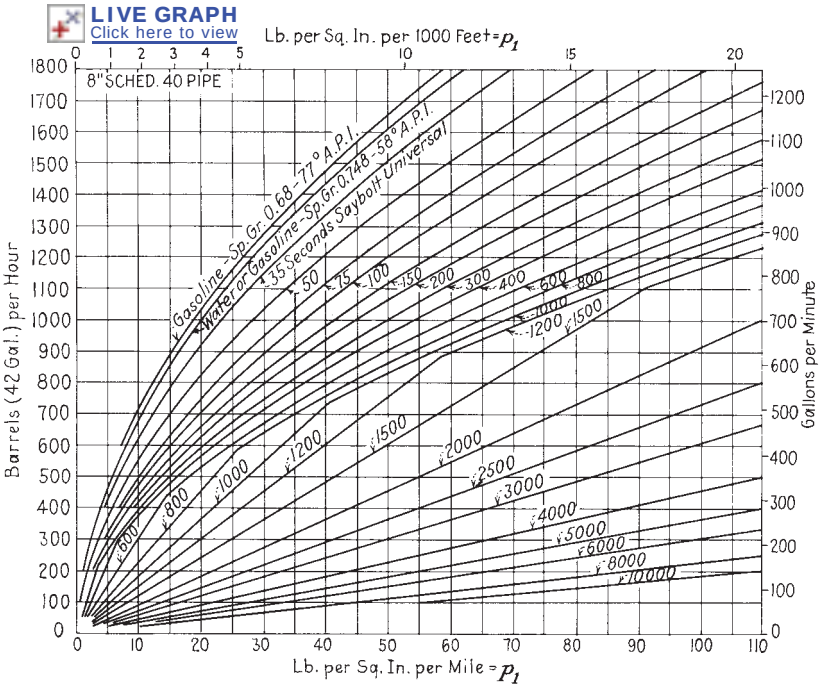

FIGURE B8.13 Pipe friction based on average Saybolt Universal viscosity and specific gravity of fluid in pipeline. Pressure drop $\Delta p = p_1 \times$ sp. gr.

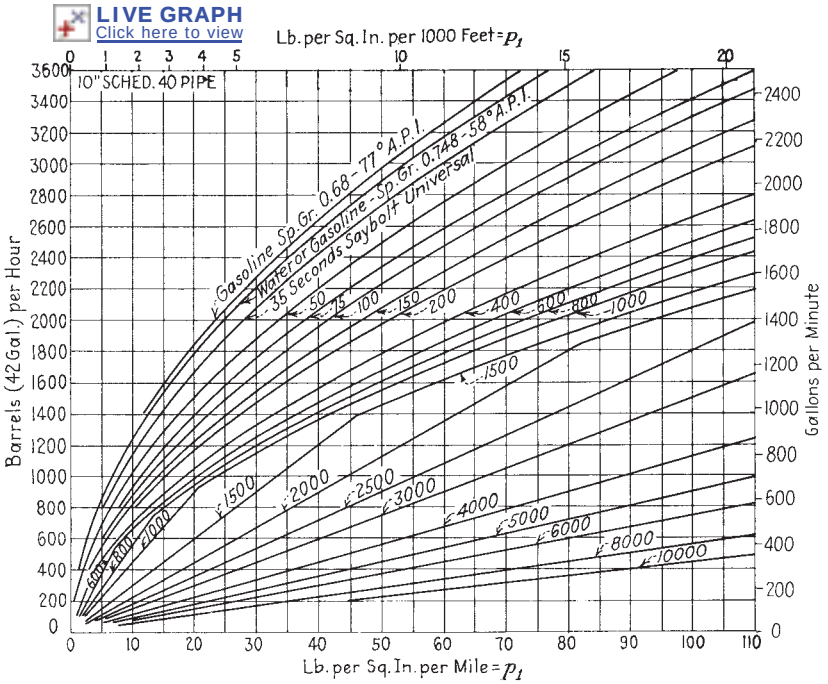

FIGURE B8.14 Pipe friction based on average Saybolt Universal viscosity and specific gravity of fluid in pipeline. Pressure drop $\Delta p = p_1 \times$ sp. gr.

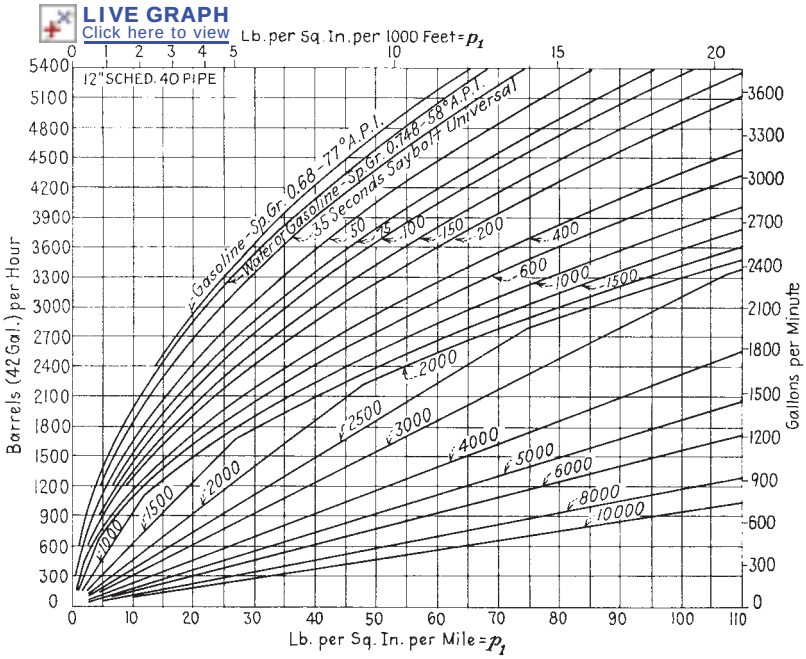

FIGURE B8.15 Pipe friction based on average Saybolt Universal viscosity and specific gravity of fluid in pipeline. Pressure drop $\Delta p = p_1 \times$ sp. gr.

API) from the respective gravities of the components. *Example:* What is the API gravity of a 40 percent mixture of a 10° API fuel and 60 percent of a 15° API fuel? Answer: $0.40 \times 10° + 0.60 \times 15° = 13°$ API.

A knowledge of viscosity and how it varies with temperature is essential for the easy handling and efficient utilization of fuel oil. Heavier fuel oils must be heated to the proper temperature in order to obtain a viscosity of 150 Saybolt Universal at the burners for the most efficient atomization. It is also important to determine to what temperature the oil should be heated in the bunkers so it can be readily pumped through the fuel oil system. Generally the maximum temperature that oil in the bunkers be heated to is 130°F (about 55°C) in an effort to reduce the viscosity for easier pumping.

When two or more oils are blended, it is necessary to determine the properties of the mixture. Several methods are available to achieve the important properties such as viscosity and most use some type of viscosity blending chart. The *Petroleum Processing Hanbook*[9] is one source of such a blending chart which is a semilogarithmic plot of kinematic viscosity versus either volume percent lower or higher viscosity liquid. A linear interpolation is used on this type of plot.

STEADY SINGLE-PHASE COMPRESSIBLE FLOW IN PIPING

Characteristics of Compressible Flow in Pipes

The term *compressible flow* implies variations in density of a fluid. These variations are the result of pressure and temperature changes from one point to another. The rate of change of density with respect to pressure is, therefore, an important parameter in the analysis of compressible flow, and it is closely connected with the velocity of sound.

Adiabatic, Constant-Area Flow with Friction. Adiabatic flow with friction is of interest in sizing safety valve discharge lines (vent lines) and other pipes where heat transfer may be neglected and where the flow may be restricted by sonic condition at the pipe exit (choked flow). Supersonic velocities will not be discussed here.

In this section, the flow of compressible gases and steam (small fluid densities) in ducts of constant cross-sectional area will be discussed. For adiabatic conditions (heat exchanged with surroundings $dQ = 0$), the energy equation for steady flow between two points, 1 and x, in a pipe may be written as follows:

$$h_x + \frac{w_x^2}{2g_c J} = h_1 + \frac{w_1^2}{2g_c J} = h_0 \tag{B8.20}$$

where h_0 is the stagnation enthalpy [see Eq. (B8.9)]. Utilizing the continuity equation:

$$\dot{G} = \frac{\dot{m}}{A} = \frac{w_x}{v_x} = \frac{w_1}{v_1} \tag{B8.21}$$

for constant values of flow rate $\dot{m}$, and area A, the following is found:

$$h_x + \left(\frac{\dot{m}}{A}\right)^2 \frac{v_x^2}{2g_c J} = h_1 + \frac{w_1^2}{2g_c J} = h_0 \tag{B8.22}$$

Equation (B8.22) represents the *Fanno line*[10] which is the locus of the conditions in a cylindrical pipe of constant diameter. Having fixed w_1 and h_1 at the starting point, the stagnation enthalpy h_0 is calculated. This enthalpy stays constant along the length L of the pipe. Choosing an arbitrary specific volume v_x, the corresponding value of h_x can be calculated from Eq. (B8.22). The intersection of v_x and h_x on the $h - s$ diagram represents a point on the Fanno line. The sonic (choked) condition at the pipe exit shown in Fig. B8.16 is defined by

$$\frac{ds}{dh} = 0 \tag{B8.23}$$

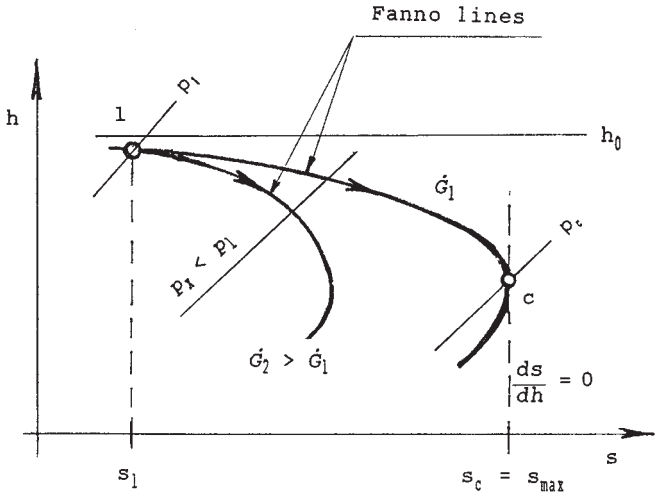

FIGURE B8.16 Fanno line on the *h-s* diagram.

Considering the work done against friction (an irreversible process with the change in entropy of the fluid within the system) and the heat generated within the fluid by internal friction during an adiabatic flow (heat exchanged with the surroundings $dq = 0$), the following expression is derived:

$$L_x = \frac{2g_c J}{f} D \int_{s_1}^{s_x} \frac{T}{w^2} ds \tag{B8.24}$$

Equation (B8.24) represents the length L_x of the pipeline, along which the pressure drops from p_1 to p_x. The described procedure yields a number of points on a Fanno line and also the coordinates of the function $T/w^2 = f(s)$. Integrating the function $T/w^2 = f(s)$ with fixed upper boundary (sonic conditions) and floating lower boundary of integration, the fluid parameters (static conditions) at any dis-

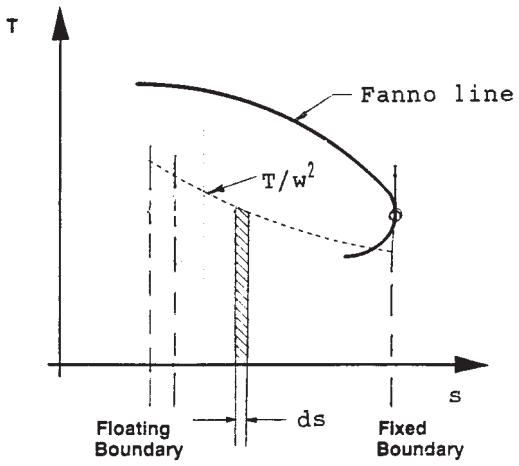

FIGURE B8.17 Integration of the function T/w^2.

tance L upstream of the sonic (choked) plane can be found (convergence on the given length L of the pipe). The procedure is explained in Fig. B8.17.

If the calculated pressure at sonic exit is lower than the receiver pressure, the additional length of the pipe required for choked conditions at the exit should be calculated. By adding this fictitious pipe length to the actual length of the pipe the "extended length" is found. This new length is now used for calculating the parameters at the start of the pipeline, after a valve, or at any distance from the choked exit.

For steam service, computerized calculations utilizing built-in steam tables (as in Ref. 5) are recommended. For most problems in gas dynamics, however, the assumption of the perfect gas law is sufficiently in accord with the properties of real gases to be acceptable.[11]

A simplified approach for frictional, adiabatic, constant-area flow (Fanno line analysis) of a perfect gas (that has constant specific heat) is presented in Ref. 11. The working formulas may be represented graphically or they may be used for computerized calculations to produce Fanno line tables for a perfect gas of any k and any assigned Ma values. As an example, see Table B8.12. It is important to notice that in Table B8.12, taken from Ref. 11, the Fanning friction factor is used (see Eq. B8.14 and lines below). Following are some of the working formulas suitable for practical computations, as presented in this reference book. The quantities marked with an asterisk (*) in written expressions (p^*, w^*, etc.) represent the values of the stream properties at the section in the pipe where Ma $= w/c = 1$ (sonic plane). Because the quantities marked with an asterisk are constants for a given adiabatic, constant-area flow, they may be regarded as convenient reference values for normalizing the equations.

Choke pressure:

$$p^* = \frac{\dot{m}}{A}\sqrt{\frac{2RT_0}{g_c k(k+1)}} \tag{B8.25}$$

TABLE B8.12 Frictional, Adiabatic, Constant-Area Flow (Fanno Line) for Perfect Gas, $k = 1.4$

Ma	T/T^*	p/p^*	p_0/p_0^*	w/w* and ρ^*/ρ	F/F^*	$4fL_{max}/D$
0.00	1.2000	∞	∞	0.00000	∞	∞
.05	1.1994	21.903	11.5914	.05476	9.1584	280.02
.10	1.1976	10.9435	5.8218	.10943	4.6236	66.922
.15	1.1946	7.2866	3.9103	.16395	3.1317	27.932
.20	1.1905	5.4555	2.9635	.21822	2.4004	14.533
.25	1.1852	4.3546	2.4027	.27217	1.9732	8.4834
.30	1.1788	3.6190	2.0351	.32572	1.6979	5.2992
.35	1.1713	3.0922	1.7780	.37880	1.5094	3.4525
.40	1.1628	2.6958	1.5901	.43133	1.3749	2.3085
.45	1.1533	2.3865	1.4486	.48326	1.2763	1.5664
.50	1.1429	2.1381	1.3399	.53453	1.2027	1.06908
.55	1.1315	1.9341	1.2549	.58506	1.1472	.72805
.60	1.1194	1.7634	1.1882	.63481	1.10504	.49081
.65	1.10650	1.6183	1.1356	.68374	1.07314	.32460
.70	1.09290	1.4934	1.09436	.73179	1.04915	.20814
.75	1.07856	1.3848	1.06242	.77893	1.03137	.12728
.80	1.06383	1.2892	1.03823	.82514	1.01853	.07229
.85	1.04849	1.2047	1.02067	.87037	1.00966	.03632
.90	1.03270	1.12913	1.00887	.91459	1.00399	.014513
.95	1.01652	1.06129	1.00215	.95782	1.00093	.003280
1.00	1.00000	1.00000	1.00000	1.00000	1.00000	0
1.05	.98320	.94435	1.00203	1.04115	1.00082	.002712
1.10	.96618	.89359	1.00793	1.08124	1.00305	.009933
1.15	.94899	.84710	1.01746	1.1203	1.00646	.02053
1.20	.93168	.80436	1.03044	1.1583	1.01082	.03364
1.25	.91429	.76495	1.04676	1.1952	1.01594	.04858
1.30	.89686	.72848	1.06630	1.2311	1.02169	.06483
1.35	.87944	.69466	1.08904	1.2660	1.02794	.08199
1.40	.86207	.66320	1.1149	1.2999	1.03458	.09974
1.45	.84477	.63387	1.1440	1.3327	1.04153	.11782
1.50	.82759	.60648	1.1762	1.3646	1.04870	.13605
1.55	.81054	.58084	1.2116	1.3955	1.05604	.15427
1.60	.79365	.55679	1.2502	1.4254	1.06348	.17236
1.65	.77695	.53421	1.2922	1.4544	1.07098	.19022
1.70	.76046	.51297	1.3376	1.4825	1.07851	.20780
1.75	.74419	.49295	1.3865	1.5097	1.08603	.22504
1.80	.72816	.47407	1.4390	1.5360	1.09352	.24189
1.85	.71238	.45623	1.4952	1.5614	1.1009	.25832
1.90	.69686	.43936	1.5552	1.5861	1.1083	.27433
1.95	.68162	.42339	1.6193	1.6099	1.1155	.28989
2.00	.66667	.40825	1.6875	1.6330	1.1227	.30499
2.05	.65200	.39389	1.7600	1.6553	1.1297	.31965
2.10	.63762	.38024	1.8369	1.6769	1.1366	.33385
2.15	.62354	.36728	1.9185	1.6977	1.1434	.34760
2.20	.60976	.35494	2.0050	1.7179	1.1500	.36091

Source: Ref. 11

Static pressure, p, in the pipe cross section where the Mach number Ma < 1, may be found from the expression:

$$\frac{p}{p^*} = \frac{1}{\text{Ma}}\sqrt{\frac{k+1}{2\left[1+(k-1)/2\text{Ma}^2\right]}} \tag{B8.26}$$

Flow velocity:

$$\frac{w}{w^*} = \text{Ma}\sqrt{\frac{k+1}{2\left[1+(k-1)/2\,\text{Ma}^2\right]}} \tag{B8.27}$$

Maximum duct length:

$$f\frac{L_{\max}}{D} = \frac{1-\text{Ma}^2}{k\text{Ma}^2} + \frac{k+1}{2k}\ln\frac{(k+1)\text{Ma}^2}{2[1+(k-1)/2\text{Ma}^2]} \tag{B8.28}$$

Equation (B8.28) gives the maximum value of $(f\,L)/D$ corresponding to any initial Mach number Ma. Notice, that for Ma = 1, the expression (B8.28) results in $(f\,L_{\max})/D = 0$. The length of duct L required for the flow to pass from a given initial Mach number Ma_1 to a given final Mach number Ma_2 may be found from the expression:

$$f\frac{L}{D} = \left[f\frac{L_{\max}}{D}\right]_{\text{Ma}_1} - \left[f\frac{L_{\max}}{D}\right]_{\text{Ma}_2} \tag{B8.29}$$

In order to find the change in some stream property, say the pressure, between the sections where the Mach numbers are Ma_1 and Ma_2 respectively, the following expression is used:

$$\frac{p_2}{p_1} = \frac{(p/p^*)_{\text{Ma}_2}}{(p/p^*)_{\text{Ma}_1}} \tag{B8.30}$$

where $(p/p^*)\text{Ma}_2$ is the value of the right-hand side of Eq. (B8.26) corresponding to Ma_2, and so forth.

Isothermal Flow in Long Pipelines. Isothermal flow with friction is of interest in connection with pipelines for transporting gas over long distances. When the lines are extremely long, there is sufficient area for heat transfer to make flow nonadiabatic and approximately isothermal, especially when the gas temperature is not much different from the temperature of the surroundings. In such cases, the flow may not be treated as incompressible and the D'Arcy-Weisbach equation cannot be used for calculating the pressure drop.

Using the assumptions of constant elevation, no work being done by the fluid, continuity, isothermal flow, and that the friction coefficient does not change with length of the pipe yields the following application equation:

$$\dot{m} = \frac{\pi}{4}\sqrt{\frac{2g_c}{fRT_1}}\sqrt{\frac{D^5}{L}p_{\text{ave}}\Delta p} \tag{B8.31}$$

For the same mass flow rate $\dot{m}$, the pipe diameter D may be decreased by increasing the average pressure p_{ave} in the pipeline and/or permitting a larger pressure drop Δp. One of the applications of Eq. (B8.31) is the economic analysis of long gas line systems requiring intermediate compression stations.

It has to be mentioned here that the Mach number

$$\mathrm{Ma} = \frac{1}{\sqrt{k}} \tag{B8.32}$$

represents a limit for continuous isothermal flow, in the same way that $Ma = 1$ represents a limit for continuous adiabatic flow.[11] The working formula for determining the maximum pipe length beyond which the continuous isothermal flow may not proceed (ideal gas approximation) is given by the following expression:

$$f\frac{L_{\max}}{D} = \frac{1 - k\mathrm{Ma}^2}{k\mathrm{Ma}^2} + \ln(k\mathrm{Ma}^2) \tag{B8.33}$$

where Ma is the Mach number at the pipe inlet. For greater lengths, choking occurs and the mass flow rate decreases.

Sample problems for this subsection are presented under ''Applications: Sample Problems B8.2–B8.7.''

Applications: Steam Systems

In a case of compressible fluids such as air or steam, when density changes are small the fluid may be considered as incompressible. Therefore, all design rules described in earlier sections are applicable to this case. For steam and gas systems, where the fluid density is small, static head is negligible and may be omitted in pressure drop calculations.

The typical velocities shown in Table B8.13 may be considered for preliminary line sizing, but economic size should be determined as a function of pressure drop, pipe cost, and so forth.

Special attention should be given to turbine main steam lines and to hot and cold reheat piping because pressure drop in those systems affects heat rate and plant performance. Cost of piping must be compared with these effects for most economical piping arrangement. Normally, total pressure drop in reheat piping and

TABLE B8.13 Typical Steam Velocity in Pipelines on Industrial Projects[1]

Steam pressure	Velocity	Pressure drop
50 psig (3.5 bar g) and lower	175 ft/s (~50 m/s)	0.4 psi/100 ft (~0.1 bar/100 m)
Over 50 psig (3.5 bar g) saturated steam	120 ft/s (~35 m/s)	1.0 psi/100 ft (~0.25 bar/100 m)
Over 50 psig (3.5 bar g) superheated steam	175 ft/s (~50 m/s)	1.0 psi/100 ft (~0.25 bar/100 m)

[1] Velocities are based on typical process industry practice.
Source: Stone & Webster.

the boiler reheater should be 7 to 9 percent of high pressure turbine exhaust pressure. It is desirable to use a smaller diameter hot reheat line and a larger diameter cold reheat line, taking a greater pressure drop in the more expensive, alloy, hot reheat line.

Extraction steam piping also affects heat rate and output, and norally this piping should be sized so that the pressure drop does not exceed about 5 percent of turbine stage pressure for the low pressure and 3 to 4 percent for the higher pressure lines.

Extraction steam lines should be designed for the pressure shown on full-load heat balance diagram at 5 percent overpressure and valves wide open (VWO).

Continuously operating steam lines in process projects shall be designed on the basis of reasonable total pressure drop and, except for short leads such as to turbines and pumps, shall not generally exceed the conditions noted in Table B8.13.

Applications: Air and Other Gas Systems

As indicated in the last section, ''Applications: Steam Systems,'' in a case of compressible fluids such as air or steam when density changes are small, the fluid may be considered as incompressible. Therefore, all design rules described in the subsections ''Characteristics of Incompressible Flow,'' ''Applications: Water Systems,'' and ''Applications: Steam Systems'' are applicable to this section. For steam and gas systems, where the fluid density is small, static head is negligible and may be omitted in pressure drop calculations.

Table B8.14 (from Ref. 7) presents pressure drop for some typical values of air flow rates through piping from ⅛ to 12 in diameter.

Applications: Sample Problems B8.2–B8.7

The most frequent application of single-phase compressible flow steam line analysis normally encountered by engineers is the sizing of safety valve vent lines. This analysis can be done either by using a computer program which is based on procedures discussed, or a hand calculation similar to that presented in this section. Users may compare their results with those obtained from an approximate, semi-empirical procedure based on tables in App. 11 of Ref. 12. It is the responsibility of the designer to make sure that the method used yields conservative results.

The primary consideration in these analyses is to ensure that the vent line will pass the required flow without exceeding recommended backpressure limitations on valves with solidly connected vents or without blowing back in the case of open vent stacks.

Problem B8.2. During abnormal operation of a system, 72,000 lb_m/h (32,659 kg/h) of air must be released from a high-pressure air tank through a 4-in (Schedule 40) commercial steel bypass line (vent line) into the atmosphere. Stagnation conditions in the vessel during this operation are: p_o = 600 psig (41.4) bar gauge (kept at a constant level by compressors), t_F = 120°F (48.9°C). Equivalent length of the vent line is 90 ft (27.43 m). Calculate the pressure p_1 that exists at the valve discharge and make your comments on the vent line size. Air may be treated as a perfect gas. Assume that this is not a typical safety valve and that the valve backpressure should not exceed 50 percent of the valve set pressure. (The safety valve vent line design criteria are well documented in the ASME Boiler and Pressure Vessel Code.)

TABLE B8.14 Flow of Air Through Schedule 40 Steel Pipe

Free air q' m ft³/min at 60°F and 14.7 psia	Compressed air ft³/min at 60°F and 100 psig	Pressure drop of air in pounds per square inch per 100 ft of Schedule 40 pipe For air at 100 lb/in² gauge pressure and 60°F temperature								
		⅛ in	¼ in	⅜ in	½ in					
1	0.128	0.361	0.083	0.018						
2	0.256	1.31	0.285	0.064	0.020					
3	0.384	3.06	0.605	0.133	0.042	¾ in				
4	0.513	4.83	1.04	0.226	0.071					
5	0.641	7.45	1.58	0.343	0.106	0.027				
							1 in			
6	0.769	10.6	2.23	0.408	0.148	0.037				
8	1.025	18.6	3.89	0.848	0.255	0.062	0.019			
10	1.282	28.7	5.96	1.26	0.356	0.094	0.029	1¼ in	1½ in	
15	1.922	. . .	13.0	2.73	0.834	0.201	0.062			
20	2.563	. . .	22.8	4.76	1.43	0.345	0.102	0.026		
25	3.204	. . .	35.6	7.34	2.21	0.526	0.156	0.039	0.019	
30	3.845	. . .		10.5	3.15	0.748	0.219	0.055	0.026	
35	4.486	. . .		14.2	4.24	1.00	0.293	0.073	0.035	
40	5.126	. . .		18.4	5.49	1.30	0.379	0.095	0.044	
45	5.767	. . .		23.1	6.90	1.62	0.474	0.116	0.055	2 in
50	6.408			28.5	8.49	1.99	0.578	0.149	0.067	0.019
60	7.690	2½ in		40.7	12.2	2.85	0.819	0.200	0.094	0.027
70	8.971			. . .	16.5	3.83	1.10	0.270	0.126	0.036
80	10.25	0.019		. . .	21.4	4.96	1.43	0.350	0.162	0.046
90	11.53	0.023		. . .	27.0	6.25	1.80	0.437	0.203	0.058
100	12.82	0.029	3 in		33.2	7.69	2.21	0.534	0.247	0.070
125	16.02	0.044			. . .	11.9	3.39	0.825	0.380	0.107
150	19.22	0.062	0.021		. . .	17.0	4.87	1.17	0.537	0.151
175	22.43	0.083	0.028		. . .	23.1	6.60	1.58	0.727	0.205
200	25.63	0.107	0.036	3½ in	. . .	30.0	8.54	2.05	0.937	0.264
225	28.84	0.134	0.045	0.022		37.9	10.8	2.59	1.19	0.331
250	32.04	0.164	0.055	0.027		. . .	13.3	3.18	1.45	0.404
275	35.24	0.191	0.066	0.032		. . .	16.0	3.83	1.75	0.484
300	38.45	0.232	0.078	0.037		. . .	19.0	4.56	2.07	0.573
325	41.65	0.270	0.090	0.043		. . .	22.3	5.32	2.42	0.673
					4 in					
350	44.87	0.313	0.104	0.050		. . .	25.8	6.17	2.80	0.776
375	48.06	0.356	0.119	0.057	0.030	. . .	29.6	7.05	3.20	0.887
400	51.26	0.402	0.134	0.064	0.034	. . .	33.6	8.02	3.64	1.00
425	54.47	0.452	0.151	0.072	0.038	. . .	37.9	9.01	4.09	1.13
450	57.67	0.507	0.168	0.081	0.042	. . .		10.2	4.59	1.26
475	60.88	0.562	0.187	0.089	0.047		. . .	11.3	5.09	1.40
500	64.08	0.623	0.206	0.099	0.052		. . .	12.5	5.61	1.55
550	70.49	0.749	0.248	0.118	0.062		. . .	15.1	6.79	1.87
600	76.90	0.887	0.293	0.139	0.073		. . .	18.0	8.04	2.21
650	83.30	1.04	0.342	0.163	0.086	5 in	. . .	21.1	9.43	2.60
700	89.71	1.19	0.395	0.188	0.099	0.032		24.3	10.9	3.00
750	96.12	1.36	0.451	0.214	0.113	0.036		27.9	12.6	3.44
800	102.5	1.55	0.513	0.244	0.127	0.041		31.8	14.2	3.90
850	108.9	1.74	0.576	0.274	0.144	0.046		35.9	16.0	4.40
900	115.3	1.95	0.642	0.305	0.160	0.051	6 in	40.2	18.0	4.91

Useful conversion of units:

1 inch = 25.4 mm; 1 ft = 0.3048 m; 1 ft³ = 0.02832 m³; $t_C = \frac{5}{9}(t_F = 32)$; for pressure conversions to other units see Table B8.1.

TABLE B8.14 Flow of Air Through Schedule 40 Steel Pipe (*Continued*)

Free air q' m ft³/min at 60°F and 14.7 psia	Compressed air ft³/min at 60°F and 100 psig	Pressure drop of air in pounds per square inch per 100 ft of Schedule 40 pipe For air at 100 lb/in² gauge pressure and 60°F temperature								
950	121.8	2.18	0.715	0.340	0.178	0.057	0.023	. . .	20.0	5.47
1 000	128.2	2.40	0.788	0.375	0.197	0.063	0.025	. . .	22.1	6.06
1 100	141.0	2.89	0.948	0.451	0.236	0.075	0.030	. . .	26.7	7.29
1 200	153.8	3.44	1.13	0.533	0.279	0.089	0.035	. . .	31.8	8.63
1 300	166.6	4.01	1.32	0.626	0.327	0.103	0.041	. . .	37.3	10.1
1 400	179.4	4.65	1.52	0.718	0.377	0.119	0.047			11.8
1 500	192.2	5.31	1.74	0.824	0.431	0.136	0.054			13.5
1 600	205.1	6.04	1.97	0.932	0.490	0.154	0.061	8 in		15.3
1 800	230.7	7.65	2.50	1.18	0.616	0.193	0.075			19.3
2 000	256.3	9.44	3.06	1.45	0.757	0.237	0.094	0.023		23.9
									10 in	
2 500	320.4	14.7	4.76	2.25	1.17	0.366	0.143	0.035		37.3
3 000	384.5	21.1	6.82	3.20	1.67	0.524	0.204	0.051	0.016	
3 500	448.6	28.8	9.23	4.33	2.26	0.709	0.276	0.068	0.022	
4 000	512.6	37.6	12.1	5.66	2.94	0.919	0.358	0.088	0.028	
4 500	576.7	47.6	15.3	7.16	3.69	1.16	0.450	0.111	0.035	12 in
5 000	640.8	. . .	18.8	8.85	4.56	1.42	0.552	0.136	0.043	0.018
6 000	769.0	. . .	27.1	12.7	6.57	2.03	0.794	0.195	0.061	0.025
7 000	897.1	. . .	36.9	17.2	8.94	2.76	1.07	0.262	0.082	0.034
8 000	1025	. . .		22.5	11.7	3.59	1.39	0.339	0.107	0.044
9 000	1153	. . .		28.5	14.9	4.54	1.76	0.427	0.134	0.055
10 000	1282	. . .		35.2	18.4	5.60	2.16	0.526	0.164	0.067
11 000	1410	. . .			22.2	6.78	2.62	0.633	0.197	0.081
12 000	1538	. . .			26.4	8.07	3.09	0.753	0.234	0.096
13 000	1666	. . .			31.0	9.47	3.63	0.884	0.273	0.112
14 000	1794	. . .			36.0	11.0	4.21	1.02	0.316	0.129
15 000	1922	. . .				12.6	4.84	1.17	0.364	0.148
16 000	2051	. . .				14.3	5.50	1.33	0.411	0.167
18 000	2307	. . .				18.2	6.96	1.68	0.520	0.213
20 000	2563	. . .				22.4	8.60	2.01	0.642	0.260
22 000	2820	. . .				27.1	10.4	2.50	0.771	0.314
24 000	3076	. . .				32.3	12.4	2.97	0.918	0.371
26 000	3332	. . .				37.9	14.5	3.49	1.12	0.435
28 000	3588	. . .					16.9	4.04	1.25	0.505
30 000	3845	. . .					19.3	4.64	1.42	0.520

For lengths of pipe other than 100 ft, the pressure drop is proportional to the length. Thus, for 50 ft of pipe, the pressure drop is approximately one-half the value given in the table . . . for 300 ft, three times the given value, etc.

The pressure drop is also inversely proportional to the absolute pressure and directly proportional to the absolute temperature.

Therefore, to determine the pressure drop for inlet or average pressures other than 100 psi and at temperatures other than 60°F, multiply the values given in the table by the ratio $[(100 + 14.7)/(P + 14.7)]$ $[(460 + t)/520]$ where P is the inlet or average gauge pressure in pounds per square inch, and t is the temperature in degrees Fahrenheit under consideration.

The cubic feet per minute of compressed air at any pressure is inversely proportional to the absolute pressure and directly proportional to the absolute temperature.

To determine the cubic feet per minute of compressed air at any temperature and pressure other than standard conditions, multiply the value of cubic feet per minute of free air by the ratio $[14.7/(14.7 + P)]$ $[(460 + t)/(520)]$.

Calculations for Pipe Other than Schedule 40

To determine the velocity of water, or the pressure drop of water or air, through pipe other than Schedule 40, use the following formulas, $v_a = v_{40}(d_{40}/d_a)^2$, $\Delta P_a = \Delta P_{40}(d_{40}/d_a)^5$, where v = velocity, ft/s; d = internal diameter of pipe, in; ΔP = pressure drop, lb/in².

Subscript a refers to the schedule of pipe through which velocity or pressure drop is desired. Subscript 40 refers to the velocity or pressure drop through Schedule 40 pipe.

Source: Ref. 7.

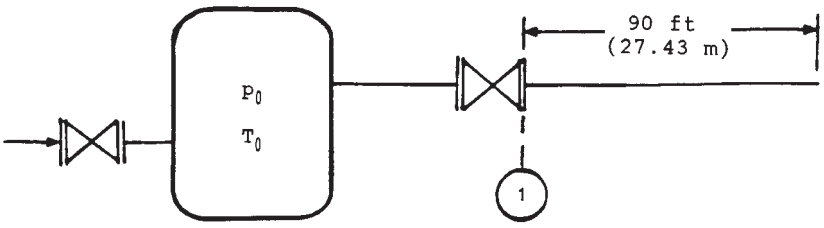

FIGURE B8.18 Reference for sample problem B8. 2.

$$\dot{m} = 72{,}000 \text{ lb/hr} = 20 \text{ lb}_\text{m}/\text{sec}$$

$$T_0 = 120^\circ\text{F} = (460 + 120) = 580^\circ\text{R}$$

$$p_0 = 600 \text{ psig} = 614.7 \text{ psia (assumed atmospheric pressure of 14.7 psia)}$$

Internal pipe diameter $D = 4.026$ in ($A = 0.0884$ ft^2).

Critical pressure at the pipe discharge (see Fig. B8.18) is found by using Eq. (B8.25):

$$p^* = \frac{\dot{m}}{A}\sqrt{\frac{2RT_0}{g_c k(k+1)}} \text{ lb}_\text{f}/\text{ft}^2$$

$$= \frac{20}{0.0884}\sqrt{\frac{(2)\,(53.3)\,(580)}{(32.174)\,(1.4)\,(2.4)}}$$

$$= 5410.35 \text{ lb}_\text{f}/\text{ft}^2 = 37.57 \text{ psia}$$

The line is choked because $p^* > p_{amb} = 14.7$ psia. Pipe $f(L/D)$, from choked exit to the valve discharge, is calculated by assuming complete turbulence of flow. From Ref. 7, for a commercial steel pipe:

$$\frac{\varepsilon}{D} = \frac{(0.00015)\,(12.0)}{4.026} = 0.00045$$

and the friction factor $f = f_T = 0.017$. Then the value of $(f\,L)/D$, counting from the choked pipe exit to the valve outlet is:

$$f\frac{L}{D} = 0.017\frac{(90)\,(12)}{4.026} = 4.5604$$

Using a computerized method (for example the Newton-Raphson method) of solving Eq. (B8.28) (notice that for Ma = 1 at the pipe discharge, the second term on the right hand side of Eq.(B8.28) is zero), with $k = 1.4$, having on the left side of this equation the above calculated $(f\,L)/D = 4.5604$ and changing the Mach number, the value of Mach number for air entering the pipe, which satisfies the equation, is found to be:

$$\text{Ma} = 0.317$$

Substituting this Ma value into Eq. (B8.26) results in

$$\frac{p}{p^*} = \frac{p_1}{p^*} = 3.4193$$

and finally:

$$p_1 = p^*\left(\frac{p}{p^*}\right) = (37.57)(3.4193) = 128.46 \text{ psia } (8.86 \text{ bar})$$

Fanno line tables for $k = 1.4$ (Table B8.12) may be used instead, but this procedure would require cumbersome interpolations. Also, note that in Ref. 11 (the source of Table B8.12) the Fanning friction factor is used, which is four times less than that of D'Arcy-Weisbach. This is the reason why Table B8.12 uses $4fL_{max}/D$) value in the last column.

Problem B8.3. Twice as much flow rate must be released from the tank described in Problem B8.2. Check if the piping is adequate.

$$p^* = (2)(37.57) = 75.14 \text{ psia}$$

Then,

$$p_1 = (75.14)(3.4193) = 256.93 \text{ psia } (17.72 \text{ bar})$$

The piping is still adequate because the calculated $p_1 < 0.5\ p_0$.

Problem B8.4. Keep the mass flow as in Problem B8.2, but double the length of the pipe. Check the pressure p_1:

$$fL/D = (2)(4.5604) = 9.1208$$

at this $f\ L/D$,

$$(p_1/p^*) = 4.4854$$

$$\text{Ma} = 0.243$$

and

$$p_1 = (37.57)(4.4854) = 168.52 \text{ psia } (11.62 \text{ bar})$$

which means that the line size is sufficient.

Problem B8.5. For the same mass flow and the same pipe as in Problem B8.2, assume that the air temperature in the vessel $t_F = 500°\text{F}$ (260°C).

$$p^* = \frac{20}{0.0884}\sqrt{\frac{(2)(53.3)(460+500)}{(32.174)(1.4)(2.4)}}$$

$$= 6960.97 \text{ lb}_\text{f}/\text{ft}^2 = 48.34 \text{ psia}$$

$$p_1 = (3.4193)(48.34) = 165.29 \text{ psia } (11.40 \text{ bar})$$

The line size is sufficient.

Problem B8.6. For the same mass flow and the same pipe as in Problem B8.2, use the pipe diameter of 2 in (Schedule 40) and calculate p_1.

$$D = 2.067 \text{ in } (A = 0.0233 \text{ ft}^2)$$

$$p^* = 37.57 \frac{0.0884}{0.0233} = 142.54 \text{ psia}$$

$$f\frac{L}{D} = (0.019)\frac{(90)(12)}{2.067} = 9.9274$$

Then

$$(p/p^*) = 4.644$$

$$\text{Ma} = 0.235$$

and

$$p_1 = (142.54)(4.644) = 661.96 \text{ psia } (45.64 \text{ bar})$$

The calculated pressure p_1 is too high. It is even higher than the pressure p_0 within the vessel. This line cannot be used for releasing the required flow.

Problem B8.7. For the same flow and the same pipe length as in Problem B8.2, use the pipe diameter of 8 in (Schedule 40), and calculate p_1.

$$D = 7.981 \text{ in } (A = 0.3474 \text{ ft}^2)$$

$$f = f_T = 0.014$$

$$p^* = 37.57 \frac{0.0884}{0.3474} = 9.56 \text{ psia}$$

Because $p^* < p_{\text{atm}}$, the line is not choked. To calculate the pressure p_1 after the valve, the additional length, L_{add}, of the pipe, required for choked conditions at the exit, should be calculated first.

Assuming

$$p_{\text{amb}} = p_{\text{atm}} = 14.7 \text{ psia}$$

$$\frac{p_{\text{atm}}}{p^*} = \frac{14.7}{9.56} = 1.5376$$

From Fanno line tables, for $(p/p^*) = 1.5376$, the following is found for the existing pipe outlet

$$fL_{\text{add}}/D = 0.2467$$

$$\text{Ma} = 0.6814$$

Therefore,

$$L_{\text{add}} = \frac{\left(f\frac{L_{\text{add}}}{D}\right)}{\frac{f}{D}} = \frac{(0.2467)(7.981)}{(0.014)(12)} = 11.72 \text{ ft}$$

and the fictitious pipe length from the choked pipe exit to the valve outlet

$$L_{\text{fict}} = 90 + 11.72 = 101.72 \text{ ft}$$

The corresponding $(f\ L/D)_{\text{fict}}$ value, starting from the choked exit to the valve, is

$$\left(f\frac{L}{D}\right)_{\text{fict}} = \frac{(0.014)(101.72)(12)}{7.981} = 2.1412$$

For this $(f\ L/D)_{\text{fict}}$, the following is obtained from the Fanno line computerized calculation, similar to that explained in Problem B8.2 (or from Fanno line tables for $k = 1.4$):

$$(p/p^*) = 2.6306$$
$$\text{Ma} = 0.4096$$

Therefore,

$$p_1 = (9.56)(2.6306) = 25.15 \text{ psia } (1.73 \text{ bar})$$

SINGLE-PHASE FLOW IN NOZZLES, VENTURI TUBES, AND ORIFICES

Theoretical Background

Liquid Service. A nozzle or an orifice in a tank or reservoir may be installed in the wall (Fig. B8.19) or in the bottom.

In the case of a nozzle, the fluid emerges in the form of a cylindrical jet of the same diameter as the throat of the nozzle, but in the case of a sharp-edged orifice, the jet contracts after passing through it, attaining its smallest diameter (vena contracta) and greatest velocity some distance (about one-half of a diameter) downstream from the opening. When installed in the bottom, the distance z from the opening in the bottom of the tank to the liquid free surface must include the length of a nozzle or the distance of the vena contracta from the bottom of the tank. The ratio of jet area A_2 at vena contracta to the area of an orifice A is called the *coefficient of contraction* C_c.

$$C_c = A_2/A \tag{B8.34}$$

For a nozzle $C_c = 1$.

Bernoulli's equation [(Eq. B8.12) without H_p and H_f] applied from a point 1 on the free surface to the center of the vena contracta, point 2, yields the following

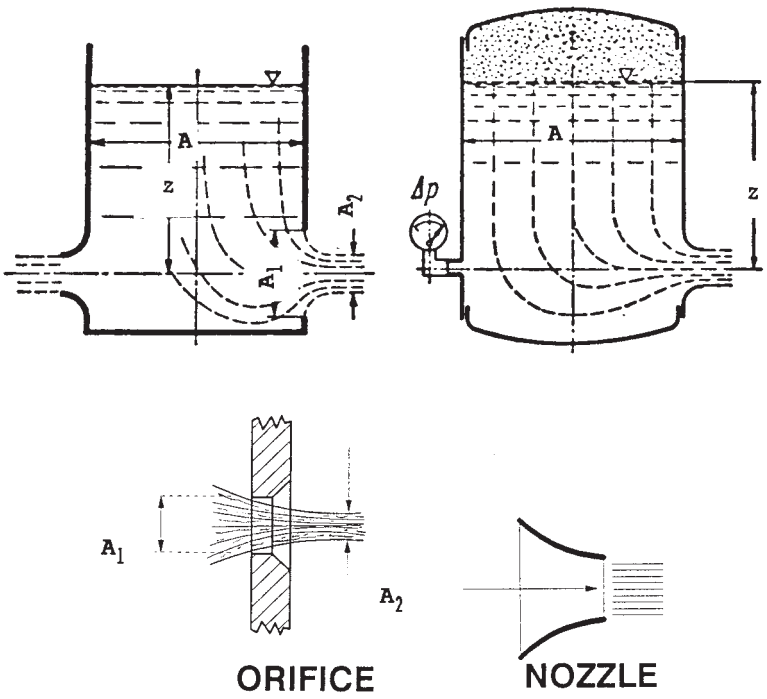

FIGURE B8.19 Typical nozzle and orifice.

expression for the theoretical (no friction) discharge velocity of fluid at the vena contracta ($w_1 = 0$)

$$w_2 = \sqrt{\frac{2g_c}{\rho}\left(p_1 - p_2 + \rho z \frac{g}{g_c}\right)} \text{ ft/s} \tag{B8.35}$$

where p_1 and p_2 are absolute static pressures (lb_f/ft^2) at the free surface in the tank and in the vena contracta respectively. If the fluid is discharged to the atmosphere, p_2 is the atmospheric pressure. For open vessels $p_1 = p_2$.

Hydraulic engineers sometimes prefer to use the following version of Eq. (B8.35):

$$w_2 = \sqrt{2g\left(\frac{p_1 - p_2}{\gamma} + z\right)} \text{ ft/s} \tag{B8.36}$$

Equation (B8.35) or (B8.36) describes the theoretical velocity because the pressure losses between the points 1 and 2 were neglected. The ratio of actual velocity w_a to the theoretical velocity w_t is called the *velocity coeffficient* C_v.

The actual volumetric discharge rate from the orifice is the product of the actual velocity at the vena contracta and the area of the jet at the vena contracta. Using the just-described coefficient of contraction C_c, the mass flow rate from the opening may be calculated from the following expression

$$\dot{m} = C_v C_c A \rho w_2 \tag{B8.37}$$

where

$$C_d = C_v C_c \tag{B8.38}$$

is called the *discharge coefficient.*

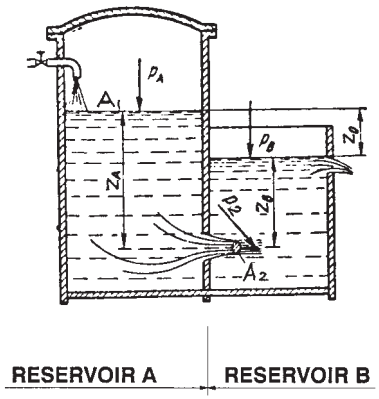

FIGURE B8.20 Typical submerged nozzle or orifice

The velocities and quantities of liquid discharged from a submerged orifice or nozzle (Fig. B8.20) are determined by the same formulas as just presented. The different symbols in Eqs. (B8.35) and (B8.36) are understood in this case as follows:

$z = z_A$ Immersion depth of the center of the opening relative to the free liquid level in reservoir A, ft

$p_1 = p_A$ Static pressure at the free surface A in reservoir, $\text{lb}_\text{f}/\text{ft}^2$

$p_2 = p_B + g\rho z_B$ Static pressure in the vena contracta jet, $\text{lb}_\text{f}/\text{ft}^2$

It is preferable that the actual coefficient of discharge C_d of an orifice or a nozzle be determined by calibration. Such calibration should encompass the entire range of flow rates to be experienced. If an orifice or a nozzle is manufactured according to the ASME specification (Ref. 13), then the appropriate values of C_d, as described in Ref. 13 may be used for flow rate calculations.

Consider now a flow nozzle installed in a horizontal pipe (Fig. B8.21), where $z_1 = z_2 = \text{const}$. Because with an incompressible fluid (i.e., a liquid) the temperature does not change, the density is constant. Thus, the continuity equation becomes

$$w_1 \frac{\pi D^2}{4} = w_2 \frac{\pi d^2}{4} \tag{B8.39}$$

and the Bernoulli equation applied from Section 1 to Section 2 is

$$\frac{w_1^2}{2g_c} + \frac{p_1}{\rho} = \frac{w_2^2}{2g_c} + \frac{p_2}{\rho} \tag{B8.40}$$

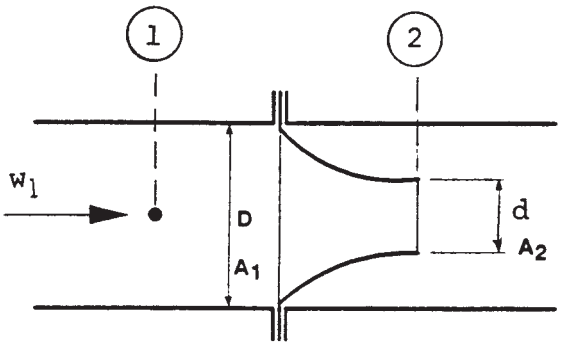

FIGURE B8.21 Flow nozzle in a pipe.

Substituting w_1 from Eq. (B8.39) into Eq. (B8.40) the following expression for the theoretical velocity w_2 is obtained (no friction):

$$w_2 = \sqrt{2g_c \frac{p_1 - p_2}{\rho} \frac{1}{1 - \beta^4}} \text{ ft/s} \tag{B8.41}$$

where $\beta = d/D$, and the approach velocity factor, F_{wa}, is

$$F_{wa} = \frac{1}{1 - \beta^4} \tag{B8.42}$$

Because most materials expand or contract as their temperature changes, an area factor F_a (Fig. B8.22) for the thermal expansion of the primary element (nozzle or orifice) must be introduced in order to find an actual flow area. In general, the actual flow rate is less than the theoretical flow. Therefore, to obtain the actual flow, the discharge coefficient C_d must be introduced (empirical value) into the theoretical Eq. (B8.41):

$$C_d = \frac{\text{actual flow rate}}{\text{theoretical flow rate}} \tag{B8.43}$$

Thus, the actual mass flow rate through a flow nozzle is

$$\dot{m} = F_a A_2 \rho C_d w_2 \tag{B8.44}$$

Equation (B8.44), which was derived for a flow nozzle, holds equally well for horizontal Venturi tubes and for orifices. The following factor is frequently used in calculations and is called the flow coefficient:

$$C = \frac{C_d}{\sqrt{1 - \beta^4}} \tag{B8.45}$$

The values of C_d and C are different for each different type of primary element: Venturi tube, flow nozzle, and orifice. Also, with flow nozzles and orifices, the

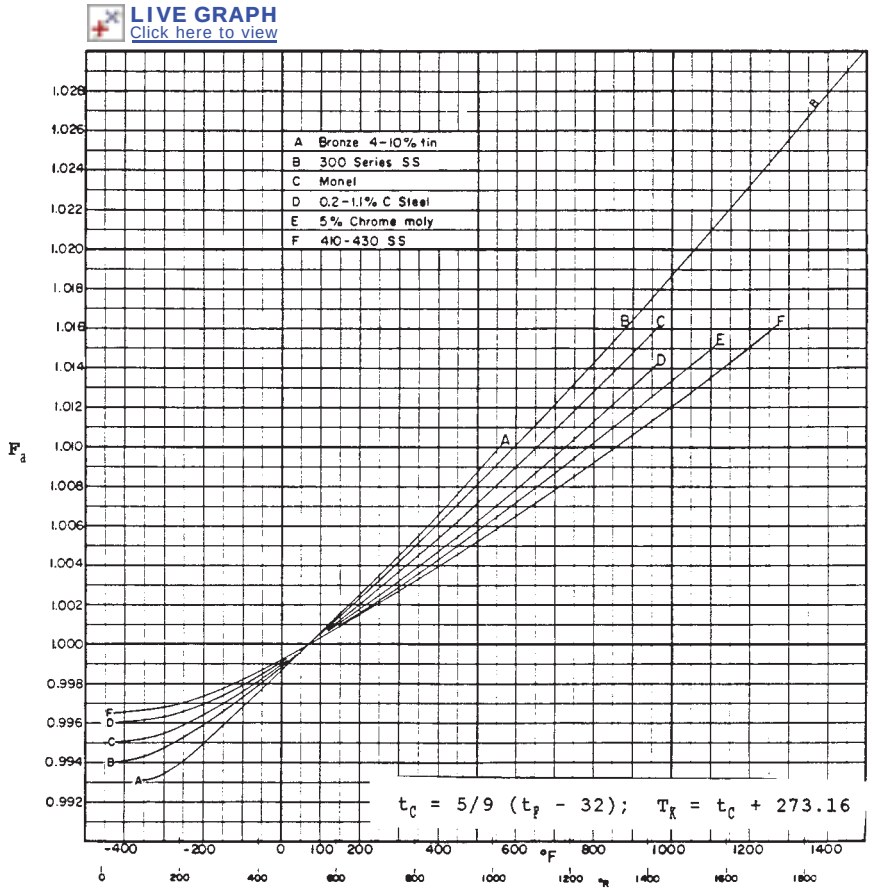

FIGURE B8.22 Area factors, F_a, for the thermal expansion of primary elements. (*From Ref. 13.*)

values depend upon the locations of the pressure taps; and, with the orifice, the values differ with the type of inlet edge, whether square and thin or rounded.

Values of C for long-radius nozzles and square-edged orifices are available in Ref. 7. For a classical Venturi tube, the discharge coefficients C_d are[13]:

	C_d
Rough-cast entrance cone	0.984
Machined entrance cone	0.995
Rough-welded sheet metal entrance cone	0.985

Each obstacle in a flow path generates a permanent pressure drop Δp_p. The pressure profile in a pipe due to an orifice insertion is shown in Fig. B8.23.

The permanent pressure loss through a primary element of a *flowmeter,* with an orifice, a nozzle, or a Venturi tube, is shown in Fig. B8.24. The Venturi tube

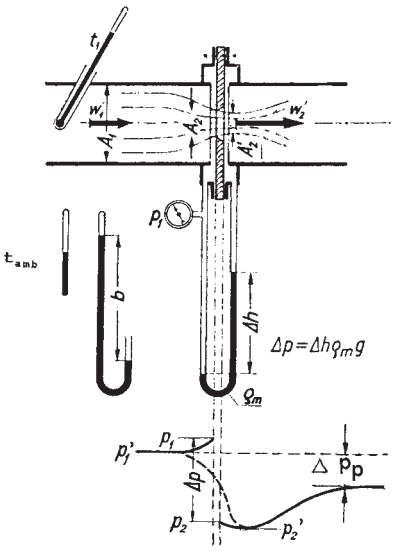

FIGURE B8.23 Pressure profile in a pipe with an orifice. (*From Ref. 15.*)

has a low overall loss due to the gradually expanding conical section, which aids in efficient reconversion of the high kinetic energy at the throat into pressure.

Steam and Gas Service. Because the static head is not considered in gas systems, there is no need to distinguish the case of outflow from a reservoir from that of flow in a pipe.

Consider the flow of a perfect gas through a converging nozzle (Fig. B8.25). By applying Eqs. (B8.7) and (B8.8) to the inlet and outlet of a nozzle, and neglecting potential energy, the following result is found for an insentropic flow:

$$w_{2s} = \sqrt{2g_c J(h_0 - h_{2s})} \tag{B8.46}$$

where h_0 is the stagnation enthalpy at the nozzle inlet [see Eq. (B8.9)].

If there are no losses due to friction or heat transfer, the change of state of a gas is isentropic (s = const), and using the gas properties relationships (Ref. 2, typical), Eq. (B8.46) yields:

$$w_{2s} = \sqrt{2g_c J c_p T_0 \left(1 - \frac{T_{2s}}{T_0}\right)} \tag{B8.47}$$

or

$$w_{2s} = \sqrt{2g_c \frac{k}{k-1} p_0 v_0 \left[1 - \left(\frac{p_2}{p_0}\right)^{(k-1)/k}\right]} \tag{B8.48}$$

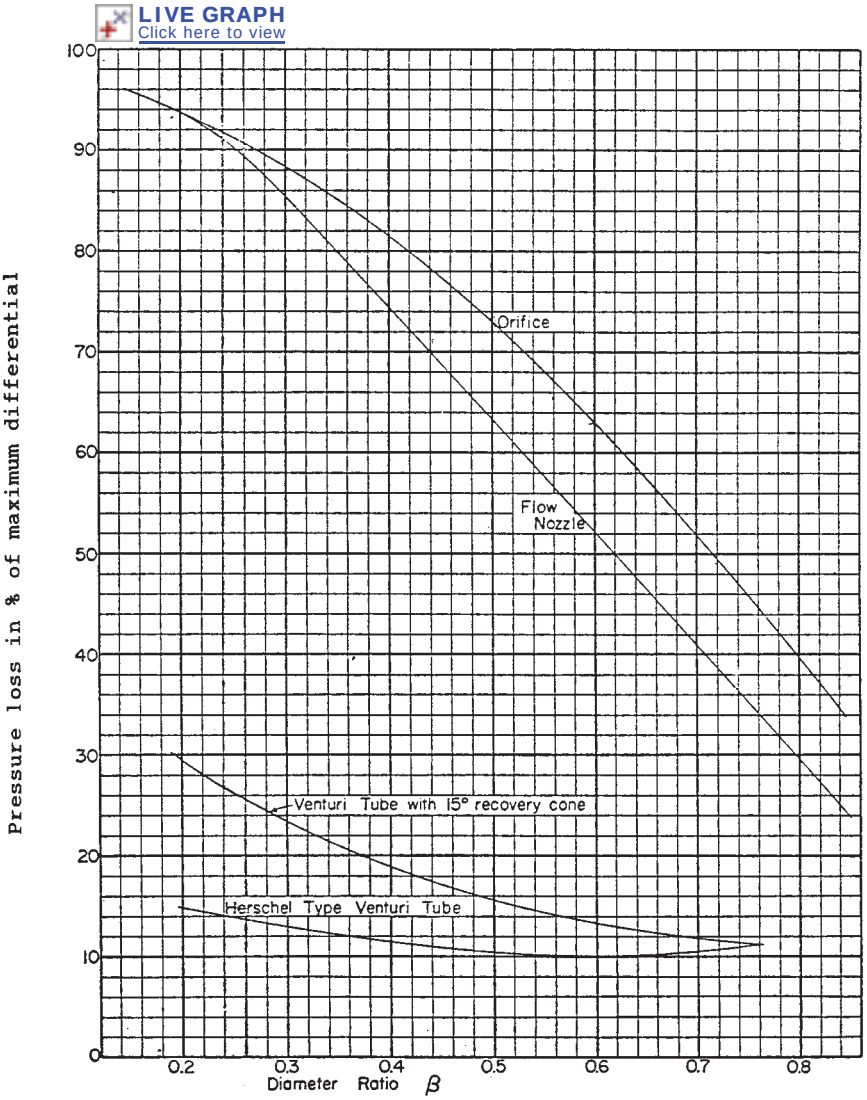

FIGURE B8.24 Permanent pressure loss through primary elements of flowmeters. (*From Ref. 13.*)

which was first derived by De St. Venant and Wantzel in 1839. Equation (B8.48) is written in terms of inlet stagnation conditions, where:

$$T_0 = T_1 + \frac{w_1^2}{2g_c J c_p} \tag{B8.49}$$

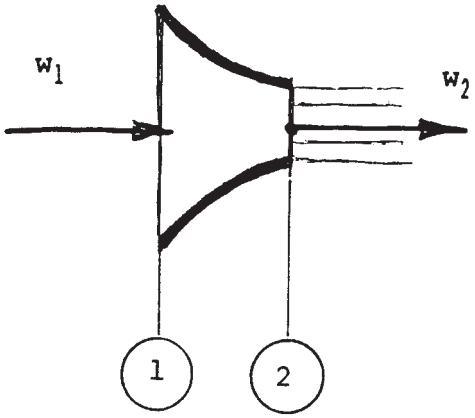

FIGURE B8.25 Fluid flow in a converging nozzle.

and for an isentropic process of a perfect gas:

$$p_0 = p_1 \left(\frac{T_0}{T_1} \right)^{k/(k-1)} \tag{B8.50}$$

The mass flow rate of a gas through the cross section area A_2 can be calculated from:

$$\dot{m} = \frac{A_2 w_{2s}}{v_{2s}} = A_2 \Psi_s \sqrt{\frac{p_0}{v_0}} \text{ lb}_\text{m}/\text{s} \tag{B8.51}$$

where

$$\Psi_s = \sqrt{2g_c \frac{k}{k-1} \left[\left(\frac{p_2}{p_0} \right)^{2/k} - \left(\frac{p_2}{p_0} \right)^{(k+1)/k} \right]} \tag{B8.52}$$

Figure B8.26 shows the mass flow rate $\dot{m}$ plotted against p_2/p_0 for a specified gas which is characterized by its $k = c_p/c_v$ value. The flow rate becomes zero when $(p_2/p_0) = 1$. As the pressure p_2 decreases, the flow rate increases to its maximum value at p^*/p_0 (critical pressure ratio). At $(p_2/p_0) < (p^*/p_0)$, Eq. (B8.51) predicts decreasing flow to zero at $(p_2/p_0) = 0$. However, experiments show that in a flow through a convergent nozzle, the pressure at the exit cross section A_2 cannot fall below the value of p^* and the flow rate does not change, no matter how low the backpressure p_2. At the critical pressure ratio the mass flow rate reaches its maximum value and the flow is said to be *choked.* The maximum flow rate at the choke point is called the *critical flow rate.* Critical or mass limiting flow is characteristic of compressible fluid systems.

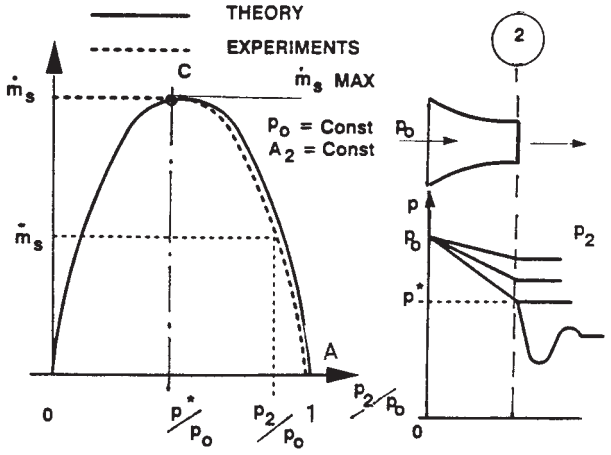

FIGURE B8.26 Mass flow rate versus p_2/p_0 ratio, and the pressure distribution within the nozzle versus p_2.

The value of the critical pressure ratio (p^*/p_0) may be found from the following conditions:

$$\frac{d\dot{m}_s}{d(p_2/p_0)} = 0 \qquad \text{or} \qquad \frac{d\Psi_s}{d(p_2/p_0)} = 0 \tag{B8.53}$$

Applying this condition to Eq. (B8.52) leads to the critical pressure ratio:

$$\beta_s = \frac{p^*}{p_0} = \left(\frac{2}{k+1}\right)^{\frac{k}{k-1}} \tag{B8.54}$$

where p_0 is described by Eq. (B8.50). Then, substituting the critical pressure ratio for p_2/p_0, Eq. (B8.52) yields:

$$\Psi_{s\,\max} = \sqrt{g_c k \left(\frac{2}{k+1}\right)^{\frac{k+1}{k-1}}} \tag{B8.55}$$

and the corresponding maximum flow rate is

$$\dot{m}_{s\,\max} = A_2 \Psi_{s\,\max} \sqrt{\frac{p_0}{v_0}} \tag{B8.56}$$

For $(p_2/p_0) > p^*/p_0$, the mass flow rate must be calculated from Eq. (B8.51) or by the simplified equation presented by Bendemann in 1907.[10] It was proved by

Bendemann that the arc AC in Fig. B8.26 can be replaced with a high degree of accuracy by a quadrant of an ellipse:

$$\left(\frac{\dot{m}}{\dot{m}_{s\,\max}}\right)^2 + \frac{\left(\frac{p_2}{p_0} - \beta_S\right)^2}{(1-\beta_s)^2} = 1 \tag{B8.57}$$

The remaining thermodynamic parameters (in addition to the critical pressure p^*) at the nozzle throat, corresponding to the maximum flow rate of an ideal gas, are the following:

1. Temperature may be determined by using the relation (see Ref. 11):

$$\frac{T^*}{T_0} = \frac{2}{k+1} \tag{B8.58}$$

For T_0 see Eq. (B8.49).

2. Specific volume may be calculated from another relation for an isentropic expansion

$$\frac{v^*}{v_0} = \left(\frac{k+1}{2}\right)^{1/(k-1)} \tag{B8.59}$$

3. The gas velocity may be calculated from the following expression

$$w_{2\,\max} = \alpha_s \sqrt{p_0 v_0} \tag{B8.60}$$

where

$$\alpha_s = \sqrt{2g_c \frac{k}{k+1}} \tag{B8.61}$$

Because $p_0 v_0 = RT_0$, also

$$w_{2\,\max} = \alpha_s \sqrt{RT_0} \tag{B8.62}$$

It will be observed that for the same perfect gas (α_s, R) the maximum velocity depends only upon its initial stagnation temperature (before a nozzle). It can be shown that Eq. (B8.60) or (B8.62) represents a velocity of sound in the choked exit plane of a nozzle:

$$w_{2\,\max} = \sqrt{g_c k R T^*} = \sqrt{g_c k p^* v^*} = c \tag{B8.63}$$

The ASME report on fluid meters (Ref. 13) presents slightly modified equations which are more suitable for precise differential-pressure flow-metering techniques. See this document for procedures and more information about flow measurement using orifices, nozzles, or Venturi tubes.

Sample problems concerning ASME fluid meters may be found in Refs. 13 and 14.

Applications: Flow Restriction

Flow-restricting orifices are used where a continuous small flow of fluid (bleeding) is required. Flow-restricting orifices are usually not designed according to requirements of the ASME specification for fluid metering devices. In most cases, they are round openings drilled in an orifice plate. Their fluid entrance may be sharp-edged, beveled, or well-rounded.

It is suggested that reasonably accurate approximations in flow rate estimations may be obtained by using equations presented in the last subsection. If the entrance is well-rounded, C values would tend to approach those for ASME nozzles, whereas openings with square entrances would have characteristics similar to those for square-edged ASME orifices. The minimum allowable orifice size should be 1/16 in to prevent clogging. The recommended thicknesses of orifice plates for carbon steel or chrome-moly steel are given in Table B8.15.

Applications: Fluid Flow Metering

Recommended conditions, procedures, and data for measuring the flow of fluids, particularly with the three principal differential-pressure meters—the orifice, the flow nozzle, and the Venturi tube—are presented in the ASME test codes.[13,14]

Applications: Sample Problem B8.8[15]

This could be a model for important safety related calculations.

Air is contained in a vessel having a volume of $V_{\text{vess}} = 80\ \text{ft}^3$ (2.27 m^3). The initial state of the gas in the vessel corresponds to its pressure of $p_0 = 250$ psia (17.24 bar), and its temperature of $t_F = 70°\text{F}$ (21.11°C). The gas line of internal diameter $d = 1$ in (25.4 mm) broke off completely at the nozzle (well-rounded inlet) and air started to leak into the surroundings at the atmospheric pressure of $p_{\text{atm}} = 14.7$ psia (1.01 bar). Assume that due to a slow process of air expansion in the vessel, while the pressure within the vessel drops, its temperature remains constant (the vessel is not insulated, and air is absorbing heat from surroundings through the vessel walls). Also, assume that the air expansion in the nozzle is isentropic.

Calculate:

1. Time t_A required to reach the pressure $p_A = 50$ psia (3.45 bar) within the vessel
2. Time t_B required to reach the pressure $p_B = 20$ psia (1.38 bar) within the vessel

Solution:

1. For air ($k = 1.4$), the critical pressure ratio [Eq. (B8.54)] is

$$\beta_s = 0.5283$$

At the end of the time period t_A the nozzle pressure ratio is

$$\frac{p_{\text{atm}}}{p_A} = \frac{14.7}{50} = 0.294 < 0.5283$$

TABLE B8.15 Restriction Orifice Plates: Pressure-Temperature Ratings. Allowable Differential Pressures Across the Orifice Plate. Plate Material: Carbon Steel or Chrome-Moly

Pipe size, NPS	Orifice plate OD, in	Temp. °F	Pressure, psi						
			Plate thickness, in						
			1/8 in	3/16 in	1/4 in	5/16 in	3/8 in	7/16 in	1/2 in
		300	333	748	1330	2078	—	—	—
1½	2⅞	600	283	637	1133	1770	2549	—	—
		900	149	335	596	932	1342	1826	2385
		300	214	482	857	1339	1928	2624	—
2	3⅝	600	182	411	730	1140	1642	2235	—
		900	96	216	384	600	864	1176	1536
		300	146	329	585	914	1316	1791	2339
2½	4⅛	600	125	280	498	778	1121	1525	1992
		900	66	147	262	410	590	803	1049
		300	99	222	395	616	888	1208	1578
3	5	600	84	189	336	525	756	1029	1344
		900	44	99	177	276	398	542	707
		300	59	134	239	373	537	731	955
4	6 3/16	600	50	114	203	317	457	623	813
		900	26	60	107	167	241	328	428
		300	28	62	110	172	248	337	440
6	8½	600	23	53	94	147	211	287	375
		900	12	28	49	77	111	151	197
		300	16	37	65	102	146	199	260
8	10⅝	600	14	31	55	86	125	169	221
		900	7	16	29	46	66	89	117
		300	10	24	42	65	94	128	167
10	12¾	600	9	20	36	56	80	109	142
		900	5	11	19	29	42	57	75
		300	7	17	30	46	67	91	119
12	15	600	6	14	25	40	57	78	101
		900	3	7	13	21	30	41	53
		300	6	14	25	39	55	76	99
14	16¼	600	5	12	21	33	47	64	84
		900	3	6	11	17	25	34	44
		300	5	11	19	30	42	58	76
16	18½	600	4	9	16	25	36	49	64
		900	2	5	9	13	19	26	34
		300	4	8	15	23	34	46	60
18	21	600	3	7	13	20	29	39	51
		900	2	4	7	10	15	20	27
		300	3	7	12	19	27	37	48
20	23	600	3	6	10	16	23	32	41
		900	1	3	5	8	12	17	22
		300	2	6	10	16	22	31	40
22	25¼	600	2	5	9	13	19	26	34
		900	1	3	4	7	10	14	18
		300	2	5	8	13	19	26	34
24	27¼	600	2	4	7	11	16	22	29
		900	1	2	4	6	8	12	15

Temperature conversion: $t_C = (t_F - 32.0)/1.8$
1 inch = 25.4 mm
For pressure conversion see Table B8.1.
Source: Stone & Webster.

and therefore Eq. (B8.56) is here applicable. This means that the decrease in mass inventory of air in the vessel in time interval t_A may be expressed by the following differential equation:

$$dm = -\dot{m}_{s\,\max}\,dt = -\Psi_{s\,\max}\,A_2\,\frac{p}{\sqrt{RT_0}}\,dt \qquad (a)$$

Under assumption of T_0 = const, the following is also true (the Clapeyron equation):

$$dm = \frac{V_{\text{vess}}}{RT_0}\,dp \qquad (b)$$

Then, from Eqs. (*a*) and (*b*), the following is derived:

$$dt = -\frac{V_{\text{vess}}}{\Psi_{s\,\max}\,A_2\,\sqrt{RT_0}}\,\frac{dp}{p} \qquad (c)$$

For $k = 1.4$, Eq. (B8.55) yields

$$\Psi_{s\,\max} = 3.8839$$

The nozzle flow area is

$$A_2 = \frac{\pi d^2}{4} = 0.00545\ \text{ft}^2$$

For air $R = 53.35\ (\text{lb}_\text{f}\cdot\text{ft})/(\text{lb}_\text{m}\cdot{}^\circ\text{R})$. Then, substituting all partial results into Equation (*c*), the following is found:

$$dt = -\frac{80}{(3.8839)\,(0.00545)\sqrt{(53.35)\,(460+70)}}\,\frac{dp}{p} = -22.476\,\frac{dp}{p}$$

and after integration:

$$t_A = 22.476 \ln\frac{p_0}{p_A} = 22.476 \ln\left(\frac{250}{50}\right) = 36.17\ \text{s}$$

2. As long as the pressure in the vessel is higher than

$$p_{\text{lim}} = \frac{p_{\text{atm}}}{\beta_s} = \frac{14.7}{0.5283} = 27.825\ \text{psia}$$

the air flow through the nozzle may be calculated by using Eq. (B8.56). For lower pressures in the vessel, however, the flow rate may be determined by using

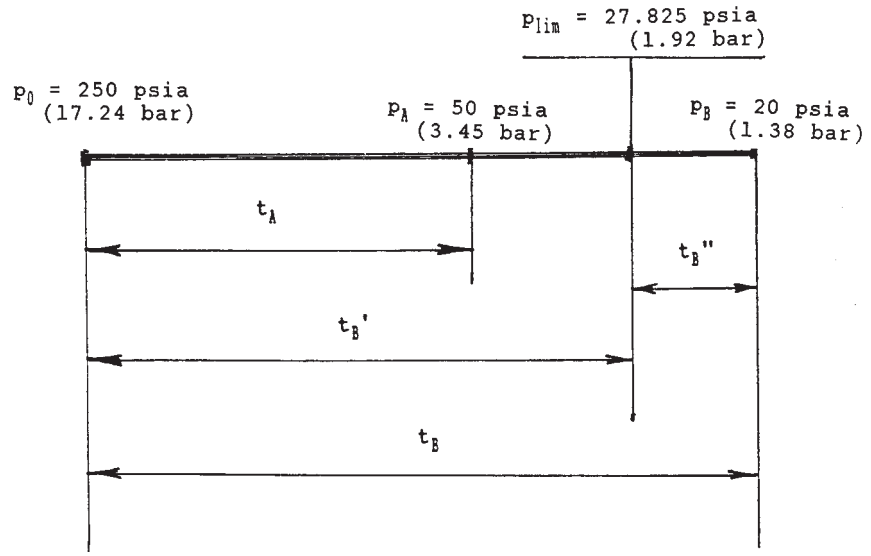

FIGURE B8.27 Various time intervals before reaching the final pressure p_B within the vessel.

Eq. (B8.57). Therefore, the time interval before reaching the pressure p_B should be divided into two steps (see Fig. B8.27). In the first step, the above written Eq. (*c*) is still valid. For this step:

$$t'_B = 22.476 \ln\left(\frac{250}{27.825}\right) = 49.35 \text{ s}$$

For the second step the following differential equation holds [see Eq. (B8.56) and the Bendemann ellipse Eq. (B8.57)]:

$$dm = -\Psi_{s\,\max} A_2 \frac{p}{\sqrt{RT_0}} \sqrt{1 - \left[\frac{p_{\text{atm}} - \beta_s p}{p(1-\beta_s)}\right]^2}\, dt \qquad (d)$$

Then, combining Eqs. (*b*) and (*d*), the following is found:

$$dt = -22.476 \frac{dp}{p\sqrt{1 - \left[\dfrac{p_{\text{atm}} - \beta_s p}{p(1-\beta_s)}\right]^2}} \qquad (e)$$

and after integration:

$$t''_B = -22.476 \frac{1}{\sqrt{-a}} \left[\sin^{-1} \frac{-(b + 2ap_B)}{\sqrt{b^2 - 4ac}} - \sin^{-1} \frac{-(b + 2ap_{\text{lim}})}{\sqrt{b^2 - 4ac}}\right] \qquad (f)$$

where

$$a = \frac{1 - 2\beta_s}{(1 - \beta_s)^2} = -0.2544 \qquad (g)$$

$$b = \frac{2\beta_s p_{atm}}{(1 - \beta_s)^2} = 10{,}052 \text{ lb}_f/\text{ft}^2 \qquad (h)$$

$$c = -\left[\frac{p_{atm}}{1 - \beta_s}\right]^2 = -20{,}138{,}536 \text{ (lb}_f/\text{ft}^2)^2 \qquad (i)$$

After substituting items (*g*), (*h*), (*i*) into Eq. (*f*), the following time interval is found:

$$t_B'' = 7.66 \text{ s}$$

Therefore, the total evacuation time from initial pressure in the vessel, $p_0 = 250$ psia (17.24 bar) to pressure $p_B = 20$ psia (1.38 bar) is equal to

$$t_B = t_B' + t_B'' = 49.35 + 7.66 = 57.01 \text{ s}$$

For those who prefer to work with computers instead of solving differential equations, there is an option of solving this problem by using numerical analysis. Choosing a sufficiently small time step, and in each step balancing the system thermodynamically, while the outflow progresses (DO LOOP), the time of reaching the critical pressure ratio (or any pressure within the vessel) may be monitored by using appropriate WRITE statements.

STEADY TWO-PHASE FLOW

Introduction

A *phase* is simply one of the states of matter and can be either a gas, a liquid, or a solid. The general subject of two-phase flow includes gas-liquid, gas-solid, and solid-liquid flow.

The term *multicomponent* is used to describe flows in which the phases do not consist of the same chemical substance. In the petrochemical industries many processes involve the evaporation (and condensation) of binary ($n = 2$) and multicomponent mixtures. Pure single-component, two-phase flows are those during evaporation and condensation of the same chemical substance. For example, steam-water flow is a single-component, two-phase flow, while air-water is a two-phase, two-component flow.

The main emphasis of the following presentation is on the two-phase flow of water.

Regimes of Gas-Liquid Flow

Description. Cocurrent, simultaneous flows of gases and liquids occur in numerous components of plant equipment such as steam generators, drain lines, and oil and natural gas pipelines.

Ever since the earliest visual observations of two-phase flow, it has been recognized that there are natural varieties of flow patterns. In addition to the random character of each flow configuration, two-phase flows are never fully developed. In fact, the gas phase expands due to the pressure drop along a pipe leading to a modification of the flow structure. The flow pattern depends also upon the geometry changes of a flow channel (bends, valves, etc.). Flow patterns will be classified according to pipe geometry and flow direction (upward, downward, cocurrent, countercurrent), and several shown in Refs. 16 and 17 are discussed in the following subsections.

Upward Cocurrent Flow in Vertical Pipes. The main flow patterns encountered in a vertical pipe are shown in Fig. B8.28.[18] Bubbly flow is certainly the most widely known configuration, although at high velocity its milky appearance prevents it from being easily recognized. Bubbles are spherical only if their diameters do not exceed 1 mm; whereas beyond 1 mm their shape is variable. Roumy[18] distinguishes two bubbly flow patterns. In the *independent bubble configuration,* bubbles are spaced and do not interact with each other. On the other hand, in the *packed configuration,* bubbles are crowded together and strongly interact with each other.

Slug flow is composed of a series of gas plugs. The head of a gas plug is generally blunt, whereas its end is flat with a bubbly wake. A simple visual observation reveals that the liquid film which surrounds a gas plug moves downward with respect to the pipe wall.

Given a constant liquid flow rate, an increase of the gas flow rate leads to a lengthening and a breaking of the gas plugs. The flow pattern evolves toward an annular flow in a chaotic way. This transition configuration is called a *churn flow.*

Dispersed annular flow is characterized by a central gas core loaded with liquid droplets and flowing at a higher velocity than the liquid film which clings to the wall. Droplets are torn off from the crest of the waves which propagate on the surface of the liquid film. They diffuse in the gas core and can eventually impinge

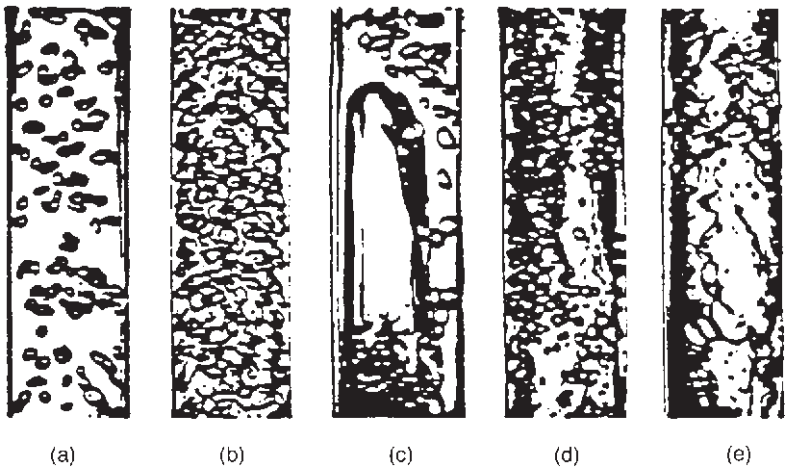

FIGURE B8.28 Upward cocurrent flow in a vertical 32 mm diameter pipe. Air-water flow pattern: (*a*) independent bubbles; (*b*) packed bubbles; (*c*) slug flow; (*d*) churn flow; (*e*) annular flow. (*From Ref. 18.*)

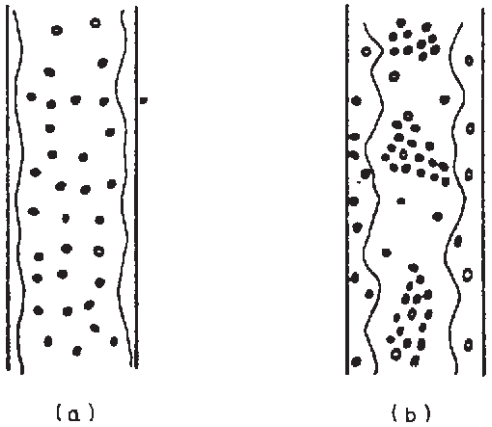

FIGURE B8.29 Annular flows: (*a*) dispersed; (*b*) wispy. (*From Ref. 19.*)

onto the film surface. Hewitt and Roberts[19] evidenced the existence of a wispy annular flow where the liquid droplets gather into clouds within the central gas core (Fig. B8.29).

Finally, if the wall temperature is high enough to vaporize the film, the droplets will constitute a *mist flow*. Figure B8.30 shows the configurations taken by a liquid-vapor flow in a heated pipe as a function of the wall heat flux. The liquid enters the pipe at a constant flow rate and at a temperature lower than the saturation temperature. When the heat flux increases, the vapor appears closer and closer to

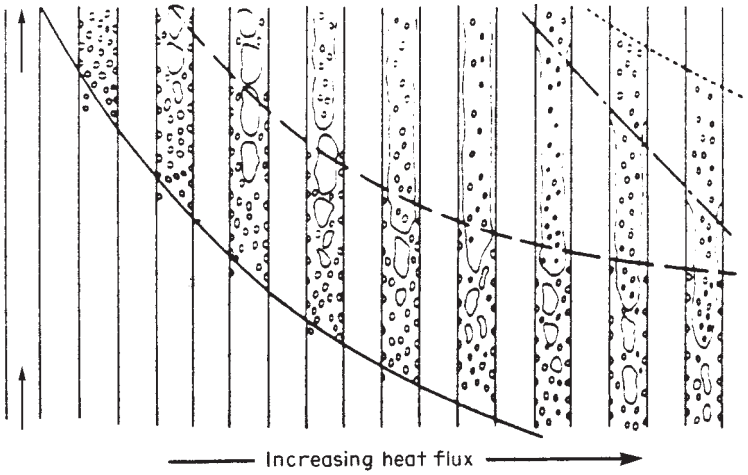

FIGURE B8.30 Convective boiling in a heated channel at a constant liquid flow rate. (—) Onset of nucleate boiling; (— — —) end of nucleate boiling; (—·—·—) Dryout; (---) limit of the superheated region. (*From Ref. 20.*)

the pipe inlet. The *local boiling length* is the extent of pipe where the bubbles are generated at the wall and condense in the liquid core, where the liquid temperature is still lower than the saturation temperature.

The usual way of presenting results of observations of flow patterns is to plot them on a *flow regime map.* A flow map is a two-dimensional representation of the flow pattern existence domains. The coordinate systems are different according to different authors and, so far, there is no agreement on the best coordinate systems. Selecting a series of flow maps is not easy, and no recommendation can be made since no method has proved entirely adequate so far.

Hewitt and Roberts' map (1969) is the most widely used chart for air-water and steam-water flows and is described in Refs. 16 and 17. The steam-water results of Bennett et al., are also well represented in the Hewitt and Roberts' diagram (see Refs. 16 and 17).

Downward Cocurrent Flows in Vertical Pipes. So far the most comprehensive studies of downward cocurrent flow patterns are due to Oshinowo and Charles.[17] These authors distinguish six different flow configurations as shown in Fig. B8.31.

The downward bubbly flow structure is quite different from the upward bubbly flow configuration. In the latter case, bubbles are spread over the entire cross section, whereas in the downward flow, bubbles gather near the pipe axis. This coring effect is similar to the phenomenon observed in a flow of liquid loaded with solid particles whose density is smaller than the liquid density.

When the gas flow rate is increased, the liquid flow rate being held constant, the bubbles agglomerate into large gas pockets. The top of these gas plugs is dome-shaped, whereas the lower extremity is flat with a bubbly zone underneath. This slug flow is generally more stable than in the upward case.

The annular configuration can exhibit several aspects. For small liquid and gas flow rates, a liquid film flows down the wall (*falling film flow*). If the liquid flow rate is higher, bubbles are entrained within the film (*bubbly falling film*). When liquid and gas flow rates are increased a *churn flow* appears, which can evolve into a *dispersed annular flow* for very high gas flow rates.

Oshinowo and Charles proposed a flow map (described in Ref. 17) which was obtained from their own experimental data. They studied two-component mixtures

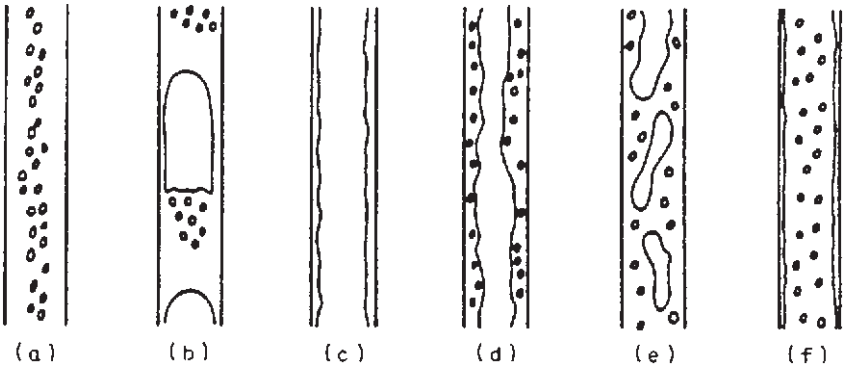

FIGURE B8.31 Downward cocurrent flow in a vertical pipe: air-water flow pattern: (*a*) bubbles; (*b*) slugs; (*c*) falling film; (*d*) bubbly falling film; (*e*) churn; (*f*) dispersed annular. (*From Ref. 21.*)

of air and different liquids flowing in a pipe 1 in (25.4 mm) in diameter at a pressure of around 25 psia (1.7 bar).

Cocurrent Flows in Horizontal and Inclined Pipes. The number of possible flow patterns in a horizontal pipe is higher than in a vertical pipe. This is due to the effect of gravity, which tends to separate the phases and to create a horizontal stratification.

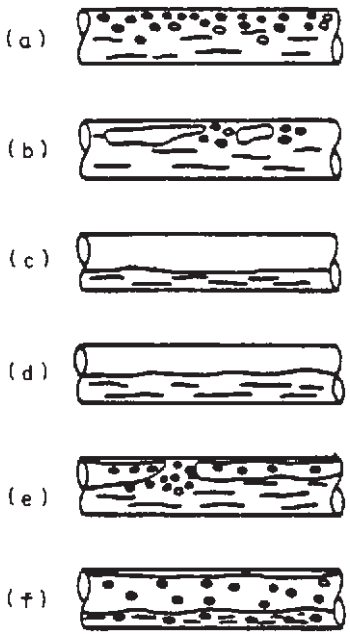

FIGURE B8.32 Flow patterns in a horizontal pipe: (*a*) bubbly flow; (*b*) plug flow; (*c*) stratified flow; (*d*) wavy flow; (*e*) slug flow; (*f*) annular flow. (*From Ref. 22.*)

Alves[22] proposed the classification shown in Fig. B8.32. In the *bubbly flow* configuration bubbles are moving in the upper part of the pipe. When the gas flow rate is increased, bubbles coalesce and a *plug flow* takes place. For low liquid and gas flow rates a *stratified flow* appears with a smooth interface. At higher gas rates waves propagate along the interface (*wavy flow*) and can reach the top wall of the pipe, giving rise to a *slug flow*. Finally, at high gas flow rates and low liquid flow rates an *annular flow* can exist, with a thicker film in the lower part of the pipe. These flow pattern names differ depending on the author. As an example, Taitel and Dukler[23] classed plug flows and slug flows under the same category (intermittent flow).

Figure B8.33 shows the evolution of a *vaporizing flow* in a horizontal pipe. The liquid enters the heated pipe with a low flow rate and at a temperature slightly lower than the saturation temperature. An important point concerns the upper part of the tube, which can dry out periodically and then suffer a sudden increase in wall temperature. If the wall temperature is high enough, the wall dries out completely, and the liquid droplets form a *mist flow*.

The earliest and the most durable of regime maps for two-phase gas-liquid flow in horizontal channels was proposed by Baker, as described in Ref. 24. It is commonly used specially in petroleum industries.

Goldmann[25] converted the Baker plot to a very informative representation of flow patterns for an adiabatic (no heat addition) steam-water system as shown in Fig. B8.34 for three different pressures.

Mandhane et al. (see Ref. 17), constructed a flow-regime map based on 5935 data points, 1178 of which concern air-water flows. Its coordinates are the superficial velocities j_f and j_g (volumetric flow rate of a given phase divided by the total cross-sectional area of pipe) calculated at the test section pressure and temperature.

The general trends of Mandhane's map were utilized by Taitel and Dukler.[23] They developed a theoretical approach for the prediction of transition between flow regimes. This approach also provides considerable insight into the mechanisms of the transitions. The generalized flow regime map for a case of horizontal pipes, proposed by Taitel and Dukler,[23,26] is presented in Fig. B8.35.

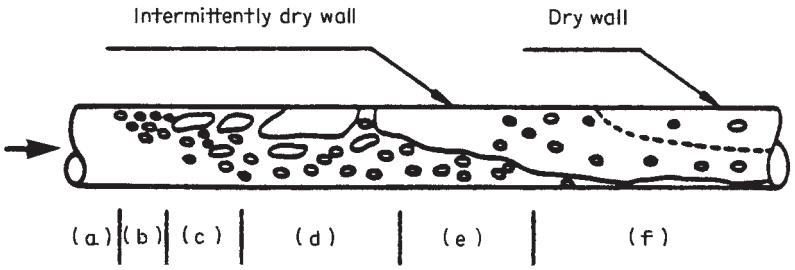

FIGURE B8.33 Evolution of flow pattern in a horizontal evaporator tube: (*a*) Liquid single-phase flow; (*b*) bubbly flow; (*c*) plug flow; (*d*) slug flow; (*e*) wavy flow; (*f*) annular flow. (*From Ref. 17.*)

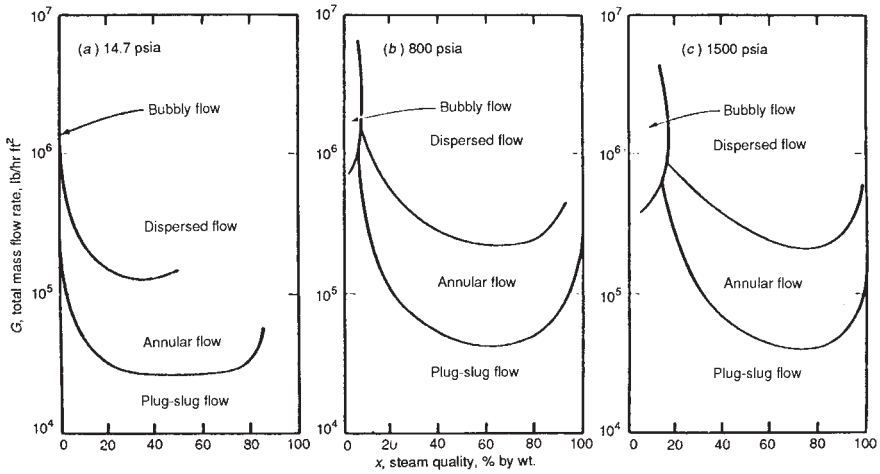

FIGURE B8.34 Flow pattern of two-phase flow. (*From Ref. 25.*)

Mass flux $\dot{G} = \dot{m}/A$ conversion: $1\ lb_m/(ft^2 \cdot h) = 0.0488\ kg/(dm^2 \cdot h)$. For pressure conversion to SI units see Table B8.1.

The five regimes considered are: *intermittent* (slug and plug), *stratified smooth, stratified wavy, dispersed bubble,* and *annular-annular dispersed* liquid flow. The condition of stratified flow is central to this analysis. The first step is to define boundaries of these flow regimes. On the generalized flow regime map the transition boundaries (lines *A, B,* and *D* in Fig. B8.35) between different flow regimes are found to be functions of h_f/D only (see Fig. B8.38). When the theory is solved in dimensionless form the following dimensionless groups emerge: *X, Y, T, F,* and *K.*

All dimensionless flow pattern transition criteria are functions of h_f/D, which in turn is a unique function of the dimensionless groups *X* and *Y,* as shown in Fig. B8.36. Thus the transition from stratified to intermittent and to annular-dispersed liquid is uniquely determined by three dimensionless groups *X, Y,* and *F.* Further, for any specified value of *Y,* the transition is uniquely determined by *X* and *F* and can be represented on a generalized two-dimensional map. For example, for horizontal flow ($Y = 0$) a series of values of *X* were selected, and the corresponding values of h_f/D were determined from Fig. B8.36. Then the value of *F* required to

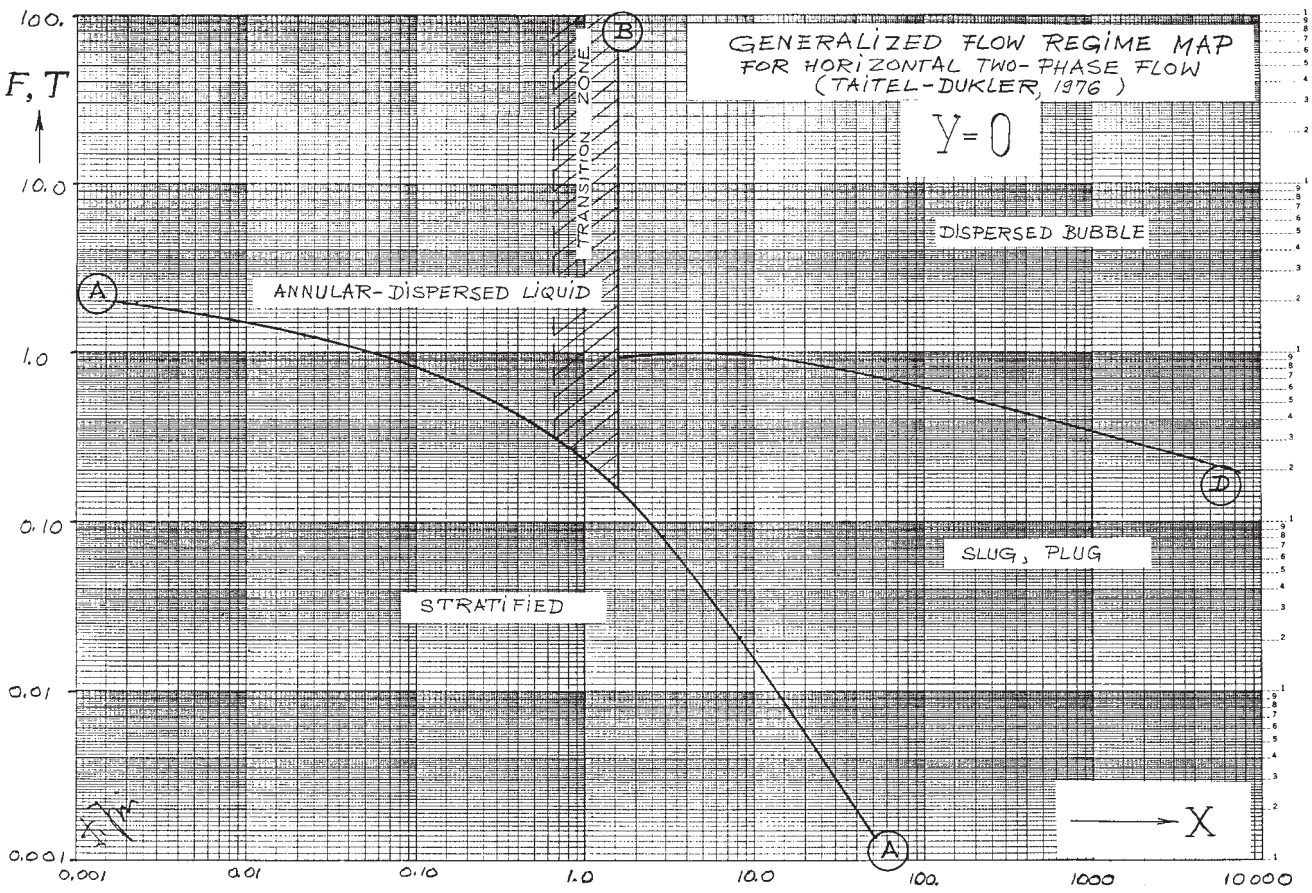

FIGURE B8.35 Generalized flow regime map for horizontal two-phase flow. (*Taitel-Dukler, 1976.*)

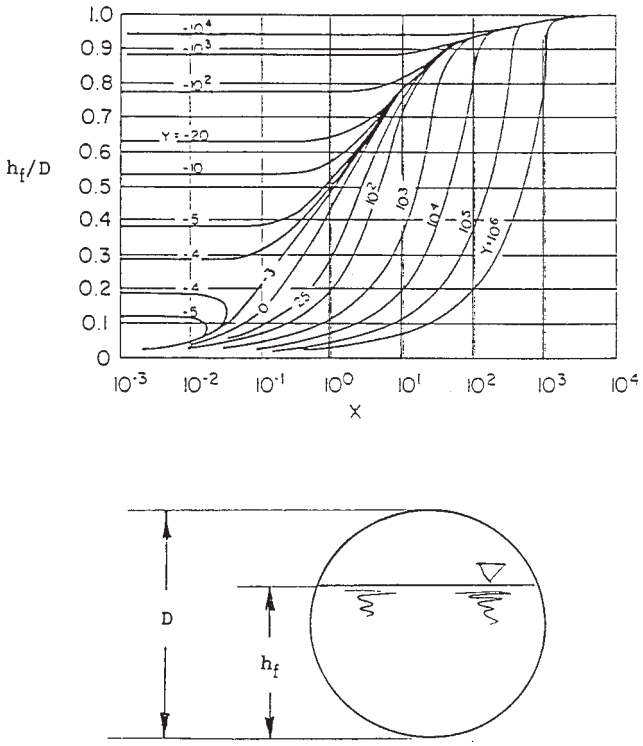

FIGURE B8.36 Equilibrium liquid level as a function of the dimensionless groups X and Y. (*From Ref. 26.*)

satisfy the theoretical transition equation given in the references can be calculated. The curve describing the relation between X and F, which satisfies this theoretical transition equation for horizontal flow, is designated as boundary A in Fig. B8.35. The calculation, as above, may be repeated for inclined pipes with other values of Y specified, by using the corresponding Y-curve in Fig. B8.36.

It is suggested that when the equilibrium liquid level in the pipe is above the pipe centerline, intermittent flow will develop, and if $h_f/D < 0.5$, annular dispersed flow will result. Because transition takes place at constant value of $h_f/D = 0.5$, a specific value of X characterizes the change in regime for any value of Y (see Fig. B8.36). For horizontal pipes ($Y = 0$), this value is $X = 1.6$, and this is plotted in Fig. B8.35 as boundary B. It was observed during experiments that the h_f/D at transition will vary between 0.35 and 0.5. This band of values is shown by the two vertical lines marked B in Fig. B8.35. Visual observations show this transition between the intermittent and annular patterns to be a gradual one that is not well-defined.

For values of X on the right of boundaries A and B in Fig. B8.35, waves will tend to bridge the pipe, forming a liquid slug and an adjacent gas bubble. At high liquid rates and low gas rates, the equilibrium liquid level approaches the top of the pipe, as is apparent from Fig. B8.36. With such a fast-running liquid stream the

gas tends to mix with the liquid, and it is suggested that the transition to dispersed bubble flow takes place when the turbulent fluctuations are strong enough to overcome the buoyant forces tending to keep gas at the top of the pipe. The terms in theoretical transition equation are again dependent only on h_f/D and thus on X and Y. For any specific value of Y, a two-dimensional representation for this transition is possible, with X and T used as the dimensionless coordinates. It is possible to map this transition on Fig. B8.35 by using the common X abscissa and T as an ordinate, as shown by curve D calculated for $Y = 0$.

To find a flow regime for actually existing pipe flow conditions, the dimensional groups X, Y, T, F, and K are calculated from the following equations, and are compared with those values in Fig. (B8.35) which correspond to the appropriate boundary line.

Parameter X, the Lockhart-Martinelli parameter

$$X = \sqrt{\frac{(dp/dz)_f}{(dp/dz)_g}} \tag{B8.64}$$

where the quantities $(dp/dz)_f$ and $(dp/dz)_g$ are the frictional pressure drops of the liquid and gas that would be observed if these fluids were flowing alone in the pipe. The value of X can be calculated with the knowledge of flow rates, fluid properties, and tube diameter (consult the references).

Parameter Y, dimensionless pipe inclination parameter (inclination angle β is positive for downward flow). Y is zero for horizontal pipes and represents the relative forces acting on the liquid in the flow direction due to gravity and pressure drop.

$$Y = \frac{(\rho_f - \rho_g)\, g \sin \beta}{g_c (dp/dz)_g} \tag{B8.65}$$

Parameter T, dimensionless dispersed bubble flow parameter: transition between intermittent (slug/plug) and dispersed bubble regimes

$$T = \sqrt{\frac{g_c (dp/dz)_f}{(\rho_f - \rho_g) g \cos \beta}} \tag{B8.66}$$

Parameter F, transition between stratified and intermittent or annular-dispersed liquid regimes (Froude number modified by density ratio)

$$F = \sqrt{\frac{\rho_g}{\rho_f - \rho_g}} \frac{j_g}{\sqrt{Dg \cos \beta}} \tag{B8.67}$$

Parameter K, (Weber number) dimensionless wavy flow parameter: transition between stratified smooth and stratified wavy regimes (not shown in Fig. B8.35)

$$K = F \sqrt{\frac{D j_f}{\nu_f}} \tag{B8.68}$$

It is, of course, not necessary to use a flow regime map at all. Given any set of flow conditions (gas and liquid rates, pressure, pipe size, and pipe inclination angle:

positive for downward flow), the flow pattern that exists for that condition can be determined by comparing appropriate calculated parameters with corresponding values on the transition lines at evaluated h_f/D, by using hand or computerized calculations based on detailed theoretical equations presented in Refs. 23 and 26, with the help of Fig. B8.36 or its computerized representation.

Countercurrent Flow of Steam and Water in Horizontal and Inclined Pipes. Countercurrent flow of steam and water may exist only when a pipe does not run full. There are two very important areas in a plant design where this kind of flow is carefully studied:

1. Design of self-venting lines where the vapor is not carried down the drainpipe with the liquid, but can rise counter to the liquid flow, continuously venting the pipe
2. Initiation of a condensation-induced water hammer in horizontal or nearly horizontal pipes containing steam and subcooled water

The stratified countercurrent flow of a gaseous phase and a liquid is governed by the open channel flow criterion expressed as a liquid Froude number:

$$\mathrm{Fr} = \frac{j_f}{\sqrt{gD}} \tag{B8.69}$$

The stratified void fraction α in a circular pipe versus dimensionless vapor gap is presented in Fig. B8.37.

The region of condensation-induced water hammer in horizontal and nearly horizontal pipes experiencing the countercurrent flow of steam and subcooled water is bound by the *absolute stability limit* at the lower flow boundary and by the *pipe-full limit* at the upper flow boundary. Bjorge and Griffith presented a one-dimensional, stratified model that predicts initiation of a water hammer in those important cases.[27,28]

Designing self-venting lines is discussed later in this section, while the condensation-induced water hammer is described in the later section ''Steam-Condensation-Induced Water Hammer.''

Pressure Drop in Gas-Liquid Flow (Nonflashing Flow)

The evaluation of the two-phase (TP) pressure drop in an evaporating or condensing channel or in a geothermal pipeline involves integrating the local pressure gradients along the channel length. This local pressure gradient is composed of three terms: a frictional term, an accelerational term, and a static head term[16,17,29]:

$$\left(\frac{\Delta p}{\Delta L}\right)_{\mathrm{TP}} = \left(\frac{\Delta p_F}{\Delta L}\right)_{\mathrm{TP}} + \left(\frac{\Delta p_A}{\Delta L}\right)_{\mathrm{TP}} + \left(\frac{\Delta p_Z}{\Delta L}\right)_{\mathrm{TP}} \tag{B8.70}$$

Using the separated flow (separated phases) model, these three components are respectively given by:

$$\left(\frac{\Delta p_F}{\Delta L}\right)_{\mathrm{TP}} = \Phi_{\mathrm{LO}}^2 \left(\frac{\Delta p_F}{\Delta L}\right)_{\mathrm{LO}} \tag{B8.71}$$

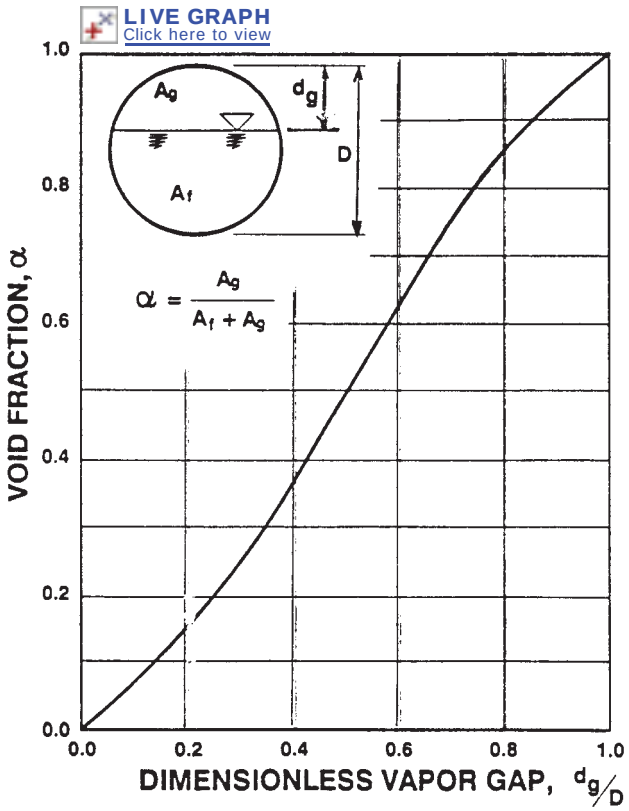

FIGURE B8.37 Void fraction in a circular pipe versus dimensionless vapor gap.

where Φ^2_{LO} is known as the *two-phase frictional pressure drop multiplier,* and $(\Delta p_F/\Delta L)_{LO}$ is the *frictional pressure drop* calculated from the D'Arcy-Weisbach equation for the total flow when the fluid (liquid and steam) is entirely in the liquid phase, as described in the section "Steady Single-Phase Incompressible Flow in Piping":

$$\left(\frac{\Delta p_A}{\Delta L}\right)_{TP} = \frac{\dot{G}^2}{g_c}\frac{\Delta}{\Delta L}\left[\frac{x^2 v_g}{\alpha} + \frac{(1-x)^2 v_f}{1-\alpha}\right] \tag{B8.72}$$

where $\dot{G}$ is the total mass flux, x is the quality, and α is the void fraction;

$$\left(\frac{\Delta p}{\Delta L}\right)_Z = \frac{g}{g_c}\sin\theta\left[\frac{\alpha}{v_g} + \frac{1-\alpha}{v_f}\right] \tag{B8.73}$$

where θ is the angle of pipe inclination to the horizontal.

To evaluate the local pressure gradient, expressions are needed for the functions Φ^2_{LO} and α. A very large number of correlations have been proposed for these functions, and a summary of the better-known correlations is given in Ref. 16. Various studies agree that the most accurate correlations for Φ^2_{LO} are those by

Baroczy, Chisholm, and Lombardi. The most accurate void fraction correlations are those of Smith, Premoli, and Chisholm, with the latter having the added advantage of great simplicity. A void fraction is sometimes expressed in terms of the slip ratio S^* (ratio of the phase velocity of the vapor to that of the liquid):

$$S^* = \left(\frac{x}{1-x}\right)\left(\frac{\rho_g}{\rho_f}\right)\left(\frac{1-\alpha}{\alpha}\right) \tag{B8.74}$$

Baroczy's correlation is widely used in the United States.[30] This correlation may be considered an extension of that of Lockhart and Martinelli, and of Martinelli and Nelson.[29] Baroczy[31] used experimental data in adiabatic conditions where the acceleration pressure drop is zero (the acceleration pressure drop is important in a case of heated channels) and where the gravity pressure drop is either zero (horizontal lines) or could be neglected. This correlation is given in two sets of curves:

1. A plot of the two-phase multiplier Φ^2_{LO} as a function of the property index PI for a fixed mass flux of 10^6 $lb_m/(ft^2 \cdot h)$ [1356 $kg/(m^2 \cdot s)$], as shown in Fig. B8.38, where:

$$\text{PI} = \frac{(\mu_f/\mu_g)^{0.2}}{\rho_f/\rho_g} \tag{B8.75}$$

2. Plots of a correction factor for mass velocity effects, Ω, as a function of the property index and mass flux, are shown in Fig. B8.39. This correction factor multiplies Φ^2_{LO} whenever $\dot{G}$ deviates from 10^6 $lb/(ft^2 \cdot h)$ [1356 $kg/(m^2 \cdot s)$]. Baroczy's correction factor for mass velocity effects varies with mass flux in a rather peculiar manner. Since several investigators have observed changes in pressure-drop behavior characteristics with flow regime, these variations may be related to flow pattern changes.

Baroczy compared his correlation method with experimental data for water-air, water-steam, and other liquids including liquid metals, organic oils, and so forth over a wide range of conditions and found the agreement good.

Critical Gas-Liquid Flow ("Flashing" Flow)

General Remarks. Critical or mass-limiting flow is characteristic of compressible fluid systems. In two-phase flow, a maximum or critical flow rate is also observed. When fluid travels in a horizontal pipeline its pressure decreases until it reaches the pipe exit. If a liquid in the upstream vessel is near the boiling point, its pressure in the pipeline may drop below the saturation point, resulting in vapor formation (*flashing*). Therefore, two-phase flow may occur starting from a certain cross section in the line. There are cases where fluid entering the pipe may already be a liquid-vapor mixture. If the pressure in the downstream receiver is reduced sufficiently to cause the flow velocity at the pipe exit to equal that of the speed of sound at local fluid conditions, the mass flow rate reaches its maximum value, and the flow is said to be *choked.* The maximum flow rate at the choke point is called *critical flow rate.*

At the present, there is no general model or correlation for critical two-phase flow that is valid for a wide range of pipe lengths, pipe diameters, and upstream conditions including subcooled liquid. For these reasons, different models may be

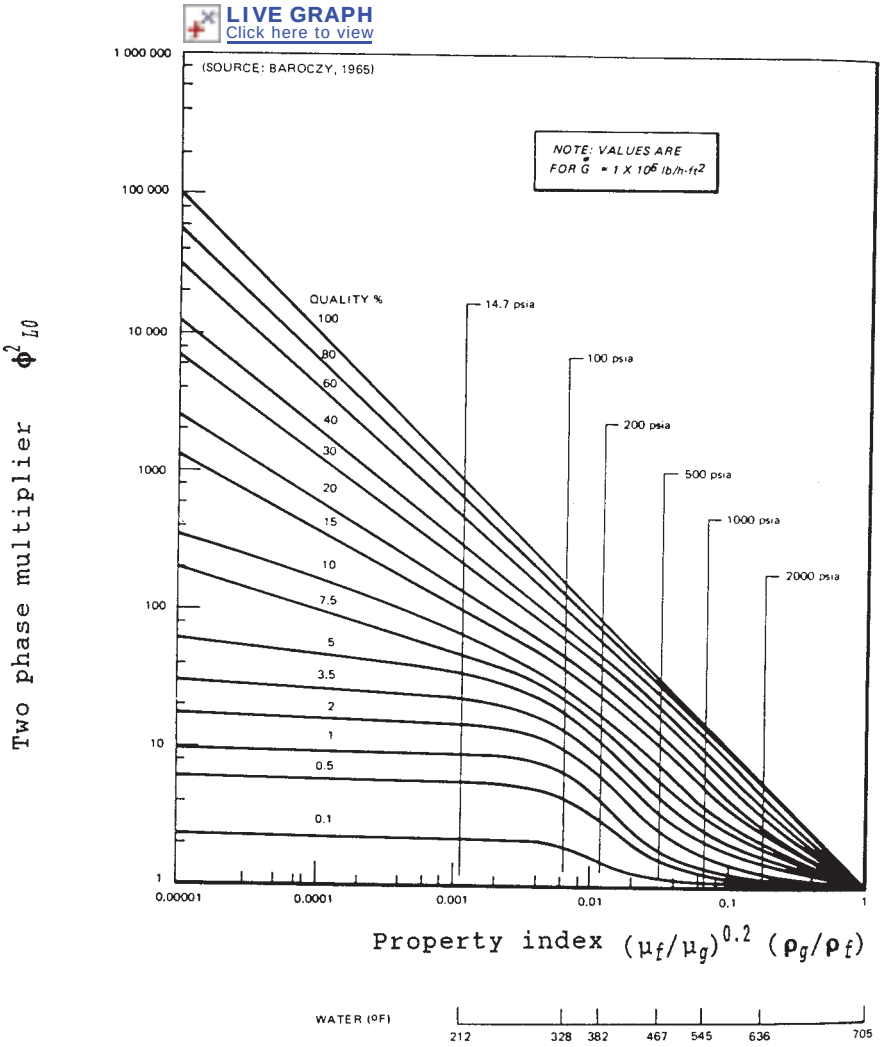

FIGURE B8.38 Baroczy frictional pressure drop correlation for $\dot{G} = 1 \times 10^6$ $lb_m/(ft^2 \cdot h)$; (1356 $kg/(m^2 \cdot s)$). (*From Ref. 31.*)

more appropriate for designing specific two-phase flow discharge systems. The most frequently used models and calculation procedures are described in the following subsections.

Fanno Model (Thermal Equilibrium, Homogeneous). All homogeneous-equilibrium models are based on three assumptions:

1. There is no slip between phases.

2. There is thermodynamic equilibrium between the liquid and vapor at all times.

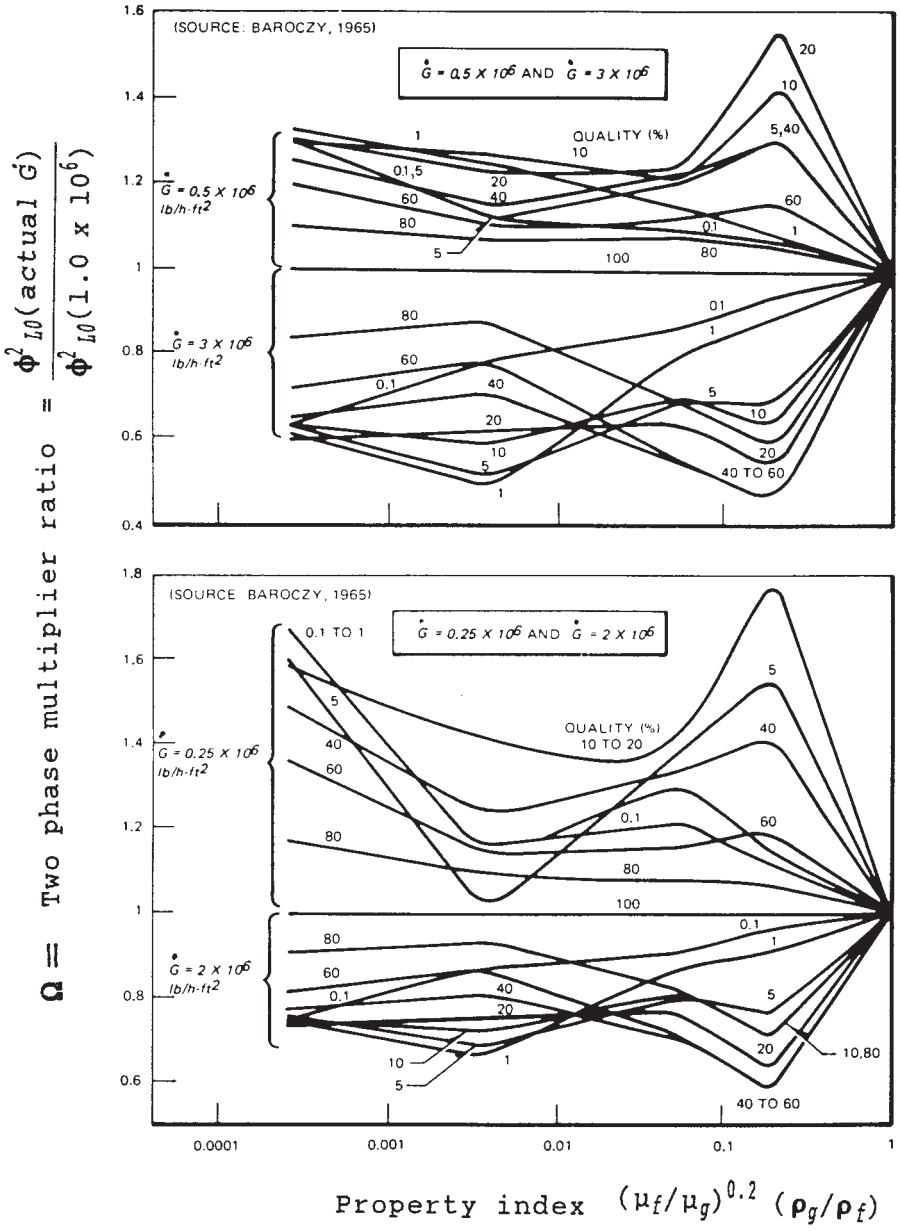

FIGURE B8.39 Baroczy correction factor for mass velocity effects. (*From Ref. 31.*)

3. The specific volume is calculated from equation

$$v = v_f + x(v_g - v_f) \tag{B8.76}$$

Equation (B8.22) represents the Fanno line[10,32] for a single-phase compressible flow, as a locus of conditions in a pipe of constant diameter. Having fixed w_1 and h_1 at the starting point, the stagnation enthalpy h_0 can be calculated. This stagnation enthalpy is constant along the length L of the pipe.

For the two-phase (wet steam) region the following expressions hold

$$h = h_f + h_{fg} \tag{B8.77}$$

$$v = v_f + xv_{fg} \tag{B8.78}$$

$$s = s_f + xs_{fg} \tag{B8.79}$$

From Eqs. (B8.22), (B8.77), and (B8.78), the following is found[32]:

$$x^2 + 2x\left[\frac{v_f}{v_{fg}} + Jg_c\left(\frac{A}{\dot{m}}\right)^2 \frac{h_{fg}}{v_{fg}^2}\right]_x + \frac{(v_f^2)_x - v_1^2 + 2Jg_c\left(\frac{A}{\dot{m}}\right)^2 [(h_f)_x - h_1]}{(v_{fg}^2)_x} = 0 \tag{B8.80}$$

Choosing a set of temperatures (or corresponding saturation pressures) below T_1, the appropriate values of h_f, h_g, v_f, v_g are calculated by using steam tables.[5] Then, solving Eq. (B8.80) for each pressure, the corresponding steam quality x is computed. Each intersection of corresponding x and p values represents the Fanno line point on the h-s diagram. The choked condition at the pipe exit is defined by maximum entropy:

$$\frac{ds}{dh} = 0 \tag{B8.81}$$

The detailed calculation procedures for finding the static pressure p_L at the distance L from the choked exit is the same as described in the subection "Adiabatic, Constant-Area Flow with Friction."

Allen Model (Thermal Equilibrium, Homogeneous). Neglecting potential energy (elevation term), Eq. (B8.11) applied to the one-dimensional, steady-state flow in a channel (no technical work), per unit mass, becomes

$$d\left(\frac{w^2}{2g_c}\right) = -vdp - d'w_f \tag{B8.82}$$

By using the differential form of the D'Arcy-Weisbach equation for work done against fluid friction

$$d'w_f = f\frac{w^2}{2g_c}\frac{dL}{D} \tag{B8.83}$$

and the differential form of the continuity equation (B8.21)

$$dw = \left(\frac{\dot{m}}{A}\right) dv \tag{B8.84}$$

the following result is found[33]:

$$v dp + \left(\frac{\dot{m}}{A}\right)^2 \left(\frac{v dv}{g_c} + \frac{f v^2}{2 g_c D} dL\right) = 0 \tag{B8.85}$$

Dividing Eq. (B8.85) by v^2 and integrating between locations l and x along the pipe, it follows that

$$\left(\frac{\dot{m}}{A}\right)^2 = g_c \frac{\int_{p_1}^{p_x} -\frac{dp}{v}}{\ln \frac{v_x}{v_1} + \frac{fL}{2D}} \tag{B8.86}$$

A similar equation is presented in the paper by Benjamin-Miller.[34]

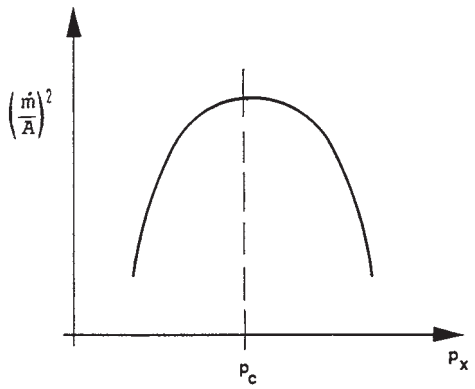

FIGURE B8.40 Function $(\dot{m}/A)^2$ versus pressure.

The function $(\dot{m}/A)^2$ has its maximum value at choked pressure $p_x = p_c$ as illustrated in Fig. B8.40. For a given pipe diameter and piping layout (equivalent length L) the choked pressure may be calculated by assuming a friction factor and evaluating the integral numerically by taking small pressure increments and summing the values $\Delta p/\bar{v}$, where $\bar{v}$ is the average specific volume within the chosen Δp limits.

To evaluate the average specific volume, the Benjamin-Miller method assumes isentropic expansion between pressures p_{x-1} and p_x, while the Allen method assumes isenthalpic expansion between those pressures. Allen suggests in his paper that the difference in specific volume, whether isenthalpic or isentropic expansion is used, will not be large.

Allen found a simple relationship between critical pressure, initial pressure, and the rate of flow:

$$p_c = \frac{\dot{m}}{A} C_A p_1 \tag{B8.87}$$

where

$$C_A = \left[\frac{1}{g_c}\left(\frac{h_{f_1} - h_{f_2}}{p_1 - p_2}\right)\left(\frac{2v_{fg1}}{h_{fg1} + h_{fg2}}\right)\right]^{1/2} \tag{B8.88}$$

In computing the constant C_A, the subscript 1 refers to saturation conditions at the source (say drain cooler exit) temperature, and the subscript 2 refers to saturation conditions an infinitely small amount below this temperature. Practically, a finite interval of one degree less than the temperature at drain cooler exit is recommended for use.

For a given stagnation enthalpy in the upstream source, and for a given mass flux $\dot{m}/A$, the corresponding pipe exit critical pressure may be found using Fig. B8.41.

In order to apply Eq. (B8.86) for finding the pressure at the outlet of the control valve, or at any distance L from choked pipe exit, the value p_x should be replaced by the calculated critical pressure p_c, and Eq. (B8.86) must be solved by trial for $p_1 = p_L$ [convergence on the lower limit of the integral in Eq. (B8.86)].

Allen succeeded in writing Eq. (B8.86) in terms of a single variable by expressing the specific volume of a mixture in terms of pressure. See Ref. 33 for more details.

Note: 1 $lb_m/(ft^2 \cdot s)$ = 4.88 $kg/(m^2 \cdot s)$
For pressure and enthalpy conversions to SI units see Tables B8.1 and B8.3.

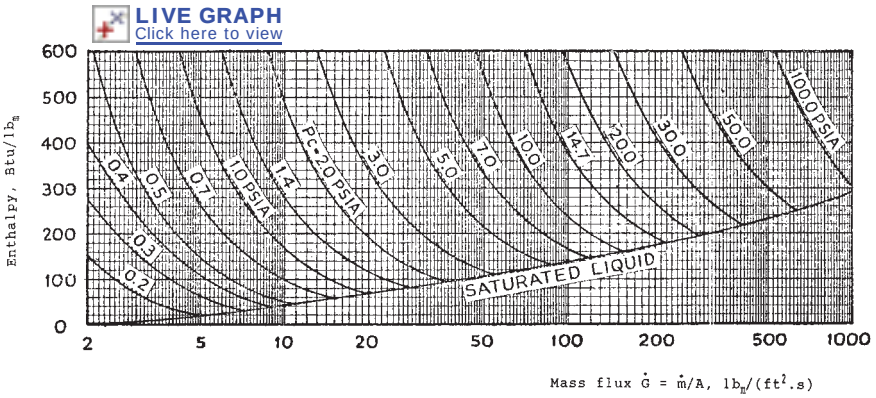

FIGURE B8.41 Pipe exit critical pressures for water-steam mixtures (*Allen Model.*)

Moody Model (Thermal Equilibrium, Nonhomogeneous). Moody considers isentropic expansion of a homogeneous fluid in a converging nozzle (Fig. B8.25). The nozzle may be considered as a pipe of diameter D_2 and length $L = 0$.[35] The two-phase flow pattern at the exit is annular with no entrainment, but the exit velocities of each phase may differ, resulting in an exit slip ratio.

The Moody model is based on the same logic as described for the previous homogeneous models, the only difference being that average vapor velocity and

average liquid velocity are not equal (nonhomogeneous annular flow). Moody developed the following expression for $\dot{G}$:

$$\dot{G} = \sqrt{\frac{2Jg_c\left[h_0 - h_f - \frac{h_{fg}}{s_{fg}}(s_0 - s_f)\right]_2}{\left[\frac{S^*(s_g - s_0)v_f}{s_{fg}} + \frac{(s_0 - s_f)v_g}{s_{fg}}\right]_2^2 \left[\frac{s_0 - s_f}{s_{fg}} + \frac{s_g - s_0}{(S^*)^2 s_{fg}}\right]_2^2}} \tag{B8.89}$$

Equation (B8.89) shows that $\dot{G}$ is a function of S^* and p_2 when h_0 and s_0 are known (upstream stagnation properties). The following expression for slip ratio S^* at the maximum flow rate was found:

$$S^* = S_2^* = \left(\frac{v_g}{v_f}\right)_2^{1/3} \tag{B8.90}$$

which indicates that S^* is the function of p_2 only. Then, for known h_0 and s_0, a maximum (choke) value of $\dot{G}_c$ is derived from the relation:

$$\frac{d\dot{G}}{dp_2} = 0 \tag{B8.91}$$

The shape of the $\dot{G}(p_2)$ function is similar to that for homogeneous flow (Fig. B8.26). Exit properties for maximum steam/water discharges $\dot{G}_c$, associated with stagnation enthalpies h_0, are shown in Fig. B8.42.

Mass flux ($\dot{G} = \dot{m}/A$) conversion : 1 $lb_m/(ft^2 \cdot s)$ = 4.88 $kg/(m^2 \cdot s)$
For pressure and enthalpy conversions to SI units see Tables B8.1 and B8.3.

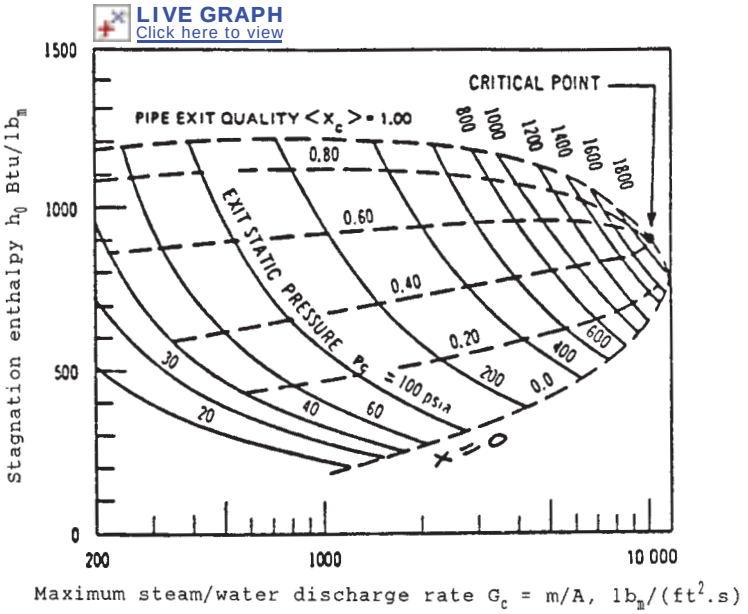

FIGURE B8.42 Exit properties for maximum steam/water discharges (*Moody Model*, from Ref. 29.)

Mass flux ($\dot{G} = \dot{m}/A$) conversion : 1 $lb_m/(ft^2 \cdot s)$ = 4.88 $kg/(m^2 \cdot s)$
For pressure and enthalpy conversions to SI units see Tables B8.1 and B8.3.

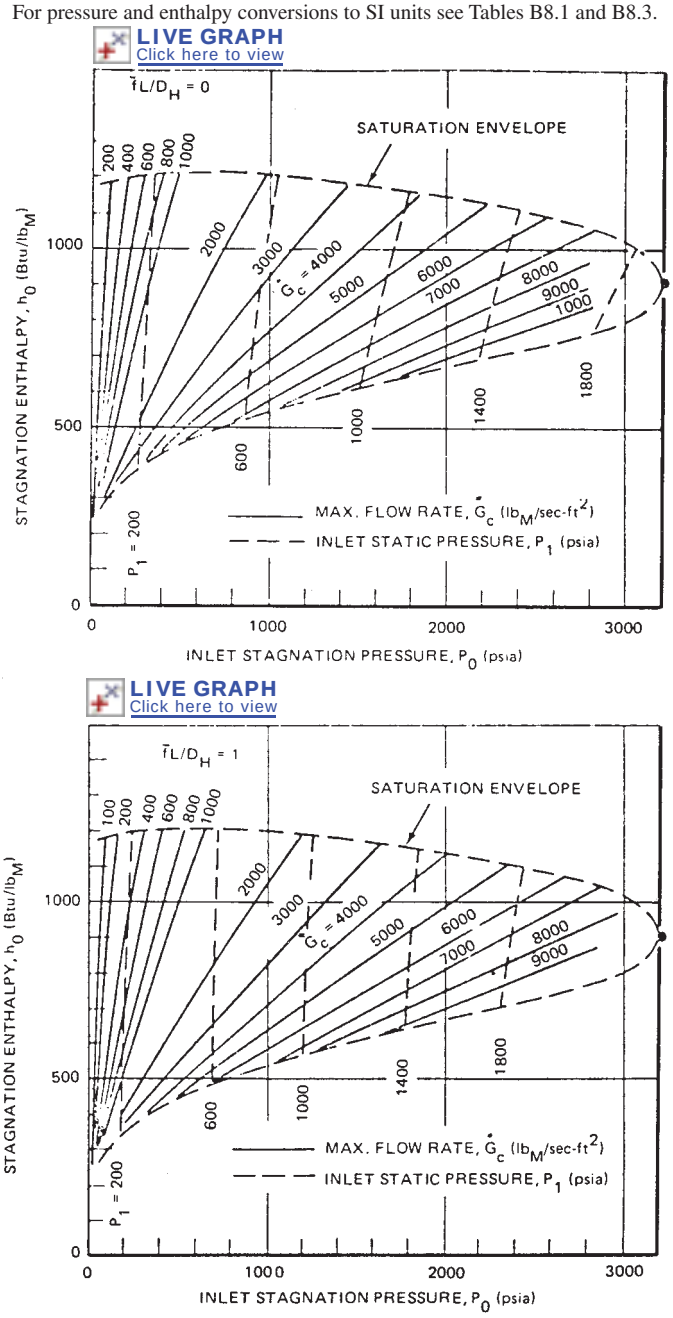

FIGURE B8.43 Pipe maximum steam/water discharge rates (*Moody Model, from Ref. 29.*)

Mass flux ($\dot{G} = \dot{m}/A$) conversion : 1 $lb_m/(ft^2 \cdot s)$ = 4.88 $kg/(m^2 \cdot s)$
For pressure and enthalpy conversions to SI units see Tables B8.1 and B8.3.

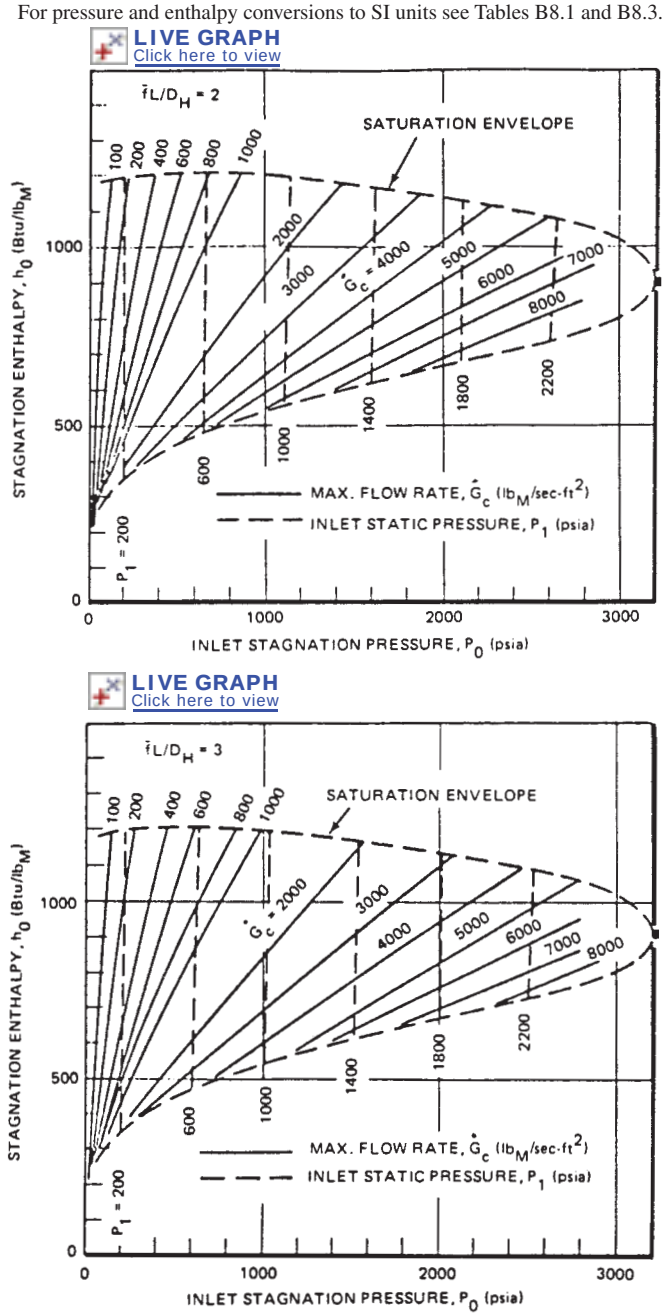

FIGURE B8.43 (*Continued*)

Mass flux ($\dot{G} = \dot{m}/A$) conversion : 1 $lb_m/(ft^2 \cdot s)$ = 4.88 $kg/(m^2 \cdot s)$
For pressure and enthalpy conversions to SI units see Tables B8.1 and B8.3.

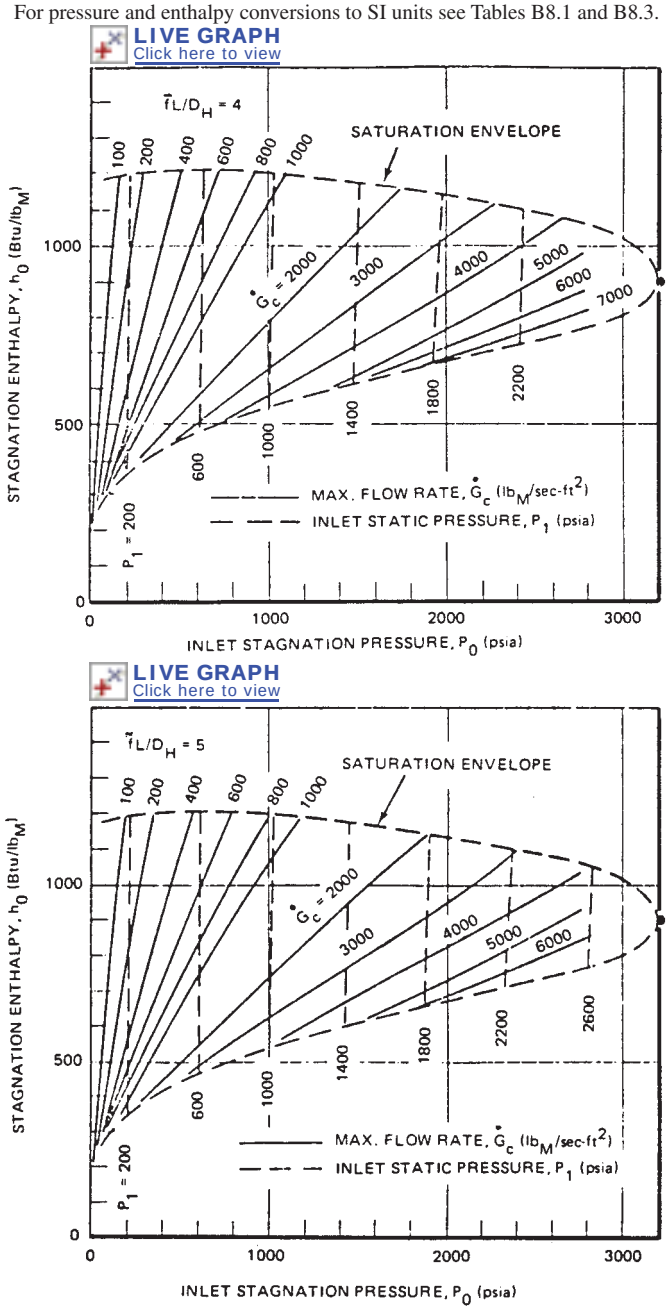

FIGURE B8.43 (*Continued*)

Mass flux ($\dot{G} = \dot{m}/A$) conversion : 1 $lb_m/(ft^2 \cdot s)$ = 4.88 $kg/(m^2 \cdot s)$
For pressure and enthalpy conversions to SI units see Tables B8.1 and B8.3.

LIVE GRAPH
Click here to view

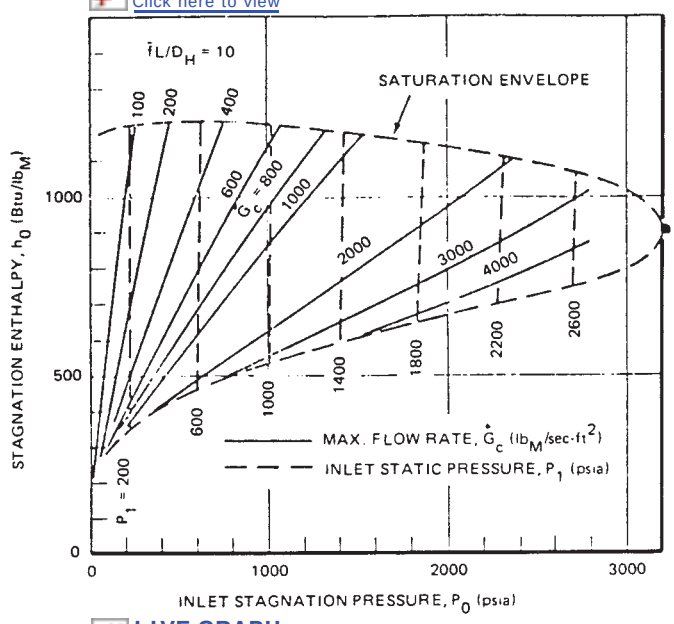

LIVE GRAPH
Click here to view

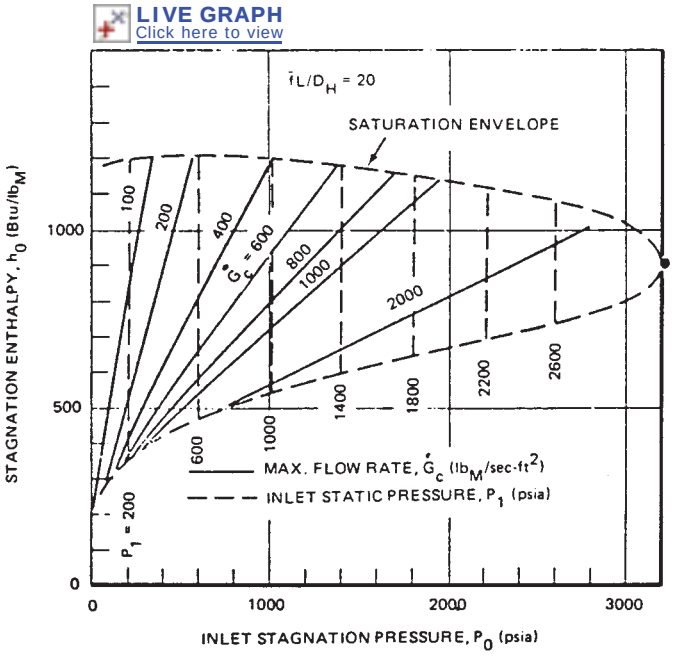

FIGURE B8.43 (*Continued*)

Mass flux ($\dot{G} = \dot{m}/A$) conversion : 1 $lb_m/(ft^2 \cdot s)$ = 4.88 $kg/(m^2 \cdot s)$
For pressure and enthalpy conversions to SI units see Tables B8.1 and B8.3.

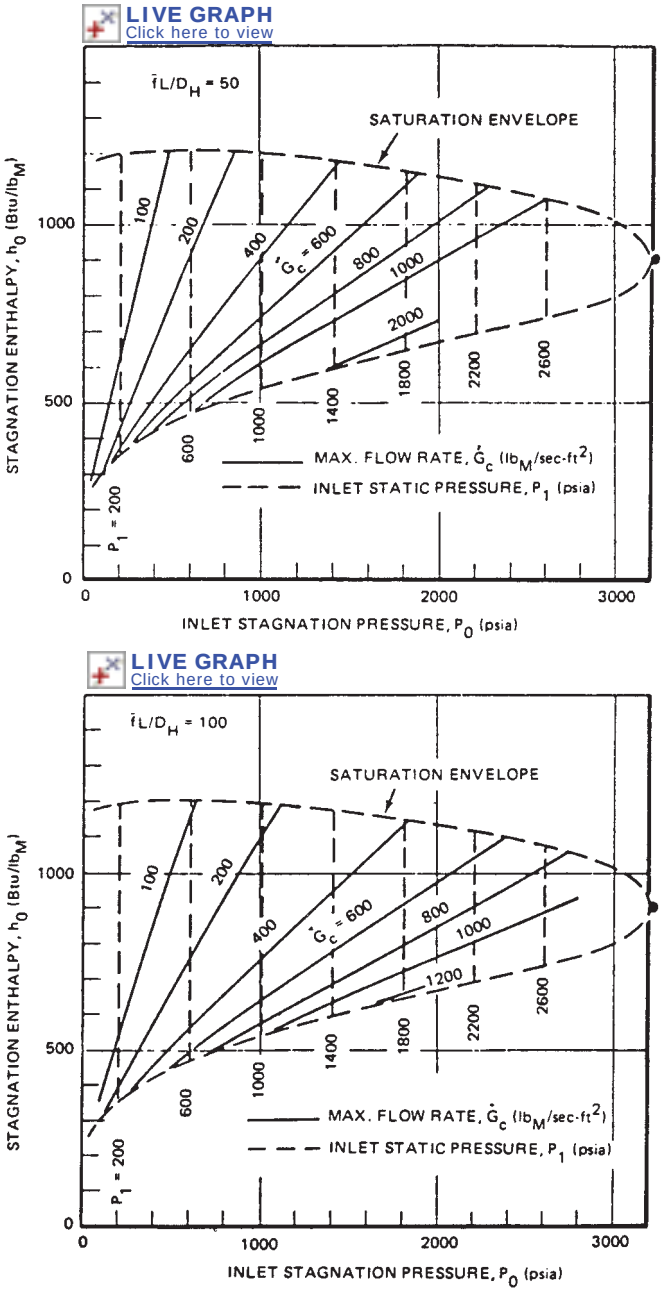

FIGURE B8.43 (*Continued*)

The thermal parameters of the fluid at a distance L from the choked pipe exit are found in a similar way to what is described earlier in the section ''Adiabatic, Constant-Area Flow with Friction.'' Computer solution of numerical integration of equations developed in Ref. 36 leads to graphs expressing the relation between the maximum (critical) two-phase discharge rate $\dot{G}_c$ from uniform pipes and the stagnation pressure p_0, the initial static pressure p_1, the fluid enthalpy h_1, and the pipe characteristics described by $\bar{f}\ L/D_H$. They are presented in Fig. B8.43 (taken from Ref. 29). Here $\bar{f}$ is the average D'Arcy-Weisbach friction factor calculated for the average liquid Reynolds number; L is the pipe length upstream from the choked exit; and $D_H = 4\ A/$(wetted perimeter) is a characteristic linear dimension (for flows in pipes of circular diameter it is equal to the pipe diameter).

References 35, 36, and 37 should be consulted for additional information concerning the development of the Moody Model.

Henry-Fauske Model (Nonequilibrium, Nonhomogeneous). The Henry-Fauske model[38] is of importance for choked two-phase flow through short pipes, nozzles, and orifices, where the fluid transit is short and thermodynamic equilibrium between phases cannot be reached. Since the phases have different densities, the pressure gradient will also tend to accelerate the lighter vapor phase more than the liquid. It is assumed in this model that at throat the actual fluid quality may be determined by introducing a nonequilibrium parameter N.

For a given stagnation condition of p_0 and x_0, the model predicts both the critical (choke) pressure and the flow rate. The theory is extended to subcooled inlet conditions. The calculated mass fluxes $\dot{G}_{\max}$ corresponding to initial stagnation conditions p_0, h_0, in the wet steam and subcooled liquid regions, are presented in Figs. B8.44 and B8.45 (based on Ref. 30). The figures indicate how the max flux $\dot{G}_{\max}$ increases with increased pressure p_0, holding the stagnation enthalpy at the same level [say 500 Btu/lb$_m$ (1163 kJ/kg)]. Steep stagnation pressure lines, especially those below 1100 psia (6.89 bar), in Fig. B8.44 indicate extreme sensitivity to the fluid enthalpy in determining the mass fluxes at low qualities, near the saturation line $x = 0$. Therefore, a very careful estimation of stagnation conditions ahead of a valve, as well as the computerized Henry-Fauske model are helpful in predicting reasonable values of mass fluxes in this wet-steam region. It is the responsibility of the designer to ensure that his or her evaluation yields conservative results.

For a specified inlet stagnation enthalpy h_0 and different stagnation pressures p_0, the values of $\dot{G}_{\max} = (\dot{m}/A)_{\max}$ and the corresponding choke pressures p_c can be found, as they are presented in a sample calculation (Table B8.16 and Fig. B8.46) performed by using a computer program.

The Henry-Fauske theory was developed for two-phase critical discharge of single-component mixture through convergent nozzles. Because the orifices (e.g., valve orifices) cannot be considered as nozzles, a discharge coefficient of 0.84, as recommended in Ref. 37, should be applied. More information on this subject may be found in Ref. 39.

Comparison of Results Generated by Different Models. As mentioned in the section ''General Remarks,'' there is no general model for two-phase critical flow that is valid for all cases of interest. Each model is only applicable for a limited range of parameters. The number of critical flow models available may cause some apprehension when the task of selecting one is approached.

In order to facilitate the selection of an appropriate model for a given problem, some useful graphs are presented in this subsection. Figures B8.47 and B8.48 show the critical (choke) pressure versus stagnation enthalpy for the mass fluxes of 50

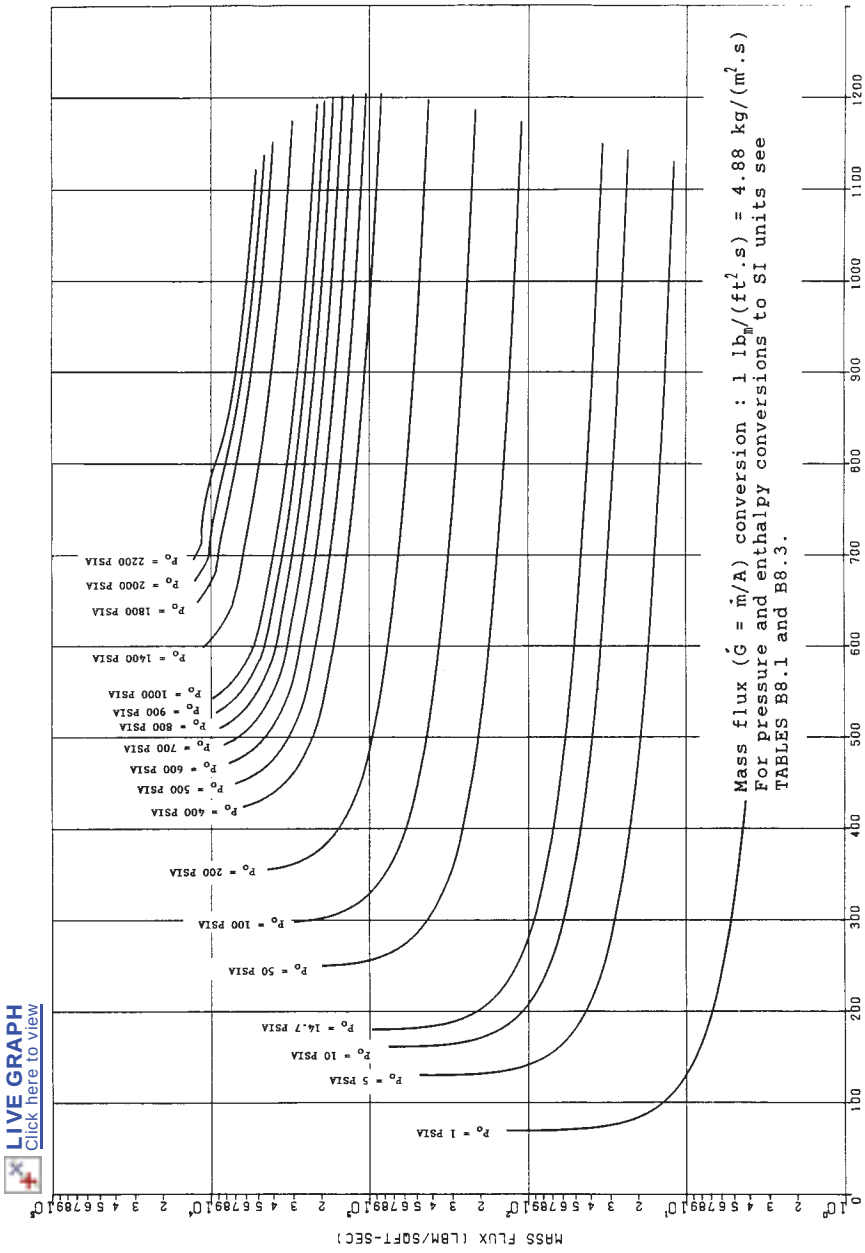

FIGURE B8.44 Two-phase critical flow (*Henry-Fauske Model; data from Ref. 30.*)

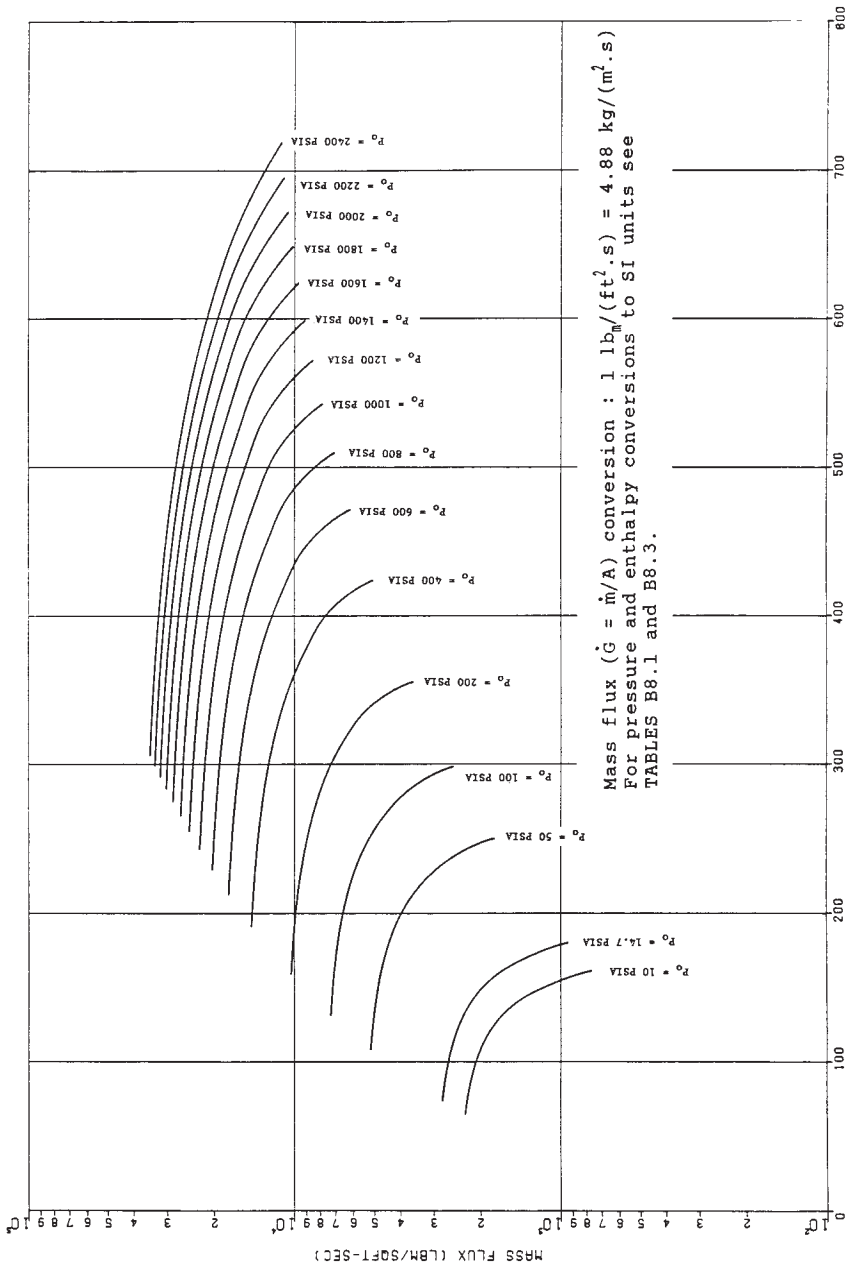

FIGURE B8.45 Subcooled critical flow (*Henry-Fauske Model; data from Ref. 30.*)

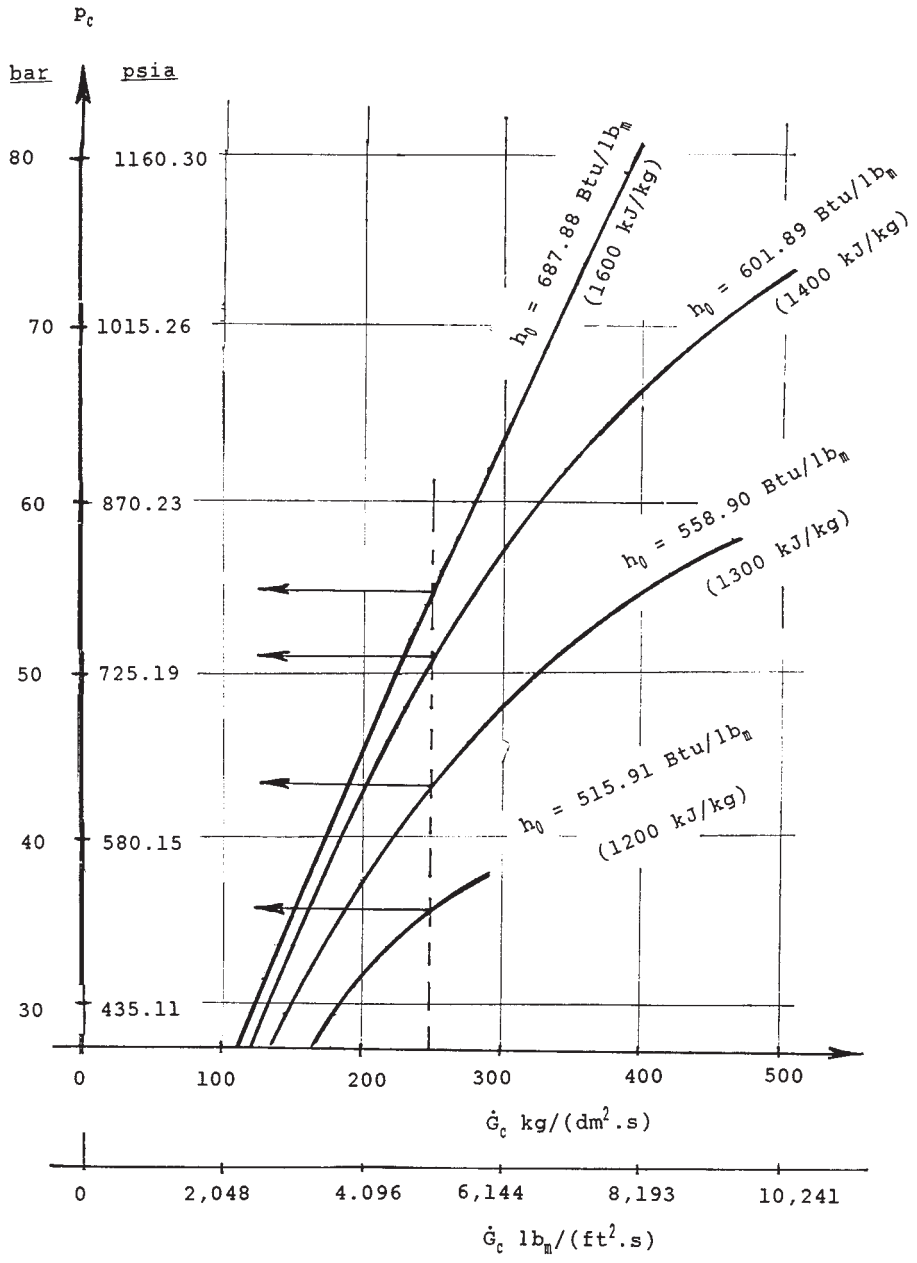

FIGURE B8.46 Critical two-phase flow by Henry-Fauske. (*Line for h_0 = 1400 kJ/kg, based on results from Table B8.16.*)

TABLE B8.16 Computer Printout for Nozzle Inlet Stagnation Enthalpy h_0 = 687.88 Btu/lb_m (1400 kJ/kg) and Various Inlet Pressures p_0 (PZERO). Here: $\dot{G}_{max}$ = GMAX, p_C = PC

HENRY-FAUSKE 2-PHASE CRITICAL FLOW

HZERO = 1400.00 kJ/kg

PZERO	GMAX	PC
bar	kg/(dm2.s)	bar
95.000	502.881	73.694
90.000	437.758	69.825
85.000	384.717	65.869
80.000	340.122	61.855
75.000	301.699	57.806
70.000	267.947	53.740
65.000	239.840	49.304
60.000	215.553	44.587
50.000	169.878	35.748
40.000	128.020	27.651
30.000	90.228	20.150
20.000	56.349	13.121
10.000	26.227	6.445
5.000	12.579	3.206
2.000	4.883	1.283

NOTE: 1 kg/(dm^2.s) = 0.01 kg/(m^2.s) = 20.48 lb_m/(ft^2.s)
For pressure, and enthalpy conversions to other units see TABLES B8.1 and B8.3.

$lb_m/(ft^2 \cdot s)$ [244.12 $kg/(m^2 \cdot s)$] and 600 $lb_m/(ft^2 \cdot s)$ [2929.46 $kg/(m^2 \cdot s)$]. The curves marked by *F, A, M,* and *H-F* represent the values corresponding to the following models respectively, Fanno, Allen, Moody, and Henry-Fauske. Figures B8.49 to B8.52[40] represent a comparison of critical flow rates predicted by various models and their relations to experimental data (also see Ref. 37 and 38 on this subject). The following conclusions can therefore be made:

1. A homogeneous equilibrium theory (Fanno model, Benjamin-Miller model, Allen model) may be used to predict critical flow rates from long pipes ($L/D \geq 40$). This theory provides a lower bound to all presented experimental data. It is generally recognized, however, that this theory underestimates the choked mass flux at low pressures and qualities. As the pressures and qualities increase, the accuracy of the answer improves.[41]
2. The Moody model predicts flow rates higher than those observed for stagnation qualities above 0.01; thus being conservative, it is recommended for U.S. water-reactor licensing calculations (e.g., loss-of-coolant accident—LOCA). It should be explained here that the computer program RELAP4/MOD5[30] is a part of the Nuclear Regulatory Commission's (NRC) water reactor evaluation model

Mass flux ($\dot{G} = \dot{m}/A$) conversion : 1 $lb_m/(ft^2 \cdot s) = 4.88\ kg/(m^2 \cdot s)$
For pressure and enthalpy conversions to SI units see Tables B8.1 and B8.3.

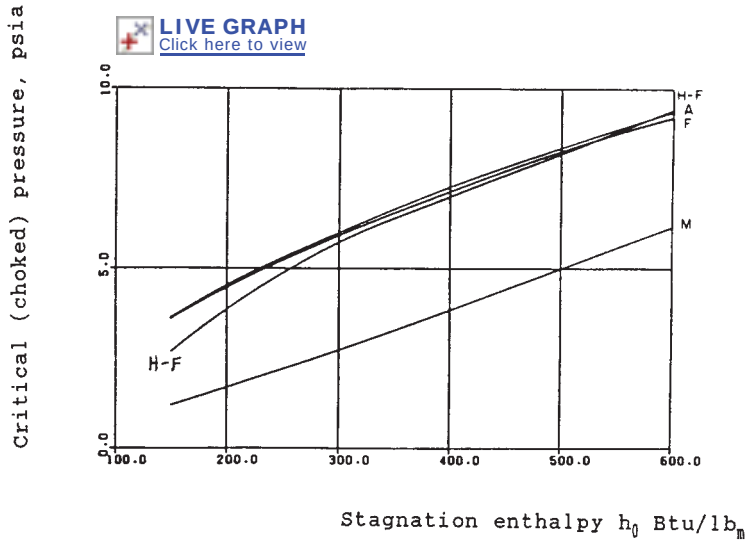

FIGURE B8.47 Predicted critical pressure versus stagnation enthalpy. Mass flux = 50 $lb_m/(ft^2 \cdot s)$. (*Stone & Webster data.*)

Mass flux ($\dot{G} = \dot{m}/A$) conversion : 1 $lb_m/(ft^2 \cdot s) = 4.88\ kg/(m^2 \cdot s)$
For pressure and enthalpy conversions to SI units see Tables B8.1 and B8.3.

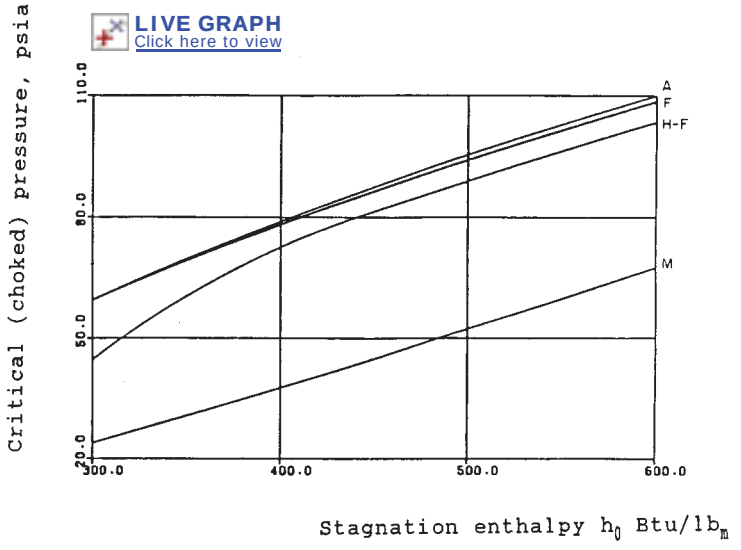

FIGURE B8.48 Predicted critical pressure versus stagnation enthalpy. Mass flux = 600 $lb_m/(ft^2 \cdot s)$ (*Stone & Webster data.*)

Mass flux ($\dot{G} = \dot{m}/A$) conversion : 1 $lb_m/(ft^2 \cdot s) = 4.88\ kg/(m^2 \cdot s)$
For pressure and enthalpy conversions to SI units see Tables B8.1 and B8.3.

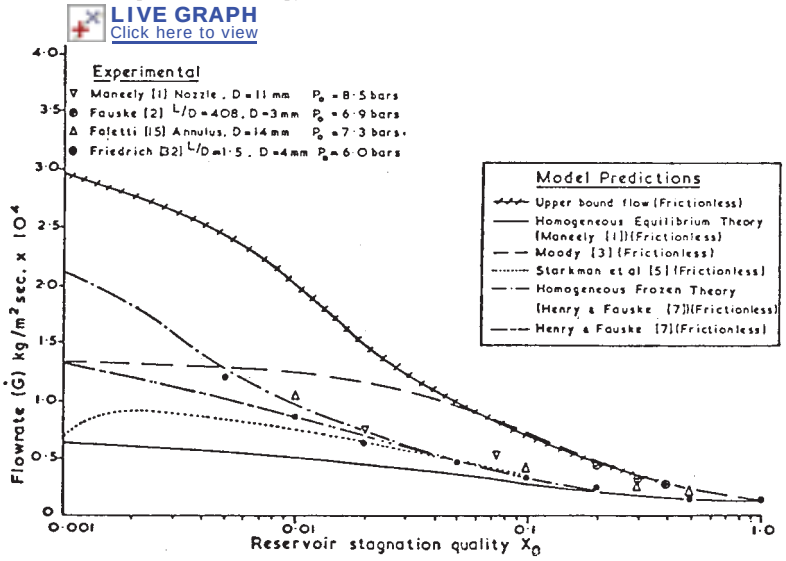

FIGURE B8.49 Comparison of critical flow models with data for p_0 = 100 psia (6.9 bar). (*From Ref. 40.*)

Mass flux ($\dot{G} = \dot{m}/A$) conversion : 1 $lb_m/(ft^2 \cdot s) = 4.88\ kg/(m^2 \cdot s)$
For pressure and enthalpy conversions to SI units see Tables B8.1 and B8.3.

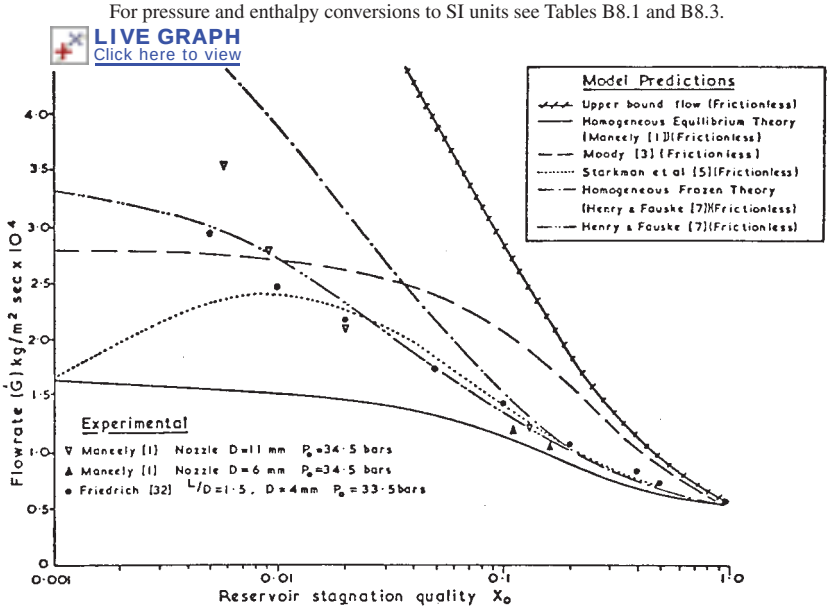

FIGURE B8.50 Comparison of critical flow models with data for p_0 = 500 psia (34.5 bar). (*From Ref. 40.*)

Mass flux ($\dot{G} = \dot{m}/A$) conversion : 1 $lb_m/(ft^2 \cdot s)$ = 4.88 $kg/(m^2 \cdot s)$
For pressure and enthalpy conversions to SI units see Tables B8.1 and B8.3.

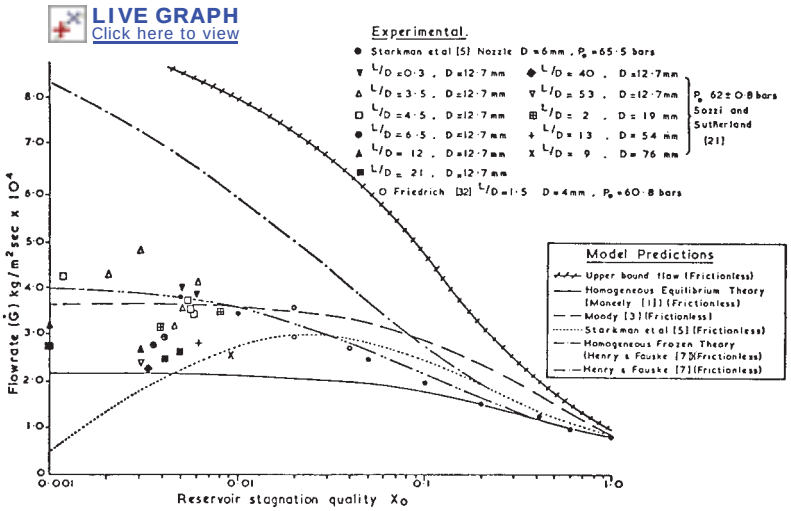

FIGURE B8.51 Comparison of critical flow models with data for p_0 = 900 psia (62 bar) (*From Ref. 40.*)

Mass flux ($\dot{G} = \dot{m}/A$) conversion : 1 $lb_m/(ft^2 \cdot s)$ = 4.88 $kg/(m^2 \cdot s)$
For pressure and enthalpy conversions to SI units see Tables B8.1 and B8.3.

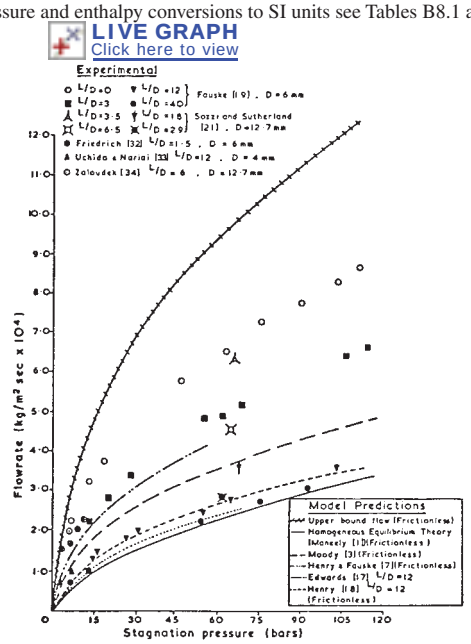

FIGURE B8.52 Discharge of saturated water through orifices, nozzles, and pipes. (*From Ref. 40.*)

(WREM). The critical flow model criterion of the WREM specifies use of the Henry-Fauske model in the subcooled region and the Moody critical flow model in the saturated region. To effect a smooth transition, therefore, the first point in the Moody critical flow tables has been placed in the last portion of the table for the Henry-Fauske critical flow model extended into the subcooled region. This limitation of the subcooled Henry-Fauske table should be realized during RELAP4 calculations.

3. The Henry-Fauske model is in reasonable agreement with short pipe ($L/D < 5$) and nozzle data for qualities greater than 0.001. Below this limit, however, agreement is less satisfactory, and the model underestimates the flow of saturated water through orifices by about 50 percent.

Applications

Design Considerations. Very often, severe problems can occur if slug flow is present in the pipeline. A number of circumstances will lead to the generation of slug flow. For instance, if an oil-gas mixture flows along a pipe on the seabed and then rises to a platform level up a vertical pipe, the liquid may collect upstream of the bend until it reaches a given level, at which point it is swept up the vertical leg, giving rise to mechanical problems in the platform equipment. In power plants, a similar phenomenon may occur in a pocketed line. Also, slug flow causes pressure fluctuations in piping, which can upset process conditions and cause inconsistent instrument sensing.

Existence of two-phase flow in a pipeline may also cause more severe fluid transient problems than occur in a single-phase condition. Should a two-phase flow condition be unavoidable in the system operation, the impact of two-phase flow transient condition should be taken into consideration in system design and piping support evaluation.

Slug flow can be avoided in piping by (1) reducing line sizes to the minimum permitted by available pressure differentials to achieve a safe mass flow rate, as indicated in Fig. B8.34; (2) designing for parallel pipe runs that will permit increasing mass flux per pipe at low load conditions by removing one pipe from service; or (3) arranging the pipe configurations to protect against slug flow (for example, in a pocketed line where liquid might collect and slug flow develop).

Slug flow will not occur in gravity-flow lines when appropriate venting is provided. Figure B8.53(*a*) shows a sketch of a non-self-venting gravity drain from a tank where the drain runs full; hence it requires a separate vent line. Figure B8.53(*b*) shows the typical design of a self-venting gravity drain which does not require a vent, but which usually has a separate vent line to maintain continuous drainage during plant transients. A hard-tee connection (i.e., flow through the branch) at a low point can provide sufficient turbulence for more effective liquid carryover. A diameter adjustment coupled with gas injection can also alter a slug-flow pattern to bubble or dispersed flow. Gas addition, however, when used solely to avoid slug flows, can be expensive.

The design of the transmission and distribution network for large district heating systems often represents more than half of the total investment cost and therefore is of vital importance to the economics of the system.[42] However, it must represent an optimized balance between economics and reliability of supplying heat to customers. From the distribution point of view, the temperature level of hot water in the district heating system should be as high as possible. The flow rates of hot water will then be reduced, the pipe sizes minimized, the pumping cost reduced, and

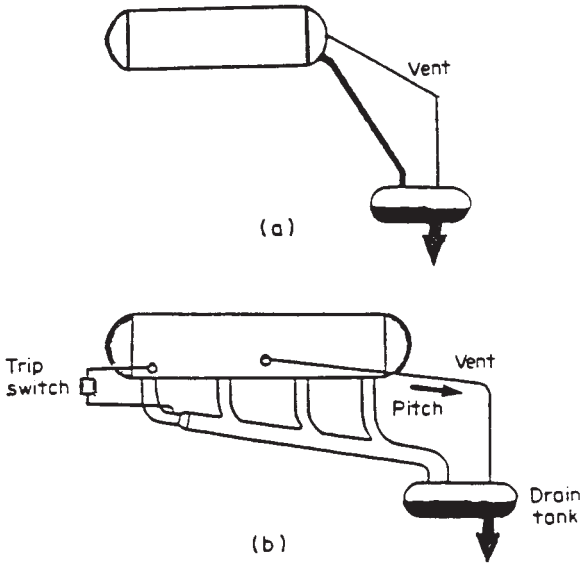

FIGURE B8.53 Drain system requirements: (*a*) design of non-self-venting gravity drains; (*b*) design of self-venting gravity drains.

the heat exchangers in the subscriber's substation will be smaller. The required temperature of the domestic water sets the minimum-possible supply temperature at 160 to 180°F (70 to 80°C). Pressure level at all points in the transmission and distribution network must always be so high that dangerous flashing or creating steam pockets will be avoided. The lowest-possible pressure in the system is therefore determined by the maximum hot water temperature and the minimum static head within the network (highest elevation).

Sample Problems B8.9 and B8.10

Sample Problem B8.9 (Self-venting line). To illustrate the design of a self-venting line, an example of calculating the diameter and minimum slope required to discharge 362,000 lb_m/h (164,200 kg/h) of 200°F (93.33°C) water (approximately 750 gpm) into a tank at ambient pressure is presented.

A properly designed drain line with gravity flow will be self-venting if the liquid Froude number (dimensionless parameter), Eq. (B8.69), is less than approximately 0.3[43]:

$$Fr = \frac{w_L}{\sqrt{gD}} \leq 0.3 \qquad (a)$$

where g = 32.174 ft/s^2 (9.80665 m/s^2) acceleration due to gravity
D = inside pipe diameter, ft (m)
w_L = velocity the liquid would have in the pipe flowing full with the given flow rate, ft/s (m/s)

$$w_L = \frac{(362{,}000\ \text{lb}_\text{m}/\text{h})\,(0.016637\ \text{ft}^3/\text{lb}_\text{m})}{(3{,}600\ \text{s}/\text{h})\,(\pi D^2/4)}$$

$$w_L = \frac{2.131}{D^2} \qquad (b)$$

Substituting (*b*) into (*a*) yields:

$$0.3 \geq \frac{w_L}{\sqrt{gD}} \geq \frac{2.131}{D^2\sqrt{32.174D}}$$

or:

$D^{2.5} \geq 1.251$, and the diameter of the self-venting line should be

$D \geq 1.094$ ft $= 13.13$ in

Use 14-in Std. pipe; inside diameter $D = 13.25$ in

The minimum slope of a self-venting line may be calculated on the basis of an assumption of constant depth of water in the line. Assuming this depth to be $D/3$, the flow in a pipe may be considered as an open channel flow. The Chezy formula describes velocity in such a flow[1] as:

$$w = C_1\sqrt{r_h(SL)}\ \text{ft/s} \qquad (c)$$

where (SL) = slope of the pipe (channel), ft/ft
$r_h = A_L/O_H$ = hydraulic radius, ft (notice that for a full flow in pipe, $r_h = 0.25\ D$)
A_L = cross-sectional area of liquid in the channel, ft^2
O_H = wetted perimeter of the conduit (the portion of the perimeter where the wall is in contact with the fluid), ft
C_1 = Chezy coefficient

The Chezy coefficient C_1 is described by the widely accepted Manning formula[1]:

$$C_1 = 1.486\,\frac{r_h^{1/6}}{n} \qquad (d)$$

where $n \approx 0.014$ is the Manning roughness factor for a metal conduit.

Formula (*d*), however, must be modified in conjunction with the SI units, to obtain, for an identical input, the same results for the minimum slope SL in both systems of units, the SI and British (the coefficient 1.486 becomes 1.000).

The calculation of the hydraulic radius is performed as follows (see Fig. B8.54 and use geometry formulas from Ref. 44, typical):

For liquid depth ratio $h/D = ⅓$, the length of arc K-N-M subtended by θ

$$S_{K\text{-}N\text{-}M} = D\cos^{-1}\left(1 - \frac{h}{R_D}\right) = 1.2310D\ \text{ft}$$

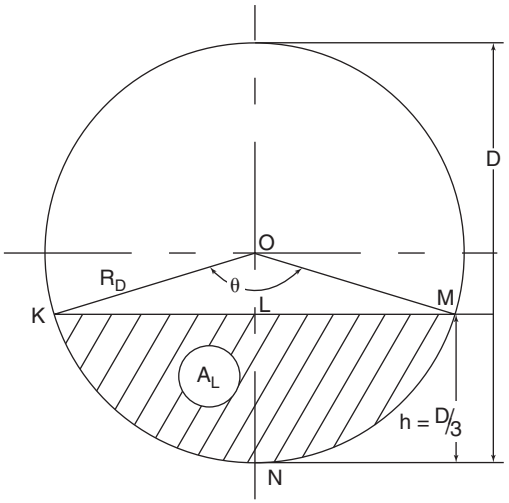

FIGURE B8.54 Cross-section geometry of a self-venting pipe.

the central angle in radians

$$\theta = \frac{S_{K\text{-}N\text{-}M}}{R_D} = \frac{(1.2310)D}{R_D} = (2)(1.2310) = 2.4619 \text{ rad}$$

segment area A_L

$$A_L = \tfrac{1}{2}(\theta - \sin\theta)R_D^2$$

$$A_L = \tfrac{1}{2}(2.4619 - 0.6285)R_D^2 = 0.9167R_D^2 = 0.2794 \text{ ft}^2$$

hydraulic radius

$$r_h = \frac{A_L}{S_{K\text{-}N\text{-}M}} = \frac{0.9167R_D^2}{(1.2310)(2)R_D} = 0.3723R_D = 0.2055 \text{ ft}$$

Then, from (*d*), the Chezy coefficient is equal to:

$$C_1 = \frac{1.486}{0.014}(0.2055)^{1/6} = 81.54$$

The actual flow velocity of liquid in the self-venting line is found from the continuity equation

$$w = \frac{\dot{m}v}{A_L} = \frac{(362{,}000)(0.016637)}{(3600)(0.2794)} = 5.99 \text{ ft/s}$$

Solving the Chezy equation (c) for the slope SL yields

$$(SL) = \frac{w^2}{C_1^2 r_h} = \frac{(5.99)^2}{(81.54)^2(0.2055)} = 0.0263 \frac{\text{ft}}{\text{ft}} = 0.315 \frac{\text{in}}{\text{ft}} \left(26.25 \frac{\text{mm}}{\text{m}}\right)$$

Industrial experience[43] requires the minimum slope for a self-venting line to be not less than 0.5 in/ft (42 mm/m). Therefore, in the case of this problem, the minimum slope should be 0.5 in/ft (42 mm/m).

Sample Problem B8.10 (Fanno Model). Consider a refrigeration system filled with Freon-12. Boiling Freon at initial temperature $t_1 = 104°F$ (40°C) is being throttled in a capillary tube of 0.059 in (1.5 mm) internal diameter at the rate of 22.05 lb_m/hr (10 kg/h). Calculate the choke pressure and the velocity of the fluid at choked-line exit conditions. The properties of refrigerant R-12 are listed in Table B8.17.

Equations (B8.77) through (B8.80) are used to generate the following table. The procedure is explained by calculating results for a chosen Fanno line point at the temperature of 86°F (30°C) (one of those points in Table B8.18):

For saturated conditions at $t = 86°F$, from Table B8.17, the following is found:

$$\begin{aligned} p_{sat} &= 108.04 \text{ psia} \\ v_f &= 0.012396 \text{ ft}^3/\text{lb}_m \\ v_g &= 0.37657 \text{ ft}^3/\text{lb}_m \\ h_f &= 27.769 \text{ Btu/lb}_m \\ h_g &= 85.821 \text{ Btu/lb}_m \\ s_f &= 0.057301 \text{ Btu/(lb}_m \cdot °R) \\ s_g &= 0.16368 \text{ Btu/(lb}_m \cdot °R) \end{aligned}$$

In a similar way, for initial conditions (saturated *liquid* at $t_1 = 104°F$):

$$\begin{aligned} p_1 &= 139.33 \text{ psia} \\ h_1 &= 32.067 \text{ btu/lb}_m \\ v_1 &= 0.012783 \text{ ft}^3/\text{lb}_m \end{aligned}$$

Pipe cross-section area:

$$A = \frac{\pi}{4} \frac{(0.059)^2}{(12)^2} = 0.0000190 \text{ ft}^2$$

Mass flux:

$$\dot{G} = \frac{\dot{m}}{A} = \frac{22.05}{(3600)(0.0000190)} = 322.4 \frac{\text{lb}_m}{(\text{ft}^2 \cdot \text{s})}$$

Equation (B8.80) may be rewritten as:

$$x^2 + Bx + C = 0$$

TABLE B8.17 Properties of Refrigerant R-12, Liquid and Saturated Vapor

Temp (F)	Pressure (lb/sq in.)		Volume (cu ft/lb)		Density (lb/cu ft)		Enthalpy (Btu/lb)			Entropy (Btu/lb-R)		Temp (F)
t	Absolute P	Gage p	Liquid v_f	Vapor v_g	Liquid $1/v_f$	Vapor $1/v_g$	Liquid h_f	Latent h_{fg}	Vapor h_g	Liquid s_f	Vapor s_g	t
−100	1.4280	27.0138*	0.009985	22.164	100.15	0.045119	−12.466	78.714	66.248	−0.032005	0.18683	−100
−98	1.5381	26.7896*	.010002	20.682	99.978	.048352	−12.055	78.524	66.469	−.030866	.18623	−98
−96	1.6551	26.5514*	.010020	19.316	99.803	.051769	−11.644	78.334	66.690	−.029733	.18565	−96
−94	1.7794	26.2984*	.010037	18.057	99.627	.055379	−11.233	78.144	66.911	−.028606	.18508	−94
−92	1.9112	26.0301*	.010055	16.895	99.451	.059189	−10.821	77.954	67.133	−.027484	.18452	−92
−90	2.0509	25.7456*	0.010073	15.821	99.274	0.063207	−10.409	77.764	67.355	−0.026367	0.18398	−90
−88	2.1988	25.4443*	.010091	14.828	99.097	.067441	−9.9971	77.574	67.577	−.025256	.18345	−88
−86	2.3554	25.1255*	.010109	13.908	98.919	.071900	−9.5845	77.384	67.799	−.024150	.18293	−86
−84	2.5210	24.7884*	.010128	13.056	98.740	.076591	−9.1717	77.194	68.022	−.023049	.18242	−84
−82	2.6960	24.4321*	.010146	12.226	98.561	.081525	−8.7586	77.003	68.244	−.021953	.18192	−82
−80	2.8807	24.0560*	0.010164	11.533	98.382	0.086708	−8.3451	76.812	68.467	−0.020862	0.18143	−80
−78	3.0756	23.6592*	.010183	10.852	98.201	.092151	−7.9314	76.620	68.689	−.019776	.18096	−78
−76	3.2811	23.2409*	.010202	10.218	98.021	.097863	−7.5173	76.429	68.912	−.018695	.18050	−76
−74	3.4975	22.8002*	.010221	9.6290	97.839	.10385	−7.1029	76.238	69.135	−.017619	.18004	−74
−72	3.7254	22.3362*	.010240	9.0802	97.657	.11013	−6.6881	76.046	69.358	−.016547	.17960	−72
−70	3.9651	21.8482*	0.010259	8.5687	97.475	0.11670	−6.2730	75.853	69.580	−0.015481	0.17916	−70
−68	4.2172	21.3350*	.010278	8.0916	97.292	.12359	−5.8574	75.660	69.803	−.014418	.17874	−68
−66	4.4819	20.7959*	.010298	7.6462	97.108	.13078	−5.4416	75.467	70.025	−.013361	.17833	−66
−64	4.7599	20.2299*	.010317	7.2302	96.924	.13831	−5.0254	75.273	70.248	−.012308	.17792	−64
−62	5.0516	19.6360*	.010337	6.8412	96.739	.14617	−4.6088	75.080	70.471	−.011259	.17753	−62
−60	5.3575	19.0133*	0.010357	6.4774	96.553	0.15438	−4.1919	74.885	70.693	−0.010214	0.17714	−60
−58	5.6780	18.3607*	.010377	6.1367	96.367	.16295	−3.7745	74.691	70.916	−.009174	.17676	−58
−56	6.0137	17.6773*	.010397	5.8176	96.180	.17189	−3.3567	74.495	71.138	−.008139	.17639	−56
−54	6.3650	16.9619*	.010417	5.5184	95.993	.18121	−2.9386	74.299	71.360	−.007107	.17603	−54
−52	6.7326	16.2136*	.010438	5.2377	95.804	.19092	−2.5200	74.103	71.583	−.006080	.17568	−52
−50	7.1168	15.4313*	0.010459	4.9742	95.616	0.20104	−2.1011	73.906	71.805	−0.005056	0.17533	−50
−48	7.5183	14.6139*	.010479	4.7267	95.426	.21157	−1.6817	73.709	72.027	−.004037	.17500	−48
−46	7.9375	13.7603*	.010500	4.4940	95.236	.22252	−1.2619	73.511	72.249	−.003022	.17467	−46
−44	8.3751	12.8693*	.010521	4.2751	95.045	.23391	−0.8417	73.312	72.470	−.002011	.17435	−44
−42	8.8316	11.9399*	.010543	4.0691	94.854	.24576	−0.4211	73.112	72.691	−.001003	.17403	−42

TABLE B8.17 Properties of Refrigerant R-12, Liquid and Saturated Vapor (*Continued*)

Temp (F)	Pressure (lb/sq in.)		Volume (cu ft/lb)		Density (lb/cu ft)		Enthalpy (Btu/lb)			Entropy (Btu/lb-R)		Temp (F)
t	Absolute P	Gage p	Liquid v_f	Vapor v_g	Liquid $1/v_f$	Vapor $1/v_g$	Liquid h_f	Latent h_{fg}	Vapor h_g	Liquid s_f	Vapor s_g	t
−40	9.3076	10.9709*	0.010564	3.8750	94.661	0.25806	0.0000	72.913	72.913	0.000000	0.17373	−40
−38	9.8035	9.9611*	.010586	3.6922	94.469	.27084	0.4215	72.712	73.134	.001000	.17343	−38
−36	10.320	8.909*	.010607	3.5198	94.275	.28411	0.8434	72.511	73.354	.001995	.17313	−36
−34	10.858	7.814*	.010629	3.3571	94.081	.29788	1.2659	72.309	73.575	.002988	.17285	−34
−32	11.417	6.675*	.010651	3.2035	93.886	.31216	1.6887	72.106	73.795	.003976	.17257	−32
−30	11.999	5.490*	0.010674	3.0585	93.690	0.32696	2.1120	71.903	74.015	0.004961	0.17229	−30
−28	12.604	4.259*	.010696	2.9214	93.493	.34231	2.5358	71.698	74.234	.005942	.17203	−28
−26	13.233	2.979*	.010719	2.7917	93.296	.35820	2.9601	71.494	74.454	.006919	.17177	−26
−24	13.886	1.649*	.010741	2.6691	93.098	.37466	3.3848	71.288	74.673	.007894	.17151	−24
−22	14.564	0.270*	.010764	2.5529	92.899	.39171	3.8100	71.081	74.891	.008864	.17126	−22
−20	15.267	0.571	0.010788	2.4429	92.699	0.40934	4.2357	70.874	75.110	0.009831	0.17102	−20
−18	15.996	1.300	.010811	2.3387	92.499	.42758	4.6618	70.666	75.328	.010795	.17078	−18
−16	16.753	2.057	.010834	2.2399	92.298	.44645	5.0885	70.456	75.545	.011755	.17055	−16
−14	17.536	2.840	.010858	2.1461	92.096	.46595	5.5157	70.246	75.762	.012712	.17032	−14
−12	18.348	3.652	.010882	2.0572	91.893	.48611	5.9434	70.036	75.979	.013666	.17010	−12
−10	19.189	4.493	0.010906	1.9727	91.689	0.50693	6.3716	69.824	76.196	0.014617	0.16989	−10
−8	20.059	5.363	.010931	1.8924	91.485	.52843	6.8003	69.611	76.411	.015564	.16967	−8
−6	20.960	6.264	.010955	1.8161	91.280	.55063	7.2296	69.397	76.627	.016508	.16947	−6
−4	21.891	7.195	.010980	1.7436	91.074	.57354	7.6594	69.183	76.842	.017449	.16927	−4
−2	22.854	8.158	.011005	1.6745	90.867	.59718	8.0898	68.967	77.057	.018388	.16907	−2
0	23.849	9.153	0.011030	1.6089	90.659	0.62156	8.5207	68.750	77.271	0.019323	0.16888	0
2	24.878	10.182	.011056	1.5463	90.450	.64670	8.9522	68.533	77.485	.020255	.16869	2
4	25.939	11.243	.011082	1.4867	90.240	.67263	9.3843	68.314	77.698	.021184	.16851	4
6	27.036	12.340	.011107	1.4299	90.030	.69934	9.8169	68.094	77.911	.022110	.16833	6
8	28.167	13.471	.011134	1.3758	89.818	.72687	10.250	67.873	78.123	.023033	.16815	8
10	29.335	14.639	0.011160	1.3241	89.606	0.75523	10.684	67.651	78.335	0.023954	0.16798	10
12	30.539	15.843	.011187	1.2748	89.392	.78443	11.118	67.428	78.546	.024871	.16782	12
14	31.780	17.084	.011214	1.2278	89.178	.81449	11.554	67.203	78.757	.025786	.16765	14
16	33.060	18.364	.011241	1.1828	88.962	.84544	11.989	66.977	78.966	.026699	.16750	16
18	34.378	19.682	.011268	1.1399	88.746	.87729	12.426	66.750	79.176	.027608	.16734	18
20	35.736	21.040	0.011296	1.0988	88.529	0.91006	12.863	66.522	79.385	0.028515	0.16719	20
22	37.135	22.439	.011324	1.0596	88.310	.94377	13.300	66.293	79.593	.029420	.16704	22
24	38.574	23.878	.011352	1.0220	88.091	.97843	13.739	66.061	79.800	.030322	.16690	24
26	40.056	25.360	.011380	0.98612	87.870	1.0141	14.178	65.829	80.007	.031221	.16676	26
28	41.580	26.884	.011409	0.95173	87.649	1.0507	14.618	65.596	80.214	.032118	.16662	28

* Inches of mercury below one atmosphere.

Temperature conversion: $t_C = (t_F - 32.0)/1.8$.

For pressure, specific volume, enthalpy, and entropy conversions to SI Units see Tables B8.1 through B8.4.

Courtesy of E. I. du Pont de Nemours & Co.

TABLE B8.17 Properties of Refrigerant R-12, Liquid and Saturated Vapor (*Continued*)

Temp (F)	Pressure (lb/sq in.)		Volume (cu ft/lb)		Density (lb/cu ft)		Enthalpy (Btu/lb)			Entropy (Btu/lb-R)		Temp (F)
t	Absolute P	Gage p	Liquid v_f	Vapor v_g	Liquid $1/v_f$	Vapor $1/v_g$	Liquid h_f	Latent h_{fg}	Vapor h_g	Liquid s_f	Vapor s_g	t
30	43.148	28.452	0.011438	0.91880	87.426	1.0884	15.058	65.361	80.419	0.033013	0.16648	30
32	44.760	30.064	.011468	.88725	87.202	1.1271	15.500	65.124	80.624	.033905	.16635	32
34	46.417	31.721	.011497	.85702	86.977	1.1668	15.942	64.886	80.828	.034796	.16622	34
36	48.120	33.424	.011527	.82803	86.751	1.2077	16.384	64.647	81.031	.035683	.16610	36
38	49.870	35.174	.011557	.80023	86.524	1.2496	16.828	64.406	81.234	.036569	.16598	38
40	51.667	36.971	0.011588	0.77357	86.296	1.2927	17.273	64.163	81.436	0.037453	0.16586	40
42	53.513	38.817	.011619	.74798	86.066	1.3369	17.718	63.919	81.637	.038334	.16574	42
44	55.407	40.711	.011650	.72341	85.836	1.3823	18.164	63.673	81.837	.039213	.16562	44
46	57.352	42.656	.011682	.69982	85.604	1.4289	18.611	63.426	82.037	.040091	.16551	46
48	59.347	44.651	.011714	.67715	85.371	1.4768	19.059	63.177	82.236	.040966	.16540	48
50	61.394	46.698	0.011746	0.65537	85.136	1.5258	19.507	62.926	82.433	0.041839	0.16530	50
52	63.494	48.798	.011779	.63444	84.900	1.5762	19.957	62.673	82.630	.042711	.16519	52
54	65.646	50.950	.011811	.61431	84.663	1.6278	20.408	62.418	82.826	.043581	.16509	54
56	67.853	53.157	.011845	.59495	84.425	1.6808	20.859	62.162	83.021	.044449	.16499	56
58	70.115	55.419	.011879	.57632	84.185	1.7352	21.312	61.903	83.215	.045316	.16489	58
60	72.433	57.737	0.011913	0.55839	83.944	1.7909	21.766	61.643	83.409	0.046180	0.16479	60
62	74.807	60.111	.011947	.54112	83.701	1.8480	22.221	61.380	83.601	.047044	.16470	62
64	77.239	62.543	.011982	.52450	83.457	1.9066	22.676	61.116	83.792	.047905	.16460	64
66	79.729	65.033	.012017	.50848	83.212	1.9666	23.133	60.849	83.982	.048765	.16451	66
68	82.279	67.583	.012053	.49305	82.965	2.0282	23.591	60.580	84.171	.049624	.16442	68
70	84.888	70.192	0.012089	0.47818	82.717	2.0913	24.050	60.309	84.359	0.050482	0.16434	70
72	87.559	72.863	.012126	.46383	82.467	2.1559	24.511	60.035	84.546	.051338	.16425	72
74	90.292	75.596	.012163	.45000	82.215	2.2222	24.973	59.759	84.732	.052193	.16417	74
76	93.087	78.391	.012201	.43666	81.962	2.2901	25.435	59.481	84.916	.053047	.16408	76
78	95.946	81.250	.012239	.42378	81.707	2.3597	25.899	59.201	85.100	.053900	.16400	78
80	98.870	84.174	0.012277	0.41135	81.450	2.4310	26.365	58.917	85.282	0.054751	0.16392	80
82	101.86	87.16	.012316	.39935	81.192	2.5041	26.832	58.631	85.463	.055602	.16384	82
84	104.92	90.22	.012356	.38776	80.932	2.5789	27.300	58.343	85.643	.056452	.16376	84
86	108.04	93.34	.012396	.37657	80.671	2.6556	27.769	58.052	85.821	.057301	.16368	86
88	111.23	96.53	.012437	.36575	80.407	2.7341	28.241	57.757	85.998	.058149	.16360	88

TABLE B8.17 Properties of Refrigerant R-12, Liquid and Saturated Vapor (*Continued*)

Temp (F)	Pressure (lb/sq in.)		Volume (cu ft/lb)		Density (lb/cu ft)		Enthalpy (Btu/lb)			Entropy (Btu/lb-R)		Temp (F)
t	Absolute P	Gage p	Liquid v_f	Vapor v_g	Liquid $1/v_f$	Vapor $1/v_g$	Liquid h_f	Latent h_{fg}	Vapor h_g	Liquid s_f	Vapor s_g	t
90	114.49	99.79	0.012478	0.35529	80.142	2.8146	28.713	57.461	86.174	0.058997	0.16353	90
92	117.82	103.12	.012520	.34518	79.874	2.8970	29.187	57.161	86.348	.059844	.16345	92
94	121.22	106.52	.012562	.33540	79.605	2.9815	29.663	56.858	86.521	.060690	.16338	94
96	124.70	110.00	.012605	.32594	79.334	3.0680	30.140	56.551	86.691	.061536	.16330	96
98	128.24	113.54	.012649	.31679	79.061	3.1566	30.619	56.242	86.861	.062381	.16323	98
100	131.86	117.16	0.012693	0.30794	78.785	3.2474	31.100	55.929	87.029	0.063227	0.16315	100
102	135.56	120.86	.012738	.29937	78.508	3.3404	31.583	55.613	87.196	.064072	.16308	102
104	139.33	124.63	.012783	.29106	78.228	3.4357	32.067	55.293	87.360	.064916	.16301	104
106	143.18	128.48	.012829	.28303	77.946	3.5333	32.553	54.970	87.523	.065761	.16293	106
108	147.11	132.41	.012876	.27524	77.662	3.6332	33.041	54.643	87.684	.066606	.16286	108
110	151.11	136.41	0.012924	0.26769	77.376	3.7357	33.531	54.313	87.844	0.067451	0.16279	110
112	155.19	140.49	.012972	.26037	77.087	3.8406	34.023	53.978	88.001	.068296	.16271	112
114	159.36	144.66	.013022	.25328	76.795	3.9482	34.517	53.639	88.156	.069141	.16264	114
116	163.61	148.91	.013072	.24641	76.501	4.0584	35.014	53.296	88.310	.069987	.16256	116
118	167.94	153.24	.013123	.23974	76.205	4.1713	35.512	52.949	88.461	.070833	.16249	118
120	172.35	157.65	0.013174	0.23326	75.906	4.2870	36.013	52.597	88.610	0.071680	0.16241	120
122	176.85	162.15	.013227	.22698	75.604	4.4056	36.516	52.241	88.757	.072528	.16234	122
124	181.43	166.73	.013280	.22089	75.299	4.5272	37.021	51.881	88.902	.073376	.16226	124
126	186.10	171.40	.013335	.21497	74.991	4.6518	37.529	51.515	89.044	.074225	.16218	126
128	190.86	176.16	.013390	.20922	74.680	4.7796	38.040	51.144	89.184	.075075	.16210	128
130	195.71	181.01	0.013447	0.20364	74.367	4.9107	38.553	50.768	89.321	0.075927	0.16202	130
132	200.64	185.94	.013504	.19821	74.050	5.0451	39.069	50.387	89.456	.076779	.16194	132
134	205.67	190.97	.013563	.19294	73.729	5.1829	39.588	50.000	89.588	.077623	.16185	134
136	210.79	196.09	.013623	.18782	73.406	5.3244	40.110	49.608	89.718	.078489	.16177	136
138	216.01	201.31	.013684	.18283	73.079	5.4695	40.634	49.210	89.844	.079346	.16168	138
140	221.32	206.62	0.013746	0.17799	72.748	5.6184	41.162	48.805	89.967	0.080205	0.16159	140
142	226.72	212.02	.013810	.17327	72.413	5.7713	41.693	48.394	90.087	.081065	.16150	142
144	232.22	217.52	.013874	.16868	72.075	5.9283	42.227	47.977	90.204	.081928	.16140	144
146	237.82	223.12	.013941	.16422	71.732	6.0895	42.765	47.553	90.318	.082794	.16130	146
148	243.51	228.81	.014008	.15987	71.386	6.2551	43.306	47.122	90.428	.083661	.16120	148
150	249.31	234.61	0.014078	0.15564	71.035	6.4252	43.850	46.684	90.534	0.084531	0.16110	150
152	255.20	240.50	.014148	.15151	70.679	6.6001	44.399	46.238	90.637	.085404	.16099	152
154	261.20	246.50	.014221	.14750	70.319	6.7799	44.951	45.784	90.735	.086280	.16088	154
156	267.30	252.60	.014295	.14358	69.954	6.9648	45.508	45.322	90.830	.087159	.16077	156
158	273.51	258.81	.014371	.13976	69.584	7.1551	46.068	44.852	90.920	.088041	.16065	158
160	279.82	265.12	0.014449	0.13604	69.209	7.3509	46.633	44.373	91.006	0.088927	0.16053	160

Source: CARRIER—Handbook of Air Conditioning System Design, McGraw-Hill Book Co., 1965.

TABLE B8.18 Calculation Results for Problem B8.10

Pressure psia	Temperature °F	Enthalpy Btu/lb_m	Entropy Btu/($lb_m \cdot$ °R)	Spec. Vol. ft^3/lb_m	Steam quality
139.33	104.00	32.07	0.06492	0.012783	0.00000
122.95	95.00	32.07	0.06502	0.024723	0.03818
108.04	86.00	32.06	0.06517	0.039340	0.07399
94.51	77.00	32.06	0.06539	0.057256	0.10774
82.28	68.00	32.05	0.06566	0.079250	0.13970
71.27	59.00	32.04	0.06600	0.106360	0.17006
61.39	50.00	32.03	0.06640	0.139801	0.19896
52.58	41.00	32.00	0.06686	0.181284	0.22648
44.76	32.00	31.95	0.06737	0.232750	0.25267
37.85	23.00	31.88	0.06791	0.297063	0.27750
31.78	14.00	31.77	0.06897	0.377216	0.30084
26.48	5.00	31.59	0.06846	0.477890	0.32244
21.89	−4.00	31.31	0.06935	0.603310	0.34187
17.94	*−13.00*	*30.87*	*0.06946*	*0.760557*	*0.35839*
14.56	−22.00	30.18	0.06910	0.953742	0.37094
11.71	−31.00	29.13	0.06797	1.189298	0.37809

where

$$B = 2\left[\frac{v_f}{v_g - v_f} + \frac{(Jg_c)}{(\dot{G})^2}\frac{(h_g - h_f)}{(v_g - v_f)^2}\right]$$
$$= 2[0.03404 + 105.300] = 210.7$$
$$C = \frac{v_f^2 - v_1^2 + 2\left(\frac{Jg_c}{\dot{G}}\right)^2(h_f - h_1)}{(v_g - v_f)^2}$$
$$= \frac{(0.012396)^2 - (0.012783)^2 - (2)(0.103394)}{(0.132623)}$$
$$= 0.155923$$

Then, the quality x is equal to

$$x = \frac{-B \mp \sqrt{B^2 - 4C}}{2} = 0.0740$$

and, from Eqs. (B8.77) to (B8.79):

$$h = h_f + x(h_s - h_g) = 32.06 \text{ Btu/lb}_\text{m}$$
$$v = v_f + x(v_s - v_g) = 0.03934 \text{ ft}^3/\text{lb}_\text{m}$$
$$s = s_f + x(s_s - s_g) = 0.06517 \text{ Btu/(lb}_\text{m}\cdot^\circ\text{R)}$$

Similar procedures for other pressures (or temperatures) result in the tabulated values. Sample data in Table B8.18 shows that the maximum entropy is 0.06946 Btu/lb$_m$, the corresponding pressure (critical or choke pressure) is 17.94 psia (1.24 bar), and the corresponding temperature is $t_{exit} = -13°F$ (−25°C). Try to relate the above presented findings to the Fanno line model presented in Fig. B8.16.

The exit velocity of the fluid is calculated from the continuity equation applied to the pipe exit condition:

$$w_{exit} = c = v_{exit}\dot{G} = (0.760557)(322.4) = 245.362 \text{ ft/s } (74 \text{ m/s})$$

TRANSIENT FLOW ANALYSIS

General Background

Hydraulic transient problems in piping systems result from faulty plant design and also from faulty plant operating procedures as, for example, rapid changes in operational functioning of components such as pumps and valves. They may produce rapid momentum changes as the column of water in the system is suddenly stopped or started. Large momentum changes can subject system components to severe force transients, and these must be considered when designing the system to ensure its safe, reliable operation.

Hydraulic transient problems may result in the formation of vapor cavities when the system pressure is reduced to the saturation pressure at a certain fluid temperature. Vapor cavities can easily form in a piping system that has a wide elevation range, if permitted to drain after the system is shut down. This behavior is known as *column separation.* In a large cooling-water system, reclosure of water columns after separation can result in destructive water hammer loads if appropriate design consideration is not given to alleviate these effects.

Analysis of hydraulic transients should be performed for all major plant systems. In addition to the maximum and minimum design pressures for components and the forcing functions for pipe supports, the analysis will help provide appropriate procedures for system startup and shutdown and operator responses to power failure.

Transients that exhibit single-phase flow can be analyzed by one-dimensional wave theory. During a transient condition, pressure waves are generated throughout the system. In complex systems, these waves may be analyzed with the aid of a computer.

Newton's second law, the equation of motion, is a vector relation. Considering the x-direction, a useful working form of the momentum theorem may be written[11]:

$$\Sigma F_x = \frac{d}{dt}\left(\frac{m}{g_c}w_x\right) = \int_{cv}\frac{\partial}{\partial t}\left(\frac{\rho}{g_c}w_x\right)dV + \int\frac{\rho}{g_c}w_n w_x dA_{out} - \int\frac{\rho}{g_c}w_n w_x dA_{in} \qquad \text{(B8.92)}$$

where the left-hand side represents the algebraic sum of the x-forces acting on the system during the time interval dt. By using vector notation, the momentum theorem for a control volume may be represented by a single equation

$$\Sigma \bar{F} = \frac{\partial}{\partial t} \int_{cv} \frac{\rho}{g_c} \bar{w} dV + \int_{cs} \frac{\rho}{g_c} (\bar{w} \cdot \overline{dA}) \bar{w} \qquad \text{(B8.93)}$$

which is the fundamental principle in the dynamics of fluid motion. In words, the resultant force acting on a control volume (*cv*) of the pipe segment is equal to the time rate of increase of linear momentum within the control volume plus the net efflux of linear momentum across the control surface (*cs*) of the pipe segment boundary. The term $\Sigma \bar{F}$ in Equation (B8.93) is the algebraic sum of all forces exerted by the surroundings on the material instantaneously occupying the control volume. These include (1) *body forces* which are proportional either to the volume or mass of the body (e.g., forces of gravitational attraction) and (2) *surface forces* which are exerted at the control surface by the material outside of the control volume on the material inside the control volume (e.g., pressure acting on the control surface). It is generally advantageous to take surface normal to the velocity wherever it cuts across the flow.

The first partial derivative term in Eq. (B8.93) is the average time rate of increase of linear momentum ($m\bar{w}/g_c$) of the system during time Δt. In the limit as Δt approaches zero, it becomes $d/dt(m\bar{w}/g_c)$. In Ref. 29 this term is called the *wave force* F_{wi} on a bounded pipe i-th segment of length L_i. A *segment* (within a control volume) is always defined as a straight pipe between elbows, turns, or between an elbow and piping component or equipment. Fluid acceleration inside the pipe generates forces on all segments that are bounded at either end by an elbow, a turn, or a piping system component.

Immediately following a flow disturbance due to a sudden flow rate reduction (by a rapid control valve adjustment) or flow-rate increase (e.g., a pipe break), a compression or a decompression wave propagates into the fluid contained by the pipe. As the fluid pressure is increased or reduced, its density changes accordingly. The compression or decompression travels at sonic speed through all pipe segments, finally arriving at the vessel where a decompression or compression wave is reflected back toward the disturbance location (valve or a rupture). As compression or decompression waves move through the pipe, the pressure at one end of each segment exceeds the pressure at the other, resulting in net forces F_{wi}.

Successive wave transmissions and associated fluid acceleration forces decay as steady discharge is achieved, and this transient term in Eq. (B8.93) vanishes when steady flow is reached. Although the wave force F_{wi} vanishes at steady flow, the second term in Eq. (B8.93) in Ref. 29, called the *blowdown force,* survives on the discharging segment. This phenomenon will be discussed in more detail in the subsection ''Pipe Rupture.''

Note again, that when steady flow is reached, the wave force vanishes. During steady-state conditions, there is no unbalanced force in the segment. Also, note that a positive segment force acts along the pipe axis opposite to the direction of flow. Equation (B8.93) is valid for bounded pipe regardless of the bend angle at either end of the segment. Large computer programs have been developed to help predict forces generated during postulated hydraulic transients in piping systems.

Pipe Rupture

If a pipe break occurs, thrust and jet forces generated by fluid discharge can cause further damage to piping and other plant components unless adequate mechanical

restrains are employed. Discharging fluid creates a reaction thrust on the ruptured pipe itself and impingement loads on objects struck by the jet of fluid. Moreover, fluid acceleration inside the pipe generates forces on all segments that are bounded at either end by an elbow or turn. Although pipe thrust may basically be considered as a steady-state phenomenon, its initiation is accompanied by a violent transient following the sudden sonic decompression wave starting at the break location.

The mechanics of the steady pipe thrust problem are similar to those involved in rocket propulsion. The steady thrust can be computed as follows. If A, is the exit area (or the area of a break), p_0, is the exit-plane pressure, ρ_e is the density of the escaping fluid to the atmosphere at pressure p_{atm}, $\dot{m}$ is the escaping mass flow rate, and w_0 is the velocity of efflux, the momentum Equation (B8.92) leads to the following expression for the thrust[11]:

$$T = \frac{\dot{m}}{g_c} w_e + (p_e - p_{\text{atm}}) A_e \text{ lb}_\text{f} \tag{B8.94}$$

In a rocket jet engine with a converging-diverging nozzle there is a minimum throat area A_t characterized by the critical pressure ratio and the sonic velocity (Ma = 1). Provided the nozzle is so designed that its enlarged exit area behind the throat (as a Venturi tube) ensures expansion down to pressure $p_0 = p_{\text{atm}}$, prevailing in the external atmosphere, the exit velocity w, becomes supersonic, and the thrust of the engine reaches its maximum. This important conclusion is valid irrespective of the type of fluid considered, whether gaseous or liquid.

If the nozzle were a simple converging nozzle, as it could be considered in a pipe break, A_0 would equal A_t (throat area). After transformation of Eq. (B8.94) by using the *ideal gas* relations, as presented in section "Single-Phase Flow in Nozzles, Venturi Tubes, and Orifices," subsection "Steam and Gas Service," the following expression for a simple convergent nozzle maximum thrust is found[11]:

$$T_{\text{conv}} = A_t \left[2p_o \left(\frac{2}{k+1} \right)^{1/(k-1)} - p_{\text{atm}} \right] \tag{B8.95}$$

Then, for *superheated steam* ($k = 1.3$), the following ideal gas thrust may reach its maximum value

$$T = A_t (1.26 p_0 - p_{\text{atm}}) \tag{B8.96}$$

and for *saturated steam* ($k = 1.1$)

$$T = A_t (1.23 p_0 - p_{\text{atm}}) \tag{B8.97}$$

If *incompressible liquid* escapes from a vessel (or broken pipe), where stagnation pressure is p_0, its subsonic exit velocity is expressed by Eq. (B8.35) (with $z = 0$ and $p_2 = p_{\text{atm}}$). Then, by using this expression for w_0 in Eq. (B8.94), the steady thrust (reaction force) can be found from the following expression:

$$T = \frac{\dot{m}}{g_c} w_e = \frac{\rho}{g_c} A_e w_e^2 = \frac{\rho}{g_c} A_e \frac{2g_c (p_1 - p_{\text{atm}})}{\rho} = 2A_e (p_1 - p_{\text{atm}}) \tag{B8.98}$$

Thus, while the speed of efflux is inversely proportional to the density, the thrust in this case is independent of the density and depends only on the area of the break (orifice) and the gauge pressure ($p_1 - p_{\text{atm}}$).

As an example, consider a vessel containing cold water at 1050 psia (72.4 bar).

As a result of a postulated 12-in (0.3-m) pipe break, water is discharged into the atmosphere. As calculated by using Eq. (B8.98) this would produce an impressive steady thrust of 225,000 lb_f (999,600 N), while the velocity of efflux, calculated from Eq. (B8.35), at its density of 62.5 lb_m/ft^3 (1020 kg/m^3), is equal to 388.1 ft/s (118.3 m/s).

If a *two-phase critical flow* escapes from a vessel or a broken pipe, one may expect somewhat different thrust characteristics. Various critical two-phase flow models, as discussed in the section ''Critical Gas-Liquid Flow,'' provide the mass flux and thermodynamic parameters (choke pressure, steam quality) at the nozzle throat in terms of vessel stagnation properties and pipe fL/D. Moody[45] used his model (see subsection ''Moody Model'') for calculating critical blowdown from a 1050 psia (72.4 bar), typical for a boiling water reactor (BWR) vessel. He found that at $fL/D = 0$ (pipe break just where it is attached to a vessel), T/A_e for critical saturated water blowdown is 183,000 lb_f/ft^2 (8,762 kN/m^2), which is about half the value of thrust/area from Eq. (B8.98) for incompressible liquid blowdown. Furthermore, T/A_e for saturated steam is 182,000 lb_f/ft^2 (8,714 kN/m^2), which is closely predicted by Eq. (B8.97). Predicted thrust and impingement properties are shown to give reasonable agreement with available data. It is also clear that increased values fL/D (pipe break at a certain distance from the vessel) would reduce the thrust. (Compare with the Fanno model discussed in section ''Critical Gas-Liquid Flow,'' subsection ''Fanno Model.'')

For more detailed discussion and numerical examples on this subject, see Refs. 29 and 45.

Typical Water Hammer Transients

Water hammer is a pressure wave, usually resulting from rapid changes in the flow rate in a pipe, which is characterized by the transformation of kinetic energy of moving fluid into pressure. Typical transients for a water-filled system include rapid valve closure, pump startup, or pump trip within the circulating water system, feedwater system, or service water system of a power plant, or the cooling water system of a process plant. The water hammer phenomena in a piping system also may result due to formation of vapor pockets at locations where the pressures are reduced to or below vapor pressure. This phenomenon is normally called *column separation.* The subsequent collapse of these vapor pockets may develop significant pressure spikes which should be taken into consideration in system design and analysis.

The basic water hammer equation is derived from equations of conservation of mass and momentum in a single pipeline. For low-flow velocities [much lower than the speed of sound in the fluid (Ma $\ll 1$)] and for columns of fluid rejoined near a closed valve or a dead end (final flow velocity $w = 0$), the produced peak (maximum) pressure of inertia is estimated from the following equation (see Refs. 1 and 46):

$$\Delta p = \frac{\rho}{g_c} c \Delta w \tag{B8.99}$$

where Δw is the relative closure velocity of the fluid before impact, ρ is the fluid density, and c is the sonic wave speed. Using the bulk modulus of elasticity of water $K = 0.3 \times 10^6$ psi (2.07×10^6 kPa) the speed of sound in water without any pipe wall effect is ~4700 ft/s (~1435 m/s). For a circular elastic steel pipe of diameter

d, in which the Young's modulus of elasticity for the wall material is $E = 30 \times 10^6$ psi (206×10^6 kPa), the wave speed is expressed by[1]:

$$c = \sqrt{\frac{g_c K/\rho}{1 + \frac{d}{e}\frac{K}{E}}} \tag{B8.100}$$

where e is pipe wall thickness. By using Eq. (B8.100) for cold water, the wave speed c varies from 4490 ft/s (1370 m/s) for $d/e = 10$ to 2360 ft/s (720 m/s) for $d/e = 300$. If the valve closure time is less than $t = 2L/c$, where L is the length of a pipe from the valve to the upstream vessel, the action is called *rapid closure.* The term *slow closure* refers to times of closure greater than $2L/c$. In the case of column separation or column rejoining (*reclosure*), large flow velocities are not necessary for significant peak pressures and segment forces. For example, for cold water with ~10 ft/s (~3 m/s) closure velocity in a 10 in pipe, a peak pressure of inertia of ~570 psi (~39 bar), as calculated from Eq. (B8.99), could produce a segment force as high as ~43,000 lb_f (~190 kN).

NUREG-0582[47] has identified a number of high-energy systems in nuclear power plants that have had a history of transient-related problems. It also discussed the major causes of transient problems which are attributable to events such as pump startup, stopping, or seizure; pump startup with inadvertently voided discharge lines; valve opening, closing, and instability; check-valve closure and delayed opening; water entrainment in steam lines; steam bubble collapse, and mixing of subcooled water and steam from interconnected systems; slug impact due to rapid condensation; and column separation and subsequent rejoining. Some of these transient events can be prevented by implementing appropriate operating procedures. However, there are other events that may occur during normal/upset, emergency, or faulted plant operating conditions. These flow transients in the piping system may cause significant dynamic loads and large reactions on the piping, piping supports, and connected equipment. These transient loads must be analyzed and incorporated into the pipe stress analysis and pipe support evaluation.

The service water system of a nuclear station illustrates the application. The system is designed to supply cooling water to remove heat from component heat exchangers throughout the station. Hydraulically, such a system is far more complex than a condenser circulating water system because there are numerous heat exchangers and considerable variations in piping elevation.

Figure B8.55 depicts the major components of a typical service water system in the case of a pressurized water reactor (PWR) unit; Fig. B8.56 shows the profile (vertical) of a portion of the system, including the control building air-conditioning water cooler (HVK) and emergency diesel engine cooling water (EGS) piping. Because of the high elevation of the HVK piping, a vapor gap will form on either side of the HVK heat exchanger when the service water pumps trip out. Also, because of the U-shaped piping configuration, a water column will be retained in the central portion of the HVK piping, as shown. After the pump has restarted, the vapor gap at the inlet piping may close rapidly—resulting in severe pressure and force transients—unless proper care is taken in the design and operation of the system.

Typical Steam Hammer Transients

Steam hammer is defined as the pressure surge generated by transient flow of superheated or saturated steam in a steam line, but not as the collapse of steam

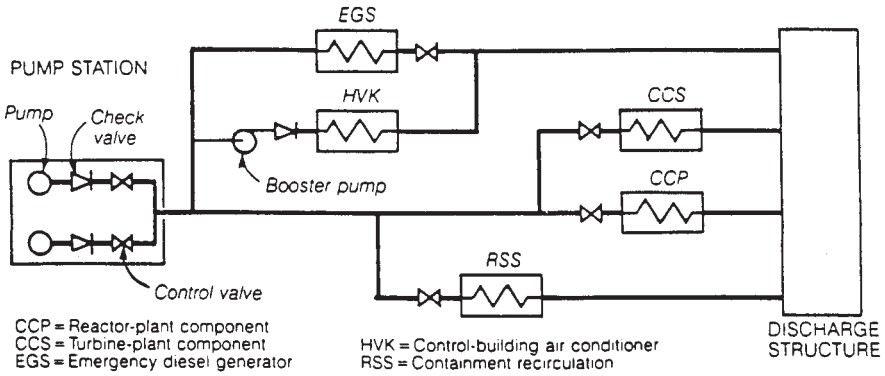

FIGURE B8.55 Major components of a service water system for a PWR-type nuclear power plant.

pockets which was described in the previous section. Usually the pressure spikes due to steam hammer are not as high as in water systems because of the large compressibility of steam.

Typical applications of a steam hammer program to perform analysis of compressible flow include studies of the turbine generator main steam and bypass system, the safety relief valve blowdown, the reactor core isolation cooling system, the high-pressure coolant injection system, and so forth. The program could apply the method of characteristics with finite difference approximations for solutions of unsteady one-dimensional compressible fluid flows. The choking phenomena of

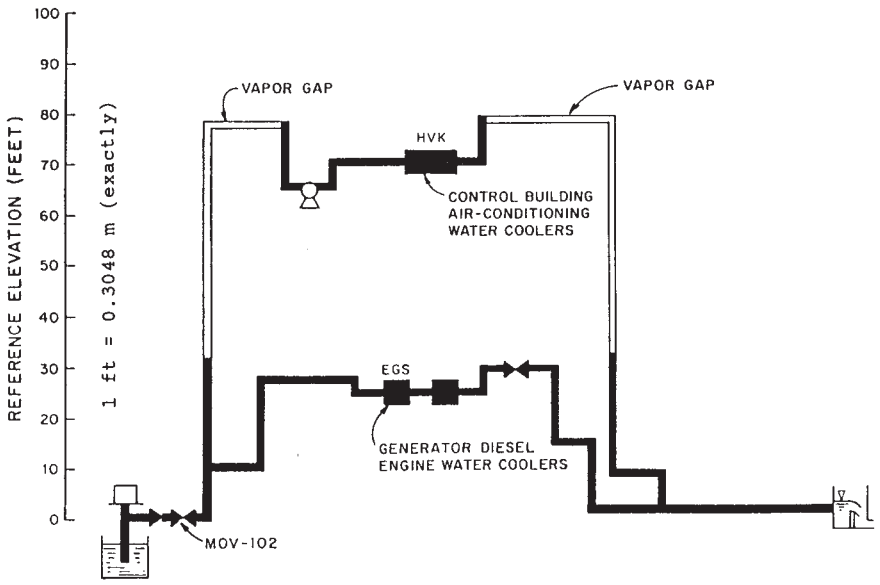

FIGURE B8.56 Partial service water system profile showing vapor gap.

steam flow are included in the program. In analyzing transients in a safety/relief-valve discharge system, the program has an option to handle the blowdown forces at the interface of steam discharging into the suppression pool.

Steam-Condensation-Induced Water Hammer

Several flow conditions may lead to severe condensation-induced water hammers, with steam and water counterflow events in a horizontal pipe being potentially the most severe. Water-cannon events (subcooled water with condensing steam in a vertical pipe) may occur if the right geometry and system conditions exist. Pressurized water entering a vertical steam-filled pipe can cause a severe transient event over a wide range of piping geometry conditions. Hot water entering a lower-pressure line is also a very common condition for many nuclear power plant piping systems, especially for those heater drain dump lines which lead to the condenser.

Condensation-induced water hammers of the steam and water counterflow type can occur in a horizontal pipe with a steam- and water-stratified environment. If the water is highly subcooled, violent condensation may occur. This rapid condensation process will generate a significant steam flow above the water surface. The shearing forces at the interface between the steam and the subcooled water can create enough turbulence to generate a water slug, which in turn will entrap an isolated steam pocket. Continued rapid condensation of the entrapped steam will accelerate the water slug into the void, causing a damaging water hammer. Two conditions must coexist in the system to initiate this condensation-induced water hammer, namely:

- A steam and subcooled water stratified flow exists in a significant length of a horizontal or near-horizontal pipe
- Substantial turbulence exists at the steam-water interface

Depending on the void fraction and subcooling in the two-phase flow environment, the magnitude of the pressure wave generated by steam condensation and bubble collapse can be devastating. These events should be prevented from occurring by all practical means (see Refs. 28, 29, 48).

In summary, the significant condensation-induced water hammer conditions are:

- Subcooled water with condensing steam in a vertical pipe
- Steam and water counterflow in a horizontal pipe
- Pressurized water entering a vertical steam-filled pipe
- Hot water entering a lower-pressure line

Practical Recommendations to Minimize Water Hammers

Protection Devices to Minimize Water Hammers. Various devices may be used to protect piping systems from damage by severe hydraulic transients. Check valves, standpipes, and accumulators prevent the occurrence of transients or reduce their effects.

Vacuum-breaker valves allow air to enter a piping system when a vacuum develops. Sometimes installed on heat exchangers, these relief valves may be located in the system where water-column separation may occur during transient conditions. Air in the system will significantly attenuate pressure spikes when water columns rejoin.

Check valves are sometimes used in service water systems to prevent column separation. Following a power loss, water in the high portion of a riser may drain out because of the large change in elevation, creating a vapor cavity. In this situation, a check valve may be installed at the bottom of the upstream riser to prevent water drainage and column separation.

A *standpipe* may be used in a cooling water system where relief of vacuum pressure is necessary. Serving as a simple surge tank, the standpipe admits water and possibly air into the system. This either eliminates column separation or reduces the severity of column reclosure because of air injection.

An *accumulator* of proper size may effectively eliminate column separation after a power failure. The device, a closed container partially filled with water topped with compressed air, is usually installed immediately downstream from a pump station along with a check valve. Following a power failure, the pump coasts down and the pump head decreases rapidly, causing the check valve to close. Compressed air in the accumulator will supply fluid flow pneumatically into the main line to minimize downsurge, and will provide a cushion on the return surge.

Field Tests for Hydraulic Transients. Frequently, field tests for hydraulic transient loading are conducted to accomplish the following:

- Verify that system design is adequate
- Determine the best way to operate a system to avoid transients
- Discover scenarios of unanticipated transients
- Validate results obtained from analytical approaches

The first three functions are often included as part of the normal startup and checkout of a new system.

Field tests serve to measure key parameters related to hydraulic transients while operating a system in a manner that could produce plausible transient events. Validation of analytical results involves benchmarking the computation method for known operating parameters; or benchmarking, combined with checking of input variables such as pump characteristics and valve opening or closing time. In many cases, transients introduced by valve opening or closing and by pump trip or startup are overpredicted, and can be improved with the help of field test data.

System Design Considerations. There are three ways to prevent or minimize fluid transients through effective system design: (1) general design practices that either reduce or eliminate a possible transient; (2) adding special systems to either control or prevent a transient; and (3) performing time-history analysis of loads, and designing a pipe support system to accommodate the transient loads.

General design practices should include:

- Designing all steam-line piping to provide continuous downward slopes with provisions for low-point drainage to preclude the formation of water pockets (upstream of a potentially isolable valve is considered to be a low point).
- Where allowed by system design function, providing slow-opening/closing valves
- Providing high-point vents or air-release valves in water-filled lines to allow system venting to eliminate the formation of air pockets
- Using vacuum breakers to minimize potential dynamic effects by providing an air cushion in fluid-carrying pipelines that could otherwise be under an occasional vacuum

Special systems that preclude or diminish the effects of fluid transients include:

- Loop-fill systems that continuously maintain a primary piping system in a filled and pressurized condition during operating modes when that system is on standby (e.g., fire-protection system and emergency core-cooling systems).
- Steam-line preheating systems that continuously maintain or allow gradual heatup of steam supply lines to reduce rapid steam condensation and the development of water slugs that generate substantial loads on the piping system.

The overall piping system stress qualification should consider as appropriate all loading conditions, including the dynamic effects of fluid transients. Piping codes prior to 1970 were rather vague in this regard; however, the more recent editions of ASME Section III of the Boiler and Pressure Vessel Code are quite specific and require this consideration. The forcing functions generated by manual or computer modeling are incorporated into the stress analyses which are used as the basis for designing a support system that can accept the loads and maintain them within the code-allowable limits for safe, continuous system operation.

Pump Net Positive Suction Head (NPSH) Transients

In dealing with net positive suction head problems, effort has been made to distinguish between NPSH required or NPSHR and NPSH available or NPSHA. The NPSHA is a function of pump design or pump requirement, while the NPSHA is a function of the pump system which must provide the required NPSH. The available NPSH must always exceed the required NPSH by a certain margin which must be positive even during transient conditions (see Ref. 49).

Large steam-electric power plants are equipped with several stages of low-pressure and high-pressure feedwater heating within the turbine cycle. There may be as many as three or four stages of low-pressure closed feedwater heaters situated between the condenser and the deaerator which supplies heated condensate to the feedwater pump. Under transient conditions when load change is sudden and large, a check valve in the steam extraction line from turbine to deaerator closes to avoid backflow and possible damage to turbine blading. Deaerator pressure at this moment decreases fairly rapidly, while colder water from the condensate system continues to enter the deaerator, and hot water continues to be withdrawn.

Turbine load rejection is a case of an even more severe transient. Immediately following a turbine load rejection from a maximum load, warm condensate will enter the deaerator initially. The temperature of the condensate, however, will eventually decay to a point exactly equal to the condenser hot-well temperature because the low-pressure heaters will no longer receive extraction steam from the turbine. It is this transient condition which should receive prime consideration in feedwater system design.

As extraction steam is cut off from the deaerator, pressure in the corresponding deaerator storage tank falls rapidly, as does the pressure at the pump suction. However, temperature and vapor pressure of water at the pump do not change until colder water from the tank has had a chance to travel down the pump suction piping. If actual pressure at the pump impeller falls below the vapor pressure there, cavitation will result. It is the production of these vapor pockets, or bubbles, and the consequent collapse as the head, or pressure, is developed in the impeller, that generates the cavitation which produces the noise, vibration, and the pitting attack of the impeller's surfaces. The measurable consequences of cavitation on a pump's

performance are a loss in flow and head resulting from voiding of vane passages, turbulence, and two-phase flow.

The design of fluid systems must clearly establish criteria that address steady-state and transient conditions from the view of system or component protection. Certain types and severity levels of transients can be accommodated by the pump but may not be tolerated by the system.

Short-term transients can be considered momentary events where the available NPSH falls below the required NPSH at a particular moment. These events will probably have no measurable effects on the pump mechanically and, because of their duration of fractions of a second to seconds, should not measurably affect performance which would be restored with restored suction conditions.

Transients which occur for periods that range from seconds to a few minutes will have a measurable impact on performance. Sustained suction conditions that are below minimum NPSH requirements will cause cavitation in the eye of the pump's suction impeller, which in turn will reduce flow and developed head. Long-term, low-NPSH transients, by design, must be avoided.

To protect the main feed pump against unwanted transient suction pressure decay and cavitation, the following steps can be considered by the plant designer:

1. Increasing static suction head by raising the deaerator or lowering the pumps. The absence of high structure in nuclear power plants creates a location problem for a deaerator.

2. Increasing deaerator storage capacity. A deaerator removes entrained oxygen from feedwater and provides a surge tank which reduces the possibility for rapid transients and provides approximately 5-min storage if a condensate pump fails.

3. Reducing pump suction pipe (downcomer) resident capacity by sizing the connecting piping as small as practical and routing it as directly as possible. Preliminary sizing of the downcomer should be based on a flow velocity of 10 ft/s (3 m/s).

4. Lowering deaerator pressure. In most fossil-fueled power plants, deaerators operate at either the fourth or fifth turbine extraction point in the eight-heater cycle which means at 80 or 160 psia (5.5 or 11 bar) respectively. Operating experience with these pressure levels is sufficient to justify the use of either.

5. Installing a booster feed pump. Auxiliary turbine-driven feed pumps require low-speed, low-head booster pumps (generally of single-stage design) ahead of the main feed pump. This booster pump is capable of handling the required capacity with the low NPSH required. A survey revealed that every power plant larger than 400 MW currently under construction uses auxiliary turbine drives for feed pumps and their boosters.

6. Injecting steam into deaerator (pegging).

7. Injecting cold water at a point sufficiently ahead of the pump suction nozzle to provide good mixing (deaerator bypass system).

While items (1) through (5) may be called preventive actions, items (6) and (7) are corrective actions.

In order to chose the base design for a particular plant, information on the magnitude of the NPSHA decay during the transient is needed. Theoretical background for computerized or hand calculations relating to these problems, as well as numerical examples, are presented in Refs. 50, 51, 52.

Pump NPSH transients have been modeled, photographed under test conditions,

and certain chronic transients have resulted in verifiable documented cases where NPSH conditions were the cause of pump problems. However, in spite of our sophistication and diligence in this area, over many decades NPSH transients and their impact remain a serious problem.

NPSH transients must be understood as well as the pump's capabilities to withstand such events; then margins can be applied initially in the design of the system.

REFERENCES

1. V. L. Streeter and E. B. Wylie, *Fluid Mechanics,* Eighth ed. McGraw-Hill Book Company, New York, 1985.
2. E. F. Obert, *Thermodynamics*, McGraw-Hill Book Company, New York, 1962.
3. H. Schlichting, *Boundary Layer Theory*, McGraw-Hill Book Company, New York, 1955.
4. W. M. Rohsenow and H. Choi, *Heat, Mass and Momentum Transfer*, Prentice Hall, Inc., Englewood Cliffs, New Jersey, 1961.
5. The American Society of Mechanical Engineers, *ASME Steam Tables,* Sixth ed. (computer program included), New York, 1993.
6. International Organization for Standardization, *Units of Measurements,* ISO Standards Handbook 2, Second ed., Geneva, Switzerland, 1982.
7. Crane Company, ''Flow of Fluids Through Valves, Fittings and Pipe,'' Technical Paper No. 410.
8. I. E. Idelchik, G. R. Malyavskaya, O. G. Martynenko, and E. Fried, *Handbook of Hydraulic Resistance*, Hemisphere Publishing Corp., 1986.
9. W. F. Bland and R. L. Davidson (eds.), *Petroleum Processing Handbook,* McGraw-Hill, New York, 1967.
10. A. Stodola, *Steam and Gas Turbines* (translated from Sixth German ed.), McGraw-Hill Book Company, New York, 1927.
11. A. H. Shapiro, *The Dynamics and Thermodynamics of Compressible Fluid Flow*, The Ronald Press Company, 1953.
12. ASME Code B31.1, 1998 ed. Appendix 11, 1.0–1.2, ''Nonmandatory Rules for the Design of Safety Valve Installations.''
13. ASME, *Fluid Meters, Their Theory and Applications*, sixth ed. ASME, 1971.
14. ASME, *Flow Measurements,* ASME Power Test Codes, The American Society of Mechanical Engineers, 1959.
15. S. Ocheduszko, J. Szargut, H. Gorniak, A. Guzik, and S. Wilk, *Zbior Zadan z Termodynamiki Technicznej*, Third ed. (in Polish) PWN, Warszawa, 1970.
16. A. E. Bergles, J. G. Collier, J. M. Delhaye, G. F. Hewitt, and F. Mayinger, *Two-Phase Flow and Heat Transfer in the Power and Process Industries*, Hemisphere Publishing Corporation, 1981.
17. J. M. Delhaye, M. Giot, and M. L. Riethmuller, *Thermohydraulics of Two-Phase Systems for Industrial Design and Nuclear Engineering*, McGraw-Hill Book Company, New York, 1981.
18. R. Roumy, ''Structure des Ecoulements Disphasiques Eau-air: Etude de la Fraction de Vide Moyenne et des Configurations d'Ecoulement,'' CEA-R-3892, 1969.
19. G. F. Hewitt, and D. N. Roberts, ''Studies of Two-Phase Flow Patterns by Simultaneous X-ray and Flash Photography,'' AERE-M 2159, 1969.
20. G. F. Hewitt, and N. S. Hall-Taylor, *Annular Two-Phase Flow,* Pergamon, New York, 1970.

21. T. Oshinowo and M. E. Charles, ''Vertical Two-Phases Flow, Part 1: Flow Pattern Correlations,'' *Can. Chem. Eng.*, vol. 52, pp. 25–35, 1974.
22. G. E. Alves, ''Cocurrent Liquid-Gas Flow in a Pipeline Contactor,'' *Chem. Eng. Prog.*, vol. 50, no. 9, pp. 449–456, 1954.
23. Y. Taitel and, A. E. Dukler, ''A Model for Predicting Flow Regime Transitions in Horizontal and Near-Horizontal Gas-Liquid Flow,'' *AlChE Journal*, 22, pp. 47–55, January 1976.
24. O. Baker, ''Simultaneous Flow of Oil and Gas,'' *Oil and Gas Journal*, vol. 53, pp. 185–190, 1954.
25. K. Goldmann, H. Firstenberg, and C. Lombardi, ''Burnout in Turbulent Flow—A Droplet Diffusion Model,'' Trans. ASME, Ser. C, *J. Heat Transfer*, 83, pp. 158–162, 1961.
26. A. E. Dukler and Y. Taitel, ''Flow Pattern Transitions in Gas-Liquid Systems: Measurement and Modeling,'' *Multiphase Science and Technology*, vol. 2, 1987.
27. R. W. Bjorge and P. Griffith, ''Initiation of Waterhammer in Horizontal or Nearly Horizontal Pipes Containing Steam and Subcooled Water,'' *Journal of Heat Transfer*, vol. 106, pp. 835–840, 1984.
28. T. J. Swierzawski, and P. Griffith, ''Preventing Water Hammer in Large Horizontal Pipes Passing Steam and Water,'' *Journal of Heat Transfer*, vol. 112, TN, pp. 523–524, 1990. (Also a technical paper TP 89-63 of the Stone & Webster Engineering Corporation, Boston, November 1989.)
29. R. T. Lahey, Jr. and F. J. Moody, *The Thermal-Hydraulics of Boiling Water Nuclear Reactor,* ANS, 1977.
30. Aerojet Nuclear Company, ''RELAP4/MOD5, A Computer Program for Transient Thermal-Hydraulic Analysis of Nuclear Reactors and Related Systems,'' User's Manual, ANCR-NUREG-1335, 1976.
31. C. J. Baroczy, ''A Systematic Correlation for Two-Phase Pressure Drop,'' NAA-SR-MEMO-11858, 1966.
32. H. D. Baehr, *Thermodynamik* (in German), Springer Verlag, 1962.
33. W. F. Allen, Jr., ''Flow of Flashing Mixture of Water and Steam Through Pipes and Valves,'' *Trans. ASME*, April 1951.
34. M. W. Benjamin and J. G. Miller, ''The Flow of a Flashing Mixture of Water and Steam Through Pipes,'' *Trans. ASME*, vol. 64, 1942.
35. F. J. Moody, ''Maximum Flow Rate of a Single Component, Two-Phase Mixture,'' APED-4378, October 1963.
36. F. J. Moody, ''Maximum Two-Phase Vessel Blowdown from Pipes,'' APED-4827, April 1965.
37. F. J. Moody, ''Maximum Discharge Rate of Liquid-Vapor Mixtures from Vessels,'' ASME Winter Annual Meeting, Houston, Texas, November 1975.
38. R. E. Henry and H. K. Fauske, ''The Two-Phase Critical Flow of One-Component Mixtures in Nozzles, Orifices, and Short Tubes,'' *ASME Journal of Heat Transfer*, pp. 179–187, May 1971.
39. D. Abdollahian and A. Singh, ''Prediction of Critical Flow Rates Through Power-Operated Relief Valves,'' ANS/ASME/AlChE, Proceedings of the Second International Topical Meeting on Nuclear Reactor Thermal-Hydraulics, vol. 2, pp. 912–918, Santa Barbara, California, 1983.
40. K. H. Ardron and R. A. Furness, ''A Study of the Critical Flow Models Used in Reactor Blowdown Analysis,'' *Nuclear Engineering and Design*, p. 39, 1976.
41. P. Griffith, ''Notes for the MIT Spring Course on Two-Phase Flow,'' 1976.
42. Swedish Trade Office, ''District Heating,'' Materials for the Swedish District Heating Workshops in the United States of America, October 10–20, 1978.

43. General Electric Company, ''Moisture Separator and Reheater Drain Systems,'' GEK-37949A, 1977.

44. R. S. Burington, *Handbook of Mathematical Tables and Formulas*, Third ed., Handbook Publishers, Inc., Reprinted in 1957.

45. F. J. Moody, ''Prediction of Blowdown Thrust and Jet Forces,'' ASME Paper 69-HP-31, 1969.

46. E. B. Wylie and V. L. Streeter, *Fluid transients*, McGraw-Hill International, 1978.

47. U.S. Nuclear Regulatory Commission NUREG-0582, ''Water Hammer in Nuclear Power Plants,'' July 1979.

48. T. J. Swierzawski and D. A. Van Duyne, ''Plant Design and Operating Considerations for Preventing Thermal-Hydraulic Water Hammers,'' ASME Paper No. 89-JPGC/Pwr-19, presented at the Joint ASME/IEEE Power Generation Conference in Dallas, Texas, October 1989.

49. I. J. Karassik, et al., *Pump Handbook*, McGraw-Hill, Inc., New York, 1976.

50. G. S. Liao and P. Leung, ''Analysis of Feedwater Pump Suction Pressure Decay Under Instant Turbine Load Rejection,'' *Journal of Engineering for Power*, Trans. ASME, Series A, vol. 94, April 1972.

51. G. S. Liao, ''Protection of Boiler Feed Pump Against Transient Suction Pressure Decay,'' *Journal of Engineering for Power*, Trans. ASME, Series A, vol. 96, July 1975.

52. G. S. Liao, ''Analysis of Drain Pumping System for Nuclear Power Plants Under Transient Turbine Loads,'' *Journal of Engineering for Power*, Trans. ASME, pp. 619-627, October 1975.